LNX, A NOVEL PDZ DOMAIN CONTAINING PROTEIN

by

Cheryl Deanna Wolting

A thesis submitted in conformity with the requirements
for the degree of Master of Science
Graduate Department of Medical Biophysics
University of Toronto

ABSTRACT

LNX, A NOVEL PDZ DOMAIN CONTAINING PROTEIN

Cheryl Deanna Wolting
Master of Science, 2000
Department of Medical Biophysics, University of Toronto

LNX, a novel protein that contains four PDZ domains, was identified through its interaction with the mammalian homologue of the cell fate determinant, Numb. A yeast two-hybrid screen was performed to identify the targets of the LNX PDZ domains. Seven proteins were identified which interact specifically with the PDZ domains of LNX in a yeast two-hybrid assay. Four of the seven proteins are novel while the other three are murine homologues of the proteins WWP1, PRA1 and syntaxin5. Two *in vitro* methods, namely mixing of fusion proteins and BiaCore analysis, were used to verify and characterize these interactions. In addition these reagents were used to identify endogenous LNX from mouse brain.

ACKNOWLEDGEMENTS

I would first like to thank my supervisor, Jane McGlade for excellent guidance and support throughout the last four years and especially during my Master's thesis. I have enjoyed working with Jane and the past and present members of the McGlade lab and I thank them for all their help. Thank you also to the members of my supervisory committee, Drs. Dan Dumont, David Rose and Daniela Rotin, for their leadership. This work was supported by a grant from the National Cancer Institute of Canada to Jane McGlade.

Thank you to Nina Jones and Bryan Snow for supplying the cDNA libraries for the yeast two-hybrid screens, Denis Bouchard for assistance with the BiaCore studies, Matt Dermer for assistance with the GST fusion proteins and deletion mutant for the yeast two-hybrid assay and Dr. Johnny Ngsee at the Loeb Research Institute in Ottawa for the pQE11-his-HA-PRA1 expression construct.

I would also like to thank my parents for their continual support and encouragement throughout my education. Last but not least, thank you to my husband, Sean, for being so understanding during my Masters (especially during the writing!).

TABLE OF CONTENTS

Table LIST OF TABLES Page

Figure LIST OF FIGURES Page

Chapter I Introduction

1.1 MULTICELLULAR ORGANISMS AND THE NEED TO COMMUNICATE

A mammalian organism is made up of millions of cells that must communicate with one another in order for the organism to survive and function normally. This communication occurs within the same cell, between neighbouring cells or between physically separated cells. A signal can provide a wide range of instructions; for example, the signal can instruct the cell to grow, move, die or maintain its current status. Different signals can give the same instructions to a given cell, and the same signal can cause different results in different cells. The response of a given cell to a signal depends, in part, on the way in which the signal is transduced within the receiving cell. Signal transduction is dependent on the cell type and its location, and also the proteins expressed within the cell when the signal is received.

Signal transduction is facilitated by interactions between proteins. These interactions can cause an enzyme to become active or inactive, facilitate proper localization of a protein or bring effector proteins within close proximity. It is well established that many interactions between proteins are facilitated by conserved, modular domains found within a protein that recognizes a target sequence or domain within another protein. These modular domains are often conserved across a wide range of multicellular organisms and are found in proteins involved in a variety of signal cascades. These domains are modular; their structure permits the domain to adopt an isolated tertiary structure separate from that of the rest of the protein. This allows many domains to exist within one protein and theoretically, the domains can be "cut-and pasted" together in almost any combination. Proteins may contain several different types of domains in any order within the protein or may contain several copies of one type of domain, where each of these domains has either a unique or common target. Each type of domain recognizes specific target sequences within the different target proteins. Comparison of these target sequences allows prediction of a consensus sequence for each conserved domain.

Protein-protein interaction domains may be found in enzymes. In enzymes, these domains function to localize the enzyme, allow substrate binding or permit regulation of enzyme activity. Other molecules consist only of modular domains and are currently classified as adaptor, docking

or scaffolding proteins. (Fig. 1-1) (Pawson and Scott, 1997). These three classifications are not absolute and some proteins appear to fall under more than one classification. The conceptual definition of the three groups is best exemplified by signaling pathways downstream of tyrosine kinase receptors. Adaptor proteins recognize an activated receptor and propagate this signal to downstream signaling pathways. Docking proteins, which also recognize receptors in their activated state, contain multiple sites that can be tyrosine phosphorylated. The phosphotyrosine residues are recognized by downstream molecules that may or may not be from different signaling pathways. The docking protein thus provides amplification of the signal from the activated receptor by supplying a much greater number of docking sites for downstream molecules than could be contained in the receptor itself. The role of scaffolding molecules in tyrosine kinase signaling pathways can either be in clustering several molecules of one protein or bringing together several different proteins that are part of the same signaling pathway. This facilitates faster and more efficient signal transduction.

Scaffolding molecules offer several advantages in signal transduction (Fanning and Anderson, 1999; Ranganathan and Ross, 1997). First, efficiency of the signal transduction cascade is increased because of the increased local concentration of signaling molecules. The fact that the proteins are concomitant upon cascade initiation permits fewer proteins (i.e., adaptors, channels, second messengers, etc.) to be produced by the cell while still allowing propagation of the signal. Second, the speed of signal transduction is increased because protein interactions do not depend on chance collisions. Instead, an activated molecule can interact with and facilitate activation of its target much faster than if it needed to first locate then activate that target molecule. An example of the importance of a multiprotein signal transduction complex is exemplified in the Drosophila photoreceptor cell that is discussed below.

1.2 PROTEIN-PROTEIN INTERACTION DOMAINS

There are now over 30 known types of protein-protein interaction domains (Bork et al., 1997; Fanning and Anderson, 1999). Several of these, such as src homology (SH)2 and SH3 domains, have been studied for many years and are well characterized. The domains that are discussed here

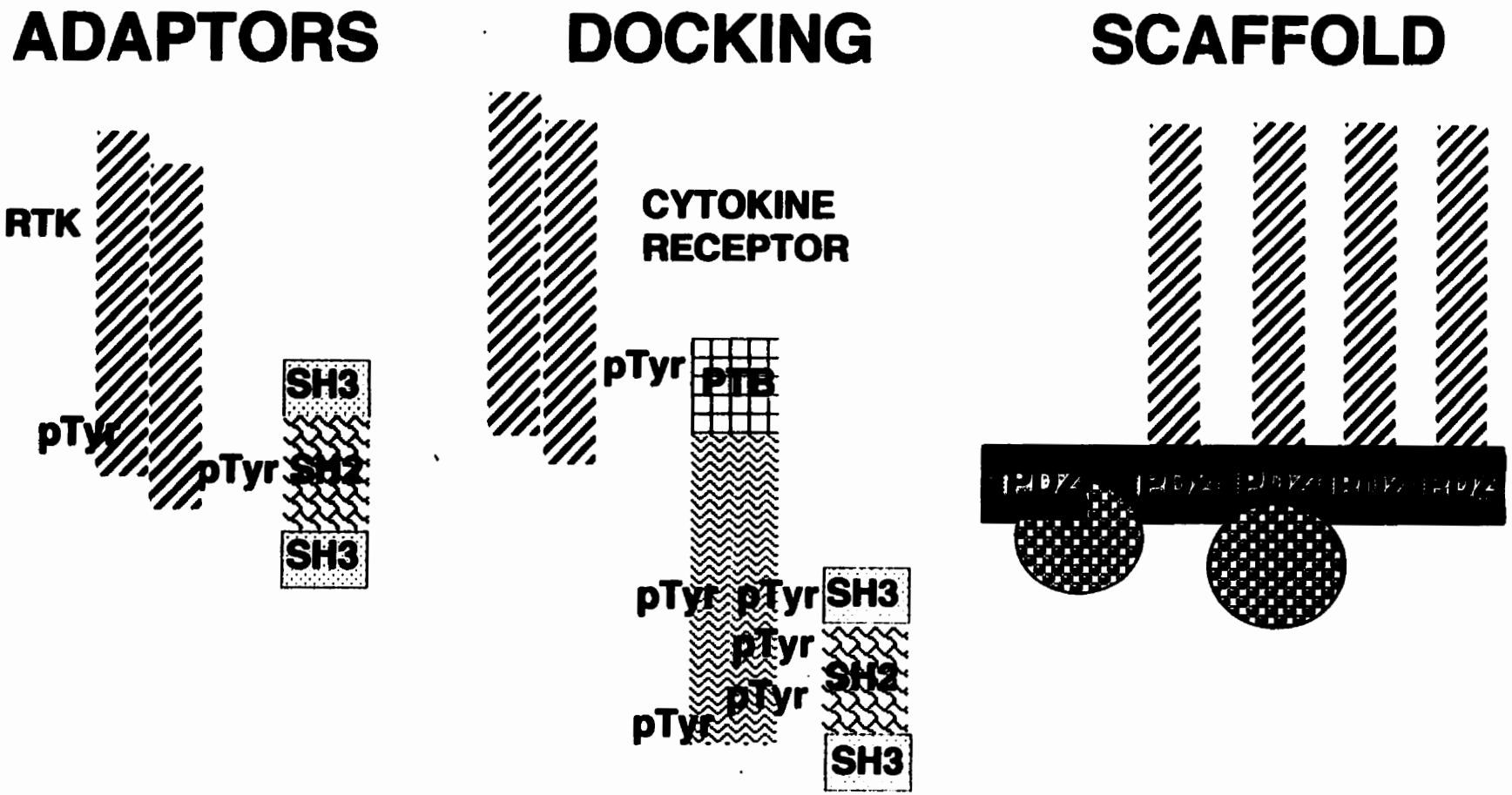

Fig. 1-1. Schematic diagram of the types of proteins involved in signal transduction pathways. RTK - receptor tyrosine kinase; pTyr- phosphotyrosine; SH2 -Src Homology 2 domain; SH3 -Src Homology 3 domain; PTB- phosphotyrosine binding domain; PDZ - PSD-95-DlgA-ZO-1 domain.

and the motifs that they recognize are outlined in Table 1-1 below. The features of the known domains provide a platform from which to begin analysis of newly identified domains.

The first protein-protein interaction domains that were described are found in the proto-oncogene src and were named SH2 and SH3 domains. The SH2 domain recognizes a phosphorylated tyrosine residue in transmembrane and cytoplasmic target proteins as well as three to five residues carboxy terminal to the phosphotyrosine (Koch et al., 1989; Sadowski et al., 1986). This interaction is regulated by the phosphorylation state of the target protein, thus it is a reversible interaction. Effectively the SH2 domain recognizes a peptide of five to ten amino acids containing the recognition site. The SH2 domain recognizes its target in a bipartite organization. A conserved binding pocket of basic residues, including one invariant arginine residue, is responsible for the interaction with the phosphorylated tyrosine residue (Pascal et al., 1994; Songyang et al., 1993; Waksman et al., 1993). The second binding surface contains variable residues which determine the specificity for the residues carboxyterminal to the phosphotyrosine; this is where specificity for different protein targets occurs (Songyang et al., 1993). For example, the SH2 domains of the Src/Lck kinase family recognize hydrophilic residues at the +1 and +2 positions relative to the phosphotyrosine and hydrophobic residues at the +3 position. The PLCγ1 and SH-PTP2 family of SH2 domains contain a hydrophobic groove adjacent to the phosphotyrosine binding pocket which is able to recognize five or more residues (Pawson, 1995).

The PTB (phosphotyrosine binding) domain, was first recognized in the docking proteins, Shc and IRS-1 (Blaikie et al., 1994; Bork and Margolis, 1995; Kavanaugh and Williams, 1994; Pelicci et al., 1992; van der Geer et al., 1995). As it turns out, this is a misnomer, as not all PTB domains require a phosphorylated tyrosine to be present in order for an interaction to occur. PTB domains from several different proteins, such as Numb (Dho et al., 1998), X11 (Borg et al., 1996), and mDab1 (Howell et al., 1999), recognize similar target sequences containing either a phosphorylated or unphosphorylated tyrosine. The consensus sequence found in many PTB target proteins is Xaa-Asn-Pro-Xaa-Tyr. In addition, hydrophobic residues five to eight residues amino terminal to the tyrosine are also recognized (Pawson and Scott, 1997). The structure of the PTB domain is composed of a seven stranded βsandwich capped by carboxy terminal αhelices

(Harrison, 1996; Zhou et al., 1996; Zhou et al., 1995). The peptide must adopt a βturn conformation just amino terminal to the (phospho)tyrosine residue in order to be recognized by the PTB. The bound peptide augments the βsheet by binding in a groove between the final βstrand of the βsheet and an αhelix. The loop preceding this final βstrand also interacts significantly with the target peptide.

The organization of βstrands and αhelices in the PTB is very similar to that of the PH (pleckstrin homology) domain, a modular signaling domain, which interacts with phosphoinositides. The PH domain recognizes the charged headgroups of phosphoinositides at the membrane and is important for targeting of signaling molecules to specific regions of the plasma membrane (Pawson and Scott, 1997). PH domains couple the proteins that contain them to signaling cascades regulated by phosphatidyl inositol kinases, inositol phosphatases and phospholipases.

The SH3 domain recognizes proline rich peptides of approximately ten amino acids within target proteins (Mayer et al., 1988; Mayer and Hanafusa, 1990). The peptides usually contain the consensus sequence Xaa-Pro-Xaa-Xaa-Pro (using the three letter amino acid code where Xaa is any amino acid). The third residue in this consensus is often a proline but this is not always the case. It has been shown that the SH3 domain recognizes the target peptide in a left-handed polyproline type II helix. The two Xaa-Pro pairs are recognized by hydrophobic pockets formed by conserved aromatic residues in the SH3 domain (Feng et al., 1994; Lim et al., 1994; Wittekind et al., 1994). There is a third pocket which often interacts with an arginine but shows some variability (Feng et al., 1994; Lim et al., 1994; Wittekind et al., 1994). It is possible that the SH3 ligand could bind in either orientation to the SH3 domain as the peptides are pseudo-symmetrical (Feng et al., 1994; Wittekind et al., 1994). Class I interaction is binding of the ligand in the amino to carboxy terminal orientation, whereas class II is binding in the carboxy to amino terminal orientation. The orientation of the ligand may determine the spatial organization of the resulting complex, which may be critical for downstream signaling events.

Another domain that recognizes proline-rich sequences is the WW domain, which binds target proteins having the consensus sequence Pro-Pro-Xaa-Tyr or Pro-Pro-Leu-Pro (Pawson and Scott,

1997). WW domains are small protein interaction domains containing 35-40 residues (Andre and Springael, 1994; Bork and Sudol, 1994; Hofmann and Bucher, 1995; Staub and Rotin, 1996). Within this domain, two tryptophan residues (from which the domain gets its name) and two proline residues are highly conserved. One WW domain containing protein, Nedd4 is important for the regulation of a Na^+ channel since mutations in the channel that disrupt recognition by the Nedd4 WW domains result in the hypertensive disorder, Liddle's syndrome (Li et al., 1995; Staub et al., 1996; Staub and Rotin, 1997).

Table 1-1. Overview of several protein-protein interaction domains and the motifs that they recognize in target molecules.

Domain	Recognition Motifs
SH2	pTyr-Xaa-Xaa-Φ 0 +1 +2 +3
PTB	Φ-Asn-Pro-Xaa-(p)Tyr -4 -3 -2 -1 0
SH3	Xaa-Pro-Xaa-Xaa-Pro
WW	Pro-Pro-Xaa-Tyr
PDZ	Glx-Ser/Thr-Xaa-Val Phe/Tyr-Xaa-Ala -3 -2 -1 0

Φ- denotes hydrophobic amino acids

There are many examples of protein-protein interaction domains that have been identified and characterized to varying degrees. Common themes can be seen in many of the interaction mechanisms used by these domains yet each has its own unique properties. Continued study of each of these domains may facilitate better understanding of the organization and regulation of signal transduction pathways. In this thesis, we will consider in detail the structure and binding specificity of the PDZ domain, a recently identified protein-protein interaction domain, in order to characterize the function of the multi-PDZ protein, LNX.

1.3 PDZ DOMAINS

PDZ domains are another modular protein-protein interaction domain which can be found in both adaptor proteins or proteins with enzymatic activity (Fig. 1-2). Like other modular domains, they

can be found in multiple copies within one protein. However, unlike most other modular domains, proteins have been found which contain only PDZ domains and no other recognizable conserved domains (Ponting et al., 1997). PDZ domains are also unique in that they can be found in proteins from mammals, *Xenopus*, *Drosophila*, *Caenorhabditis elegans*, to budding and fission yeast and even bacteria (*Bacillus subtilis*) (Ponting et al., 1997). This widespread conservation has not been seen with other recognized protein-protein interaction domains.

The PDZ domain was named for the first three proteins in which it was discovered: the post-synaptic density protein of 95kDa, PSD-95, the Drosophila tumour suppressor discs large (Dlg) and the tight junction protein ZO-1 (Kennedy, 1995; Ponting et al., 1997). It was previously called the GLGF domain (Cho et al., 1992), to reflect the four amino acid motif (Gly-Leu-Gly-Phe) that is conserved in the domain, and the DHR (Bryant et al., 1993), for discs large homology region. Many PDZ domains recognize the last few amino acids in the carboxy terminal tail of their target proteins, which can be transmembrane or cytoplasmic proteins (Ponting et al., 1997; Saras and Heldin, 1996; Songyang et al., 1997). Some PDZ domains may also recognize internal sequences. However, the recognition of a target molecule by a PDZ domain always occurs via a similar structural mechanism, as will be discussed below.

In order to characterize the target binding specificity of PDZ domains, Songyang et al. (1997) performed peptide library screens with nine different PDZ domains. In the first screen, a library of eight-residue degenerate peptides was incubated with the individual PDZ domains and the peptides selected by each domain were sequenced to generate a consensus motif. All nine PDZ domains preferred peptides with a hydrophobic carboxy terminal amino acid, (i.e. valine, isoleucine or leucine, and occasionally alanine or methionine). From this point on the last amino acid of the protein will be referred to as the amino acid in the "0" position, the second last amino acid is in the "-1" position, the third last amino acid is in the "-2" position and so on. Most of the PDZ domains examined selected a hydroxyl residue at the -2 position, either serine, threonine or

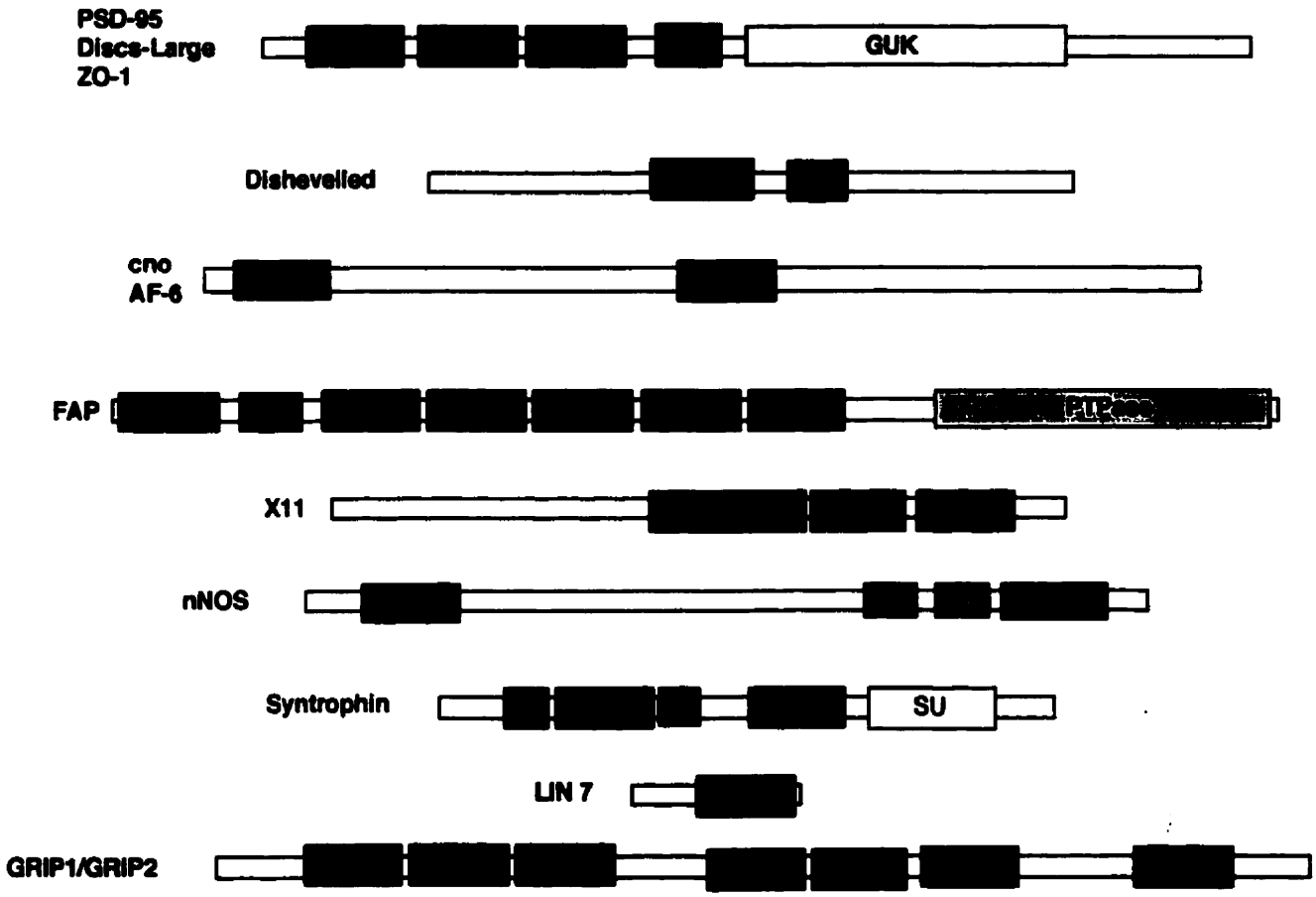

Fig. 1-2. Examples of PDZ domain-containing proteins. PDZ - PSD-95-DlgA-ZO-1 domain; SH3 - Src Homology 3 domain; GUK - guanylate kinase domain; DEP - dsh/egl-10/pleckstrin domain; RasBD - Ras binding domain; M- membrane binding site; PTPase - phosphatase; PTB - phosphotyrosine binding domain; CB - coenzyme binding region; PH - plecstrin homology domain; SU - syntrophin unique region.

tyrosine. For those PDZ domains with known protein targets, the consensus sequence predicted by the peptide library screen corresponded well to the known target recognition sites.

To identify the specificity at other residue positions, an oriented peptide library was created with nine residues peptides restricted to serine, threonine or tyrosine at the -2 position (Songyang et al., 1997). Some PDZ domains showed specificity for residues back to the -8 position with a mild preference for lysine, glutamine and aspartate in the -8 to -5 positions. Others showed specificity for hydrophobic amino acids in the -2, -1 and 0 positions. Songyang et al. (1997) proposed that PDZ domains could be separated into two groups based on their specificity at the -2 position. Group I PDZ domains prefer hydroxyl amino acids such as serine or threonine. This group includes all three PDZ domains of the mouse Discs large homologue and PDZ3 and PDZ5 of PTP-bas/FAP-1, a phosphotyrosine phosphatase. Group II PDZ domains prefer a hydrophobic amino acid such as phenylalanine or tyrosine at the -2 position. This included the single PDZ domain-containing proteins, p55, human Lin2, Tiam1 and AF-6.

Based on the structure of two PDZ domains which had already been solved, several conserved residues were identified which were integrally involved in peptide recognition (Doyle et al., 1996; Morais Cabral et al., 1996) (discussed below; Fig. 1-3). Songyang et al. (1997) utilized the residue predicted to be the first amino acid of the second αhelix (αB1) to divide each specificity group into two subgroups. This residue had been most strongly correlated with recognition of the -2 position of the peptide by structural analyses (Doyle et al., 1996; Morais Cabral et al., 1996). Group IA PDZ domains, containing a histidine residue at the αB1 position, recognize serine or threonine (and occasionally tyrosine) at the -2 position. Group IB consists of molecules for which the αB1 position is also basic (i.e., arginine or lysine) but the -2 target residue is not known. On the other hand, Group IIA PDZ domains have a hydrophobic residue at αB1 and recognize a hydrophobic residue at the -2 position. Group IIB PDZ domains have an acidic residue at the αB1 position (i.e., Asp, Glu, Gln, Asn) and prefer hydrophobic -2 position residues.

An alternatively oriented peptide library was generated and used to screen the nine PDZ

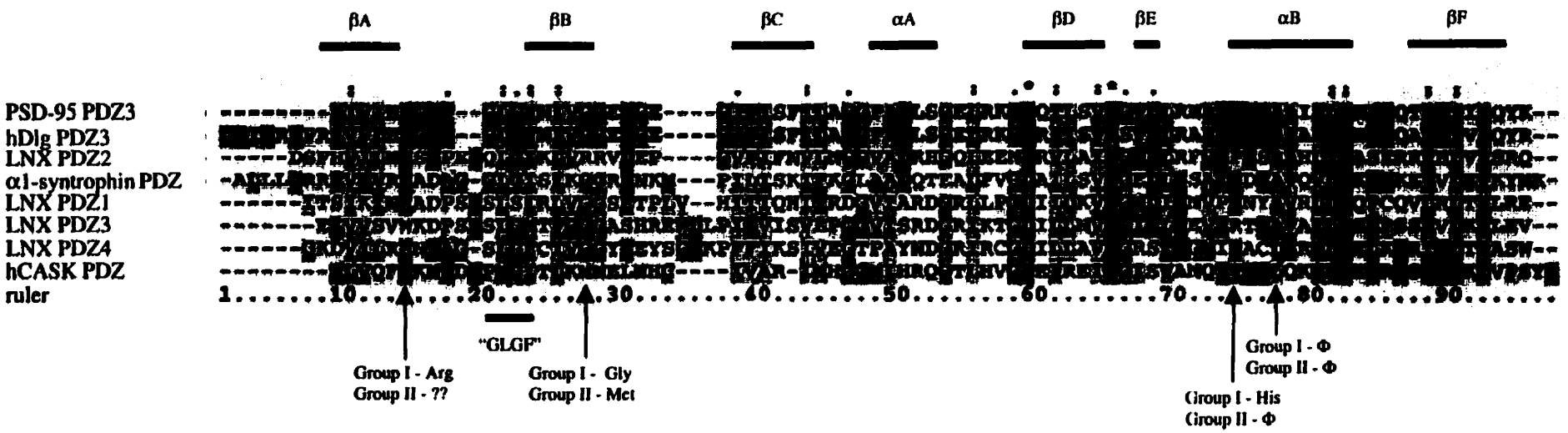

Fig. 1-3. Alignment of PDZ domains discussed in Chapter 1. The third PDZ domains from PSD-95 and hDlg, all four PDZ domains of LNX, and the single PDZ domains from α1-syntrophin and hCASK are included. Alignment was generated with ClustalX. Secondary structures as per Doyle et al. (1996) are marked above. Ruler denotes number of residues, residues discussed in text are indicated below. Φ denotes hydrophobic amino acids.

domains. This library, containing a fixed internal tyrosine, was intended to represent possible internal peptide sequences that might be recognized by a PDZ domain (Songyang et al., 1997). The peptides had the following sequence: NH2-Met-Ala-Xaa-Xaa-Xaa-Xaa-Tyr-Xaa-Xaa-Xaa-Xaa-Ala-Lys-Lys-Lys-NH2. None of the PDZ domains recognized a specific consensus sequence from this library and the authors thus proposed that PDZ domains do not bind internal sequences. We now know that there are several problems with this conclusion. First, it is not known why the authors believe that a peptide with a fixed internal tyrosine automatically represents an internal peptide. The only apparent rationale for using a fixed internal tyrosine is that a -2 position tyrosine might be recognized by both groups of PDZ domains. However, the authors themselves report that only one Group I PDZ domain recognized tyrosine at the -2 position, thus four of the nine PDZ domains are immediately irrelevant to this screen. Secondly, from the structural data it is now known that an internal peptide recognized by a PDZ domain must adopt a βstrand-like structure to fit in the binding groove (Hillier et al., 1999) (discussed below). Therefore, a conformationally constrained peptide library will likely yield more relevant results. Indeed, it has been observed that a PDZ domain will recognize a cyclized version of the same peptide which it will not bind after the intrachain disulfide bond has been broken (Gee et al., 1998).

The third PDZ domain of the rat protein PSD-95 (amino acids 302-402; PSD-95 PDZ3) has been crystallized alone and in complex with a nine residue peptide derived from a PDZ3-interacting protein identified in a yeast two-hybrid screen (Fig. 1-4) (Doyle et al., 1996). The domain adopted a six-stranded βsandwich organization, where the fourth βstrand (βD) participated in both sheets. Comparison of the complexed and peptide-free structures indicated that little conformational change occurred in the PDZ domain upon ligand binding. The amino and carboxy termini of the domain are in close proximity in the tertiary structure and are found on the opposite face of the domain with respect to the ligand binding face confirming the prediction that PDZ domains are modular protein interaction domains.

A peptide binding groove forms on the surface of the domain between the second βstrand (βB) and the second αhelix (αB) (Doyle et al., 1996). The last four amino acids of the peptide are highly ordered in the crystal; the backbone of the peptide interacts with the backbone of βB by

Fig. 1-4. Crystal structure of PSD-95 PDZ3 (backbone - teal; αhelix - green, βstrand - gold) in complex with peptide (free teal-coloured strand) which lies between αB and βB (PDB accession number, 1BE9) as viewed in Cn3D (available from ftp://ncbi.nlm.nih.gov/cn3d).

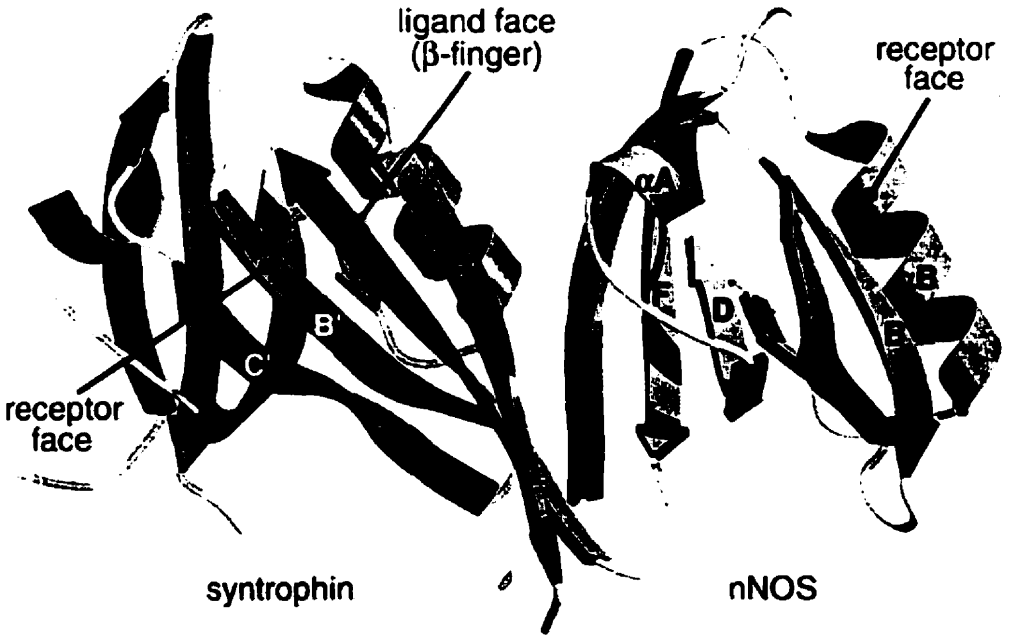

Fig. 1-5. Ribbon diagram of nNOS-α1-syntrophin co-crystal structure from Hillier et al., 1999. αhelices of nNOS labeled αA and αB; βstrands of nNOS labeled A-H; βstrands of syntrophin labeled B' and C'.

hydrogen bonding. This addition of a βstrand by peptide binding increases the βsheet by one, a binding mechanism known as βaugmentation. The side chains of the -2 and -3 position residues in the peptide interact with the side chains of residues in αB, βB and βC. These residues thus provide the specificity of the PDZ domain for a given peptide sequence.

The loop between βA and βB that lies at the end of this peptide binding groove contains the signature motif of PDZ domains, Gly-Leu-Gly-Phe (GLGF). The way in which this loop contributes to target peptide binding is unique among modular protein interaction domains. This loop was named the carboxylate binding loop for its role in anchoring the free carboxylate at the end of the peptide. It forms a stearic block at the end of the peptide binding groove so that only the extreme carboxy terminus of peptides are predicted to be structurally able to fit in this binding site. The binding of the carboxylate moiety by the GLGF sequence orients the terminus of the peptide such that the 0 position valine projects directly into a hydrophobic pocket, made up of several residues in the carboxylate binding loop.

Comparison of the PDZ domain structure to the structure of other modular protein interaction domains revealed a striking similarity to PH and PTB domains (Doyle et al., 1996; Harrison, 1996). The position of βstrands and αhelices are very similar, however differences are seen in the connectivities between secondary structures. The peptide recognition by PTB and PDZ domains also appears to have several similarities; the positioning of the peptide between a βstrand and an αhelix and the addition of an antiparallel βstrand to facilitate βaugmentation are both conserved.

There are fewer residues involved in peptide recognition by PSD-95 PDZ3 (four) than are recognized by other modular protein interaction domains such as SH2, SH3 and PTB (five to ten). However, the number of hydrogen bonds (approximately ten), and the area which is solvent excluded upon binding (400Å^2) is very similar in all four of these domains (Doyle et al., 1996).

Soon after this publication, another group reported the structure of the third PDZ domain of the human homologue of the Drosophila discs large tumour suppressor DlgA (Morais Cabral et al., 1996). This group described the PDZ structure as a five stranded antiparallel βbarrel with three

αhelices. There are two differences in secondary structure between the crystals of hDlg PDZ3 and PSD-95 PDZ3. hDlg PDZ3 does not have βE, as seen in PSD-95 PDZ3, although the loop between β4 and α2 of hDlg PDZ3 is in a very similar position to where βE of PSD-95 PDZ3 is found. Also, there is an additional αhelix at the end of hDlg PDZ3 which packs against the outside of the βbarrel that is not found in PSD-95 PDZ3. However, the secondary structures that are shared between the two are very similar in size and positioning.

A program which uses only geometric criteria derived from the atomic coordinates was used to identify possible peptide binding cavities on the surface of hDlg PDZ3 (Morais Cabral et al., 1996). Only one groove that would be large enough to accommodate a ligand was identified. This groove corresponds to the peptide binding groove identified by Doyle et al. (1996). The binding pocket is made up of residues from β2, α2 and the β1β2 loop at the end of the groove. A partially buried arginine was also identified in the conserved hydrophobic pocket. This arginine was also found to be important for PSD-95 PDZ3 and is reminiscent of the buried arginine found in the hydrophobic phosphotyrosine binding pocket of SH2 domains (Morais Cabral et al., 1996). A peptide of Thr-Asp-Val-COOH was modeled in the predicted peptide binding groove. The interaction predicted closely resembled the peptide binding seen in PSD-95 PDZ3. An alignment of several PDZ domains with hDlg PDZ3 combined with superposition of secondary structural elements shows that most insertions and deletions found in other PDZ domains are restricted to the loop regions.

Independent determinations of crystal structure of two related PDZ domains generated very similar structure models. Both models provide the same explanation for the unique interaction of PDZ domains with carboxy terminal amino acids. Both PDZ domains studied fit into the class I specificity group described by Songyang et al. (1997). Within each of the two classes of PDZ domains, sequence identity is around 60-70%. Between class I and class II PDZ domains, however, sequence identity is as low as 20% and may call into question the structural conservation between the two classes of domains.

For this reason, the crystal structure of the CASK PDZ domain was determined (Daniels et al., 1998). CASK was identified in rat as a protein that interacts with the intracellular domain of neurexins, extracellular matrix binding proteins (Hata et al., 1996). CASK has a PDZ domain, a type II calmodulin kinase domain (CaMKII), an SH3 domain and a guanylate kinase (GuK) domain. It is the mammalian homologue of the *C. elegans lin-2* gene product, which is involved in Let-23 localization in epithelial cells (Hoskins et al., 1996; Kaech et al., 1998). The human CASK protein has been found to interact with both syndecans, a family of heparan sulfate proteoglycans, and protein 4.1, an actin/spectrin binding protein (Daniels et al., 1998). The CASK PDZ domain was classified as a class II PDZ domain by examining the carboxy terminal sequences of these known CASK binding partners.

Crystallization of the CASK PDZ domain revealed the presence of six βstrands and two αhelices in very similar organization to the PSD-95 PDZ3 structure (Daniels et al., 1998). Despite the sequence differences in the carboxylate binding loop (Phe-Met-Gly-Ile versus Gly-Leu-Gly-Phe) the structure of the loop and the pattern of hydrogen bonding was the same in the CASK PDZ domain as was seen in the third PDZ domain of PSD-95. The important differences in sequence between the class I and class II domains are in residues involved in ligand binding. In class II PDZ domains, the residue corresponding to Met507 in the βBβC loop is often a serine or hydrophobic residue whereas class I PDZ domains have a glycine in this position. A valine is present in all three class II PDZ domains examined at the position corresponding to Val549 in the αB helix, however class I PDZ domains have a polar residue, for example histidine or arginine, in this position (Fig. 1-3). The position of Leu552 is conserved as a hydrophobic residue in both class I and II domains. This comparison of critical residues corresponds to the criteria originally used to classify PDZ domains (Songyang et al., 1997). Despite low sequence identity between the two classes of PDZ domains, we see highly conserved structure and binding mechanisms.

1.4 PDZ DOMAIN HOMO- AND HETERO-DIMERIZATION

One aspect of PDZ domains that is not explained by these structural descriptions is the ability of some PDZ domains to bind other PDZ domains or to bind internal targets. With the previously

described restrictions on peptide binding, how do PDZ-PDZ interactions occur? Is it possible that a domain and an internal sequence interact in the same binding groove? Or is there another binding face on the domain for these types of interactions? There are not yet any publications describing the interaction between a PDZ domain and an internal region from a non-PDZ domain containing protein, however, a PDZ heterodimer has been studied.

The PDZ domain of neuronal nitric oxide synthase (nNOS) interacts with the PDZ domains from both PSD-95 (PDZ2) and α1-syntrophin (Brenman et al., 1996; Brenman et al., 1996). The full PDZ domain of each protein is required for both nNOS interactions. In addition, thirty residues carboxy terminal to the nNOS PDZ domain are also required (Brenman et al., 1996). It is now known that these interactions are relevant to nNOS function *in vivo* (Aoki et al., 1993; Brenman et al., 1995; Kameya et al., 1999). The region of nNOS involved in PDZ-PDZ interactions (amino acids 1-130) was used to determine the crystal structure alone and in complex with the α1-syntrophin PDZ domain (Hillier et al., 1999).

The structure of the nNOS region alone revealed a polarized structure whereby residues 1-100 formed a conventional PDZ domain as seen in other crystal structures and the final thirty residues formed a conformationally constrained βfinger on the opposite face of the protein with respect to the conventional ligand binding face (Hillier et al., 1999; Tochio et al., 1999). In the co-crystal of the α1-syntrophin PDZ domain with nNOS (1-130) (Fig. 1-5), the βfinger acted as a ligand in the α1-syntrophin peptide binding groove (Hillier et al., 1999). The first strand of the βfinger acts as a pseudo-peptide motif that mimics peptide binding in its sequence specific interactions. The sequence Leu-Glu-Thr-Thr-Phe in the first strand of the βfinger interacted with residues in βB and αB in a manner similar to that seen in the PSD-95-peptide co-crystal. Rather than having a free carboxylate group anchored by the Gly-Leu-Gly-Phe motif, a sharp βturn occurred at the tip of the βfinger. The heterodimer, therefore, does not adopt the normal two-fold rotational symmetry seen in other dimer structures but binds in a linear head-to-tail fashion due to the polarized structure of nNOS residues 1-130.

The entire PDZ domain including the carboxy-terminal thirty residues of nNOS are thus required for interaction with α1-syntrophin because of the extensive interactions that occur between the βfinger and the canonical nNOS PDZ domain in order to achieve proper conformational stability (Hillier et al., 1999). This heterodimerization buries twice as much of the surface of α1-syntrophin as is buried in conventional peptide binding. The residues in α1-syntrophin that are important for the tertiary interactions with nNOS are conserved between α1-syntrophin and PSD-95 PDZ2.

The head-to-tail arrangement of this PDZ heterodimerization may confer several unique characteristics to PDZ domain containing proteins (Hillier et al., 1999). This may be the mechanism by which subcellular localization of the catalytic domain of nNOS occurs while also adding a new receptor site for alternate proteins. Alternatively, this type of interaction may permit oligomerization of these and other PDZ domain containing proteins. Finally, branching interactions may be possible in multiple PDZ domain-containing proteins allowing recruitment of a wide variety of signaling molecules to a given complex.

The structure determination suggests that the interactions between nNOS (1-130) and PSD-95 PDZ2 or PSD-93 PDZ2 may occur in a similar manner. In fact, biochemical studies of the nNOS-PSD-95 and nNOS-PSD-93 interactions support this prediction (Christopherson et al., 1999). However, there are biochemical results which contradict the model whereby the nNOS PDZ domain could simultaneously interact with target peptides and other PDZ domains (Jaffrey et al., 1998). It is presently difficult to reconcile the results provided by these two groups. Structural evidence is very convincing, however these experiments are performed with a protein or proteins in isolation from the *in vivo* setting which may cause perturbations from the norm. On the other hand, biochemical experiments can conceal some aspects of the interaction that we do not yet understand since we often adopt the simplest mechanism by which we can describe the observed results. Further structural and biochemical experiments need to be performed to clarify the mechanisms of these interactions.

1.5 FUNCTION OF PDZ DOMAIN-CONTAINING PROTEINS

1.5.1 INAD in the Drosophila photoreceptor 'signalplex'

INAD is a multi-PDZ domain-containing protein that plays an important role in the Drosophila visual system (Fig. 1-6). Chemical mutagenesis was used to generate mutant strains of Drosophila which were characterized using electroretinogram (ERG) measurements (Pak and Pinto, 1976). The mutant strains were characterized as having either an abnormal light coincident receptor potential (LCRP) or an abnormal prolonged depolarization afterpotential (PDA). Mutants with defects in LCRP were characterized as no receptor potential A (*norpA*), slow receptor potential A (*slrpA*) or transient receptor potential A (*trpA*). Strains with PDA defects were described as either inactivation-no-afterpotential (*ina*) or no-inactivation-no-afterpotential (*nina*) mutations; within each type of PDA mutant, several complementation groups were defined. Four of the gene products mutated in these strains are now known to interact directly via protein-protein interactions. They are *norpA*, which encodes a phospholipase (PLCβ) (Bloomquist et al., 1988), *trp*, which encodes a store-operated Ca^{++} channel (Montell and Rubin, 1989), *inaC*, which encodes an eye-specific protein kinase C (eye-PKC) (Smith et al., 1991) and *inaD*, which encodes a 5 PDZ domain containing protein (Shieh and Niemeyer, 1995). Many studies have examined the mutant strains and characterized the role of the individual gene products in phototransduction (Chevesich et al., 1997; Huber et al., 1996; Huber et al., 1996; Shieh and Zhu, 1996). The mechanism by which these four genes are connected was not clear until the identification of the PDZ domain (Kim et al., 1995; Kornau et al., 1995) and, specifically, the presence of five such domains in the *inaD* gene product (Tsunoda et al., 1997).

INAD acts as a scaffold and this role in the transduction of the light activated signal in the Drosophila eye was demonstrated by a combination of *in vitro* interactions, *in vivo* colocalization and physiological assays (Tsunoda et al., 1997). INAD is an integral molecule in the formation of a complex that contains most of the proteins involved in photoreceptor signal transduction. TRP, PLCβ and eye-PKC have been shown to interact with INAD in both immunoprecipitation and *in vitro* binding assays in Drosophila head extracts. However, neither Gqα nor rhodopsin have been detected in the INAD immunocomplex despite their high concentrations in photoreceptor cells. GST fusion proteins of the individual PDZ domains showed that each

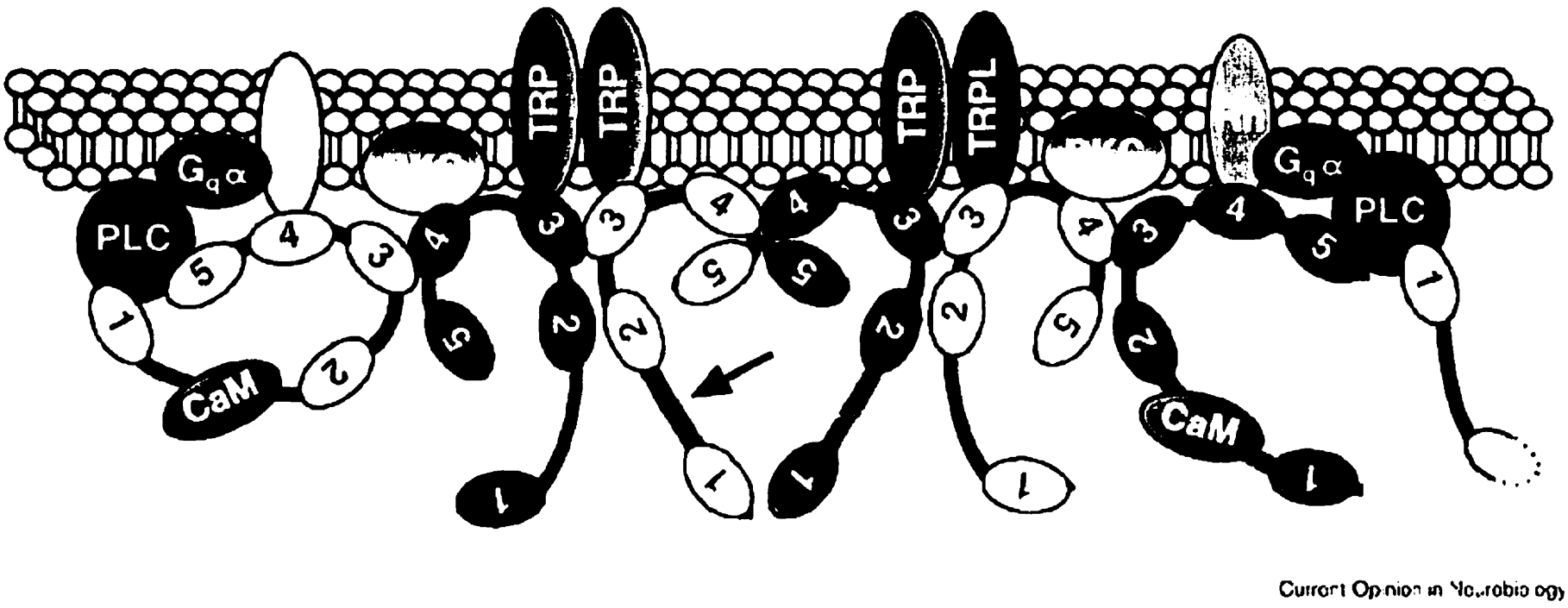

Fig. 1-6. Model of 'signalplex' in Drosophila rhabdomere nucelated by INAD from Montell, 1998. The arrow indicates one of the INAD molecules; PDZ domains of INAD labelled 1-5; PLC - phospholipase Cβ; Gqα - large G protein; CaM - calmodulin; Rh - rhodopsin; PKC - eye-specific protein kinase C; TRP and TRPL - store-operated Ca^{++} channels.

domain had a preferred target protein; PDZ3 bound most strongly to TRP, PDZ4 preferred eye-PKC and PDZ5 bound PLCβ. These interactions were shown to be independent of one another because INAD bound the remaining two proteins when the third was absent in each of the three mutant strains: *norpA, trp* and *inaC*. As well, the $inaD^{215}$ mutant gene was isolated and sequenced; this revealed a Met442Lys substitution in PDZ3.

Two additional *inaD* mutant strains were generated in order to better characterize the phototransduction cascade (Tsunoda et al., 1997). The $inaD^{1}$ mutation generated a premature stop codon so that translation ends at residue 270, halfway into PDZ2. The $inaD^{2}$ allele caused a Gly605Glu mutation in PDZ5 and showed decreased expression levels of INAD. Examination of the Drosophila rhabdomeres of all three INAD mutant strains showed mislocalization of specific interacting molecules, changes in protein levels and altered ERG phenotypes (Tsunoda et al., 1997). As would be expected from the biochemical studies, TRP, PLCβ and eye-PKC were all affected in the $inaD^{1}$ strain whereas only PLCβ and TRP were affected in the $inaD^{2}$ and $inaD^{215}$ strains, respectively.

From the results obtained above, it was proposed that a complex, called a 'transducisome', exists within the rhabdomere of the Drosophila photoreceptor cell. This complex is responsible for anchoring many of the proteins involved in light-dependent signal transduction cascades and explains the remarkable sensitivity and specificity of signal transduction in photoreceptor cells. The temporal resolution of signal transduction in photoreceptor cells is excellent. This cascade is the fastest known G protein coupled cascade to date: it takes only 20ms to go from light incidence to receptor depolarization and approximately 100ms to restore membrane polarity after the signal is terminated. It is predicted that this type of 'transducisome' mechanism may also be used in other types of cells. By controlling the recruitment of different signaling molecules into a variety of transduction complexes, the cell optimizes its responses to many extracellular signals.

This model has been subsequently extended by Xu et al. (1998). Using techniques with increased sensitivity (relative to those used by Tsunoda et al., 1997), direct interaction of INAD with rhodopsin, TRPL, eye-PKC and calmodulin was demonstrated. The results indicate that

many different types of molecules are able to bind the same PDZ domains and each target protein is able to bind to more than one PDZ domain. Thus, it is not possible for one molecule of INAD to nucleate the entire phototransduction signaling cascade, suggesting that INAD may homomultimerize. The self-association of INAD through PDZ3 or PDZ4 was observed via cotransfection and affinity chromatography.

Interestingly, differences in binding ability were seen between a construct encoding just PDZ3 and one encoding PDZ3 plus 28 carboxy terminal residues (PDZ3L) (Xu et al., 1998). Each result described can be reconciled to the structural description of PDZ-PDZ interactions described above (Hillier et al., 1999). In each instance where homomultimerization was seen, at least one of the constructs utilized contained the PDZ3L region, which is consistent with the possible existence of βfinger between PDZ3 and PDZ4 of INAD.

The authors propose that INAD, via its PDZ-peptide and PDZ-PDZ interactions, nucleates a 'signalplex', defined as an extended network of INAD homomultimers to which more than five targets bind (Fig. 1-6) (Xu et al., 1998). In addition, molecules such as rhodopsin and TRPL may interact with the signalplex reversibly. The dynamic association of some of the phototransduction cascade proteins may be regulated by two proposed mechanisms (Montell, 1998). First, light dependent Ca^{++} influx may induce a conformational change in INAD that allows reversible association with certain target molecules. The second possibility is that light-dependent phosphorylation of rhodopsin or TRPL regulates their interaction with INAD. The signalplex may serve two functions that are not mutually exclusive (Montell, 1998). It may play a role in activation of the cascade by creating a localized high concentration of critical second messengers (Ca^{++}, IP_3, DAG). It may also be important for the negative feedback regulation mediated by the light- dependent rise in Ca^{++}.

Many aspects of the visual phototransduction signal cascade remain to be understood. However, the large body of knowledge of the proteins involved and the available physiological assays permit further study and better understanding of this pathway. These results may relate to other

multi-PDZ domain-containing proteins within different signaling systems and their mechanisms of action. Thus, the signalplex may also be employed in other signal transduction pathways.

1.5.2 Function of PAR-3 in asymmetric cell division during C. elegans development

The process by which a zygote consisting of one cell becomes a multicellular organism is a complex pathway of cell division and cell fate determination. The asymmetric division of cells into two distinct daughter cells is critical to the generation of cell diversity during development (Horvitz and Herskowitz, 1992). Asymmetric cell division can be due to extrinsic or intrinsic factors. Extrinsic cues for asymmetric cell division include cell signaling between sibling cells after division and/or signaling from other cells. Intrinsic cues include the asymmetric localization of determinants within the two sibling cells and/or the division of the mother cell along an asymmetric plane creating sibling cells of different size. In order to distribute intrinsic cell fate determinants differently to two sibling cells, two events must be coordinated. First, the cell fate determinant must asymmetrically localize within the mother cell and second, the division plane must align along the axis of asymmetry (Rhyu and Knoblich, 1995).

Both of these events are observed during early embryonic cleavages in *C. elegans* development (Guo and Kemphues, 1996) (Fig. 1-7). P granules, which are cytoplasmic inclusions, are asymmetrically distributed and specifically retained in the germline blastomeres during four cell division events early in development. The mechanism of asymmetric distribution of the cytoplasmic determinants has been studied with strains of *C. elegans* with partitioning defects (*par*) (Kemphues et al., 1988). Six genes were identified which disrupt the size of the daughter cells, division timing, spindle orientation or molecular composition of the first cell division. These genes were classified into two groups. Group I genes, which include *par-1* and *par-4*, have a severe effect on cytoplasmic localization of determinants, but a mild effect on spindle orientation. Group II genes, *par-2*, *par-3*, *par-5* and *par-6*, have a severe effect on spindle orientation but less severe effect on cytoplasmic localization. *par-1* encodes a putative serine/threonine kinase and *par-2* contains a putative ATP-binding site and a RING finger domain. Current models for the roles of these two proteins will not be discussed except in relation to *par-3*.

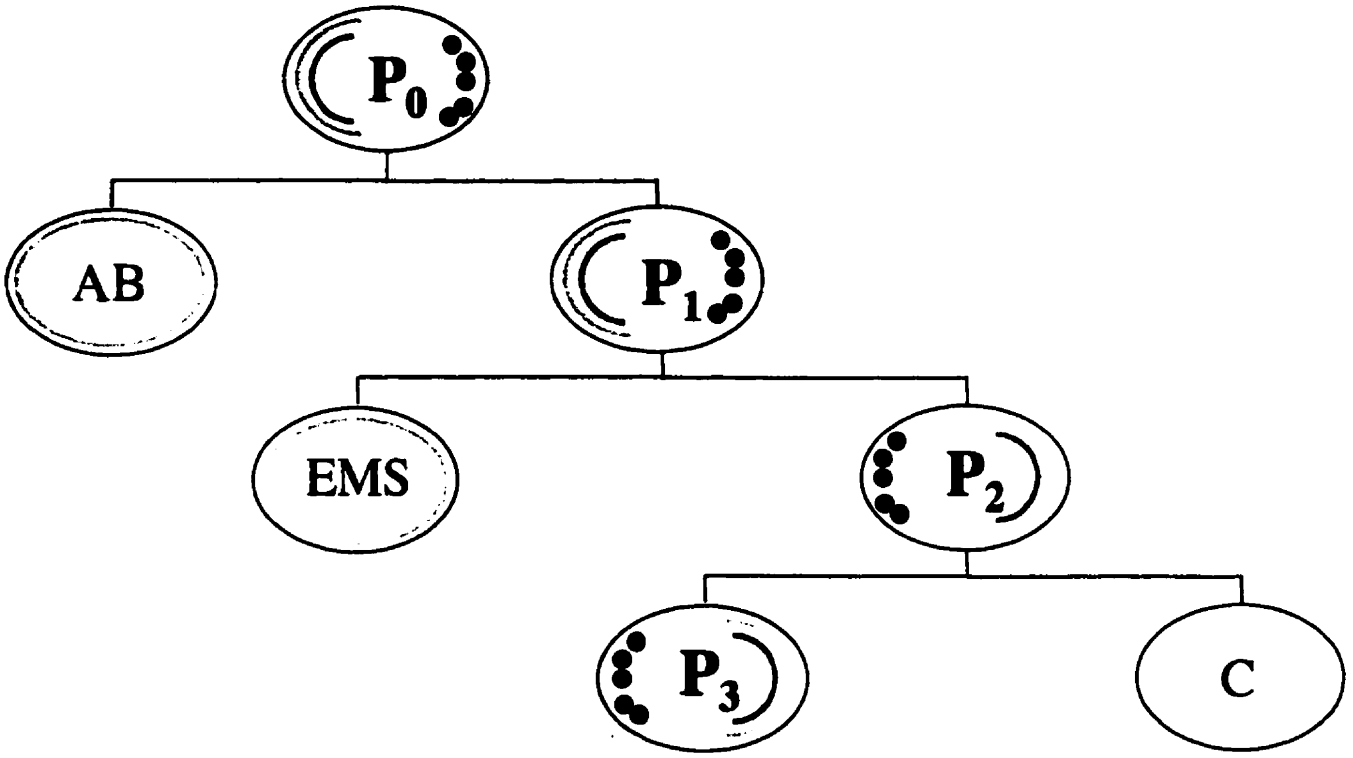

Fig. 1-7. Schematic diagram of asymmetric cleavages during early stages of *C. elegans* development. P granules (black dots) are retained in germline (P) daughter cell at each stage. PAR-3 (orange) and PAR-6 (purple) are asymmetrically localized to posterior periphery during division. PAR-3 is located throughout the periphery of somatic daughter cells (AB, EMS and C).

The *par-3* gene was isolated and extensively characterized with respect to PAR-3 localization in wild-type and *par* strains (Etemad-Moghadam et al., 1995). The predicted 138 kDa protein contains three PDZ domains and several proline-rich regions similar to those seen in ZO-1 and ZO-2, two other PDZ domain containing proteins. Maternal expression of *par-3* is required for establishment of the anterior-posterior (A-P) polarity and control of the cleavage pattern in early embryos. The asymmetric localization of PAR-3 to the anterior periphery of the embryo depends on PAR-2 but not PAR-1 nor PAR-4. Indeed, PAR-2 posterior localization prior to the first cleavage of the embryo is dependent on PAR-3, indicating an interdependency of these two proteins for localization and function. PAR-1 and P granule asymmetric distribution to the periphery of the posterior pole of the embryo also depend on the presence of PAR-3.

The localization of PAR-3 to the anterior pole of dividing germline blastomeres results in the inheritance of a large proportion of PAR-3 by the somatic cell lineage (Etemad-Moghadam et al., 1995). PAR-3 is not asymmetrically localized in somatic cells but is distributed evenly throughout the periphery. PAR-3 is also present in the P lineage and is asymmetrically localized in the germline blastomeres. This asymmetric distribution appears to restrict the localization of PAR-1 and PAR-2 to the posterior pole. It has also been observed that PAR-3 independently requires functional *par-5* and *par-6* for proper peripheral distribution (Guo and Kemphues, 1996).

There are several similarities in the observed disruptions of embryonic asymmetries in *par-3* and *par-6* mutant *C. elegans* strains (Watts et al., 1996). Study of *par-6* and its gene product revealed that 1) it is required for stable peripheral localization of both PAR-3 and PKC-3, 2) it contains one PDZ domain and 3) it has an overall expression pattern during early embryo cleavages that resembles that of PAR-3. PAR-3 and PAR-6 were shown to be interdependent for correct anterior peripheral localization.

A mammalian homologue of PAR-3, called ASIP, was identified in an expression library screen with an atypical protein kinase C, PKCζ (Izumi et al., 1998). ASIP contains three PDZ domains and an atypical PKC (aPKC; includes PKCζ and PKCλ) binding site. It has three regions of high

similarity to the *C. elegans* cell polarity determinant, PAR-3. Conserved region 1 (CR1) is located in the amino terminal portions of ASIP and PAR-3, CR2 is comprised of the three PDZ domains and CR3 is located within the aPKC-binding site. Co-localization of ASIP and PKCλ in polarized MDCK II cells grown to confluence in culture was shown to be restricted to tight junctions, consistent with a role for ASIP in establishing and/or maintaining cell polarity. This work also led to the isolation of a *C. elegans* aPKC homologue, PKC-3 (Tabuse et al., 1998). Tabuse et al. (1998) showed that PKC-3 is required for establishing embryonic polarity, is localized to the anterior periphery of the *C. elegans* embryo and that PKC-3 and PAR-3 are mutually required for asymmetric distribution. It is possible that an interdependent ternary complex of PAR-3, PAR-6 and PKC-3 could encode the intracellular signal for the establishment of polarity (Tabuse et al., 1998). It has now been demonstrated that the interaction between PAR-3/ASIP and aPKC is conserved across species (Izumi et al., 1998).

Coincident with these publications describing mammalian *par-3* homologues was the identification of a Drosophila *par-3* homologue, called *bazooka* (Kuchinke et al., 1998). The *bazooka* mutation of Drosophila was identified in a screen for mutant strains exhibiting patterning defects (Wieschaus et al., 1984) and was later shown to control epithelial cell polarity in the Drosophila embryo (Muller and Wieschaus, 1996). The *bazooka* gene was cloned and its product was shown to be homologous to PAR-3 (Kuchinke et al., 1998). Examination of the effect of the *bazooka* mutation in neuroblast differentiation reveals that the *bazooka* gene product plays a role in orienting the axis of intrinsic apico-basal polarity of the cell with respect to the A-P axis of the embryo. However the absence of BAZOOKA does not severely effect central nervous system (CNS) development. Thus the Drosophila *par-3* homologue *bazooka* is similarly involved in polarity cues integral to cleavage patterns in the early embryo.

The examples discussed above describe the function of multi-PDZ proteins in cell signaling and development. We have utilized these examples in trying to understand the function of LNX, the novel multi-PDZ protein that is the subject of the work in this thesis.

1.6 THE INTRINSIC CELL-FATE DETERMINANT, NUMB

Another well-studied example of an intrinsic cell fate determinant is Drosophila *numb* (dNb). *numb* was originally described as a mutation affecting the sensory organ precursor (SOP) lineage in the peripheral nervous system (PNS) and specific neurons in the central nervous system (CNS) (Uemura et al., 1989). dNb is a membrane-associated protein that is asymmetrically localized during cell divisions giving rise to distinct daughter cell fates (Knoblich et al., 1995; Rhyu et al., 1994; Spana and Doe, 1996; Spana et al., 1995; Vervoort et al., 1997). The segregation of dNb to one of two daughter cells during asymmetric cell division is thought to be responsible for the inhibition of signaling from the transmembrane receptor, Notch (Guo et al., 1996; Spana and Doe, 1996).

Mammalian homologues of *numb* have been isolated and characterized (Verdi et al., 1996; Zhong et al., 1996; Zhong et al., 1997). mNb is functional when expressed in Drosophila demonstrating functional conservation across species (Verdi et al., 1996; Zhong et al., 1996). mNb has been shown to asymmetrically localize during specific cell divisions in the developing cortical plate of the mouse embryo suggesting that it has a role in mammalian neurogenesis (Zhong et al., 1996). A chicken homologue of Nb has also been identified and shown to be asymmetrically localized in neuroepithelial cells (Wakamatsu et al., 1999). Chicken Nb is also able to inhibit the repression of neuronal differentiation by chicken Notch. This suggests that mammalian Nb functions in a similar manner to dNb. However, since mNb is expressed in most adult mouse tissues, it is likely that Nb also has other functions.

It is now known that there are four isoforms of mNb (Dho et al., 1999) and hNb (Verdi et al., 1999) as well as a separate gene encoding another *numb* related protein called Numb-like (Nbl) (Zhong et al., 1997). The differential expression patterns of these five mammalian Numb proteins suggests that each has a distinct function in the cells in which it is expressed. The four mNb isoforms differ by either the presence or absence of two small inserts. The first insert is in the amino terminal PTB domain and consists of 11 amino acids. This insert is thought to mediate the plasma membrane localization of the mNb isoforms in which it is found (Dho et al., 1999). The second insert is 49 amino acids and is found in the carboxy terminal proline rich region. This Nb

isoforms which contain the insert appear to be involved in cell proliferation rather than differentiation (Dho et al., 1999; Verdi et al., 1999).

Studies of the function of mammalian Nb are ongoing in our laboratory. Gene targeted and transgenic mice which overexpress Nb are being generated and characterized. The putative interactions of Nb with Notch and a novel kinase domain-containing molecule are also being investigated.

1.7 LNX, A NOVEL PDZ-DOMAIN CONTAINING PROTEIN

In order to identify protein targets of the mammalian Numb (mNb) PTB domain, a yeast two-hybrid screen was performed (Dho et al., 1998). The kinase domain of the platelet-derived growth factor receptor was co-expressed in the yeast during the library screen (Lioubin et al., 1996). This permitted phosphorylation of any potential tyrosine phosphorylation sites in the library fusion proteins since PTB interactions were predicted to require phosphotyrosine for target recognition (Kavanaugh and Williams, 1994). Seven of ten isolated clones were overlapping sequence of the same protein that we have termed LNX (ligand of Numb, protein X). The largest cDNA (2.5 kb) was used to screen a 16.5-day mouse embryo cDNA library to isolate the full-length cDNA and a protein of 728 residues was predicted from the 2.8 kb cDNA that was isolated (referred to as LNX long). Conceptual translation of the cDNA revealed five conserved domains, an amino-terminal RING finger domain followed by four PDZ domains (Fig. 1-8). A peptide sequence containing a possible PTB recognition site (LDNPAY) was identified between the RING finger and the first PDZ domain.

Northern blot analysis of adult mouse tissues for LNX expression revealed two major bands of 2.6 and 2.8 kb. The 2.6 kb band was detected only in heart and brain while the 2.8 kb band was present in heart, lung, skeletal muscle and kidney. The presence of the two bands indicated that another isoform of LNX may exist. The 2.5 kb partial cDNA of LNX, originally isolated from the yeast two-hybrid screen, was used to screen a mouse brain cDNA library to search for the other isoform. A smaller LNX cDNA was isolated that encoded a 628 residue protein referred to as LNX short. This protein contained an amino terminal sequence that is distinct from LNX long,

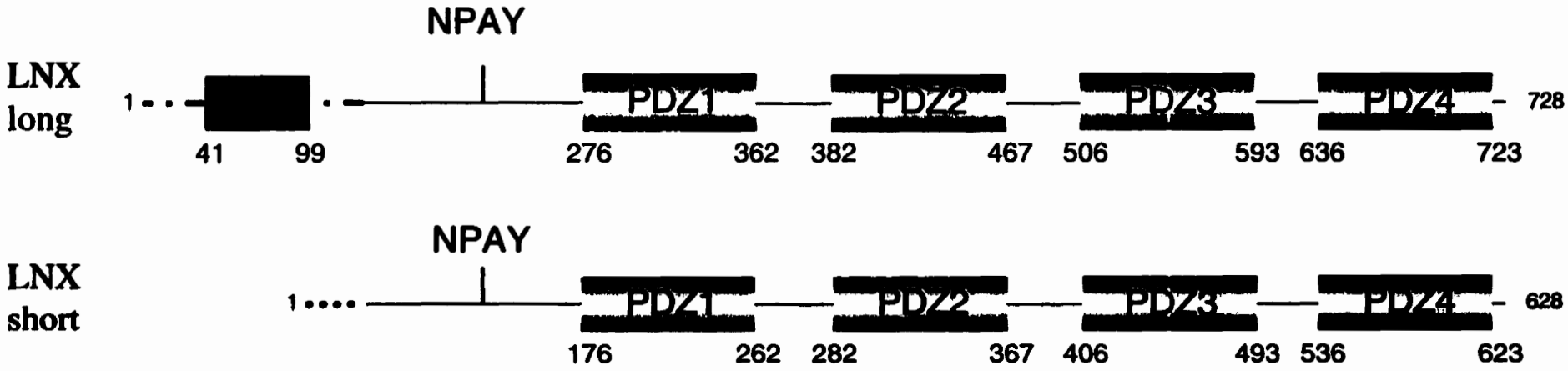

Fig. 1-8. Protein-protein interaction motifs in the two isoforms of LNX, LNX long and LNX short. The amino acid sequence is identical between the two isoforms from residue 132 of LNX long to the carboxy terminus.

but it is identical to LNX long from residue 132 of LNX long (residue 32 of LNX short) to the end. To confirm that the two isoforms of LNX represented the two major bands seen in the northern, the same northern blot was hybridized with the cDNA encoding only the RING finger domain of LNX long. Bands of 2.8 kb were observed in heart, lung, skeletal muscle and kidney. This suggests that the shorter cDNA encodes a LNX isoform that lacks the RING finger domain and has an unique expression pattern from LNX long.

In vitro interaction between LNX and the Numb PTB domains was confirmed through two separate techniques (Dho et al., 1998). Cell lysates from LNX long transfected 293T cells were incubated with various GST PTB fusion proteins. The PTB domains from mNb, mNbl and dNb precipitated LNX. It has now been shown that both PTB isoforms of mNb are able to interact with LNX (Dho et al., 1999). In addition, overlay assays were performed to demonstrate direct interaction between mNb PTB and dNb PTB with hemagglutinin (HA) tagged LNX long.

Several GST fusion proteins encoding various regions of LNX were used to elucidate the region of LNX which interacts with mNb (Dho et al., 1998). The fusion protein that included the NPAY sequence located between the RING finger and PDZ1, called RING/NPAY, precipitated mNb from A431 cell lysates. However, the fusion protein containing PDZ1 and part of PDZ2 interacted weakly with Nb. At the time it was thought that this interaction was non-specific, however, it has since been recognized that the mNb carboxy terminal amino acids resemble a PDZ recognition site (-SSDLQKTFEIEL*) and it is possible that mNb bound to this part of LNX via its carboxy-terminal tail. However we have subsequently shown that it is unlikely that this occurs (see Chapter 3 *Section 3.3.1*).

The mNb binding site in LNX was mapped using several techniques (Dho et al., 1998). Mutations in either the sequence in LNX predicted to be recognized by mNb or in the mNb PTB domain were generated. These results demonstrated that the mNb PTB domain recognizes the LNX 'LDNPAY' peptide sequence independent of tyrosine phosphorylation. As well, the leucine (L), asparagine (N) and tyrosine (Y) were shown to be critical for recognition by mNb. These experiments characterize the novel protein LNX and its interaction with Nb in mammalian cells.

The interaction is specifically demonstrated to occur between the PTB domain of Nb and the NPAY motif found in both LNX long and LNX short. The function of the interaction between LNX and Nb in mammalian cells is unknown.

The arrangement of protein-protein interaction domains in LNX lends itself to a role in protein complex scaffolding This scaffolding may be a mechanism by which LNX plays a role in the function of Numb in cell-fate signals or in directing its asymmetric localization. In order to characterize the role of LNX in signal transduction and in relation to Numb function, it is important to characterize the LNX protein and identify LNX PDZ binding partners. The goal of this thesis work was to perform a yeast two-hybrid screen to identify molecules that interact with LNX. The interactions between LNX PDZ domains and their target molecules were characterized using BiaCore analysis and *in vitro* binding experiments. In addition, endogenous LNX short protein was isolated using immunoaffinity and *in vitro* affinity purification employing recombinant proteins identified in the yeast two-hybrid screen.

All of the results presented in chapters two and three were generated by myself. The BiaCore analysis in figures 3-2, 3-3 and 3-4 were generated with the assistance of Denis Bouchard. The deletion mutant analysis in figure 2-13 and the *in vitro* mixing experiment in figure 3-5 were generated with the assistance of Matt Dermer.

Chapter II Identification of molecules which interact with LNX via the yeast two-hybrid screen

2.1 RATIONALE

There are many methods for detecting protein-protein interactions. Biochemical methods involve studying the interacting proteins directly from cell or tissue lysates. Library-based methods allow expression and interaction of proteins followed by isolation of the DNA encoding a protein of interest. One of our primary objectives was to identify proteins that interact with LNX; we therefore compared the available methods for identifying protein-protein interactions.

Biochemical techniques that can be used to identify protein-protein interactions include affinity chromatography, affinity blotting ("far western"), immunoprecipitation or chemical cross-linking. Some of these methods allow for greater sensitivity so that weak or transient interactions can be detected; others occur in a native or near-native environment, meaning that biological relevance of the interaction can be immediately established. However, it is often more labor-intensive to identify the proteins with which the protein of interest is interacting. Using these methods to detect protein-protein interactions, the protein of interest is selected and purified. Identification of interacting proteins could occur either by directly sequencing the protein (e.g., Edman degradation, mass spectrometry) or by generating antibodies against the protein then using the antibodies to screen an expression library to isolate the gene. Biochemical methods were not appropriate for our purposes, as we had not yet isolated endogenous LNX protein.

Several library-based methods for detecting protein-protein interactions are available and widely used. Library-based screens permit the gene encoding the interacting protein to be easily isolated and are performed in organisms with rapid doubling times to allow screening to occur rapidly. Thus, a library-based screen would be most appropriate for this study. Several library-based screening methods are compared below.

Expression libraries are cDNA libraries that package into phagemids and can inject their DNA into bacterial cells. The bacteria are then induced to express the protein encoded by the cDNA

and the proteins are immobilized. A labeled protein or peptide can then be used as a probe with the immobilized library proteins to allow interaction to occur. This method permits ease of preparation of a probe (either fusion protein or chemically synthesized peptide) and manipulations of the probe *in vitro* if post-translational modifications are necessary. However, the proteins encoded by the library must fold within the bacterial cells, which may result in incorrect conformation. The proteins expressed in the bacterial cells must then bind to a nitrocellulose filter and retain their conformation under these conditions. The interaction between the library encoded protein and the protein or peptide used as a probe occurs completely *in vitro* and the investigator arbitrarily imposes the conditions for interaction. Although this allows variation in the detection level of an interaction, these conditions may or may not reflect the intracellular situation. As well, the library-encoded proteins cannot undergo most eukaryotic post-translational modifications inside *E. coli*. The interaction in an expression library screen between the probe and the immobilized protein is not amplified as greatly as in the other library-based systems which causes decreased sensitivity in the screen.

Phage display can also be used for identifying protein-protein interactions. In this method, the size of the library-encoded proteins is limited as they are expressed as a fusion to a phage coat protein. Again, the protein must fold within the bacterial cell and must also in this case be secreted by *E. coli* to allow exposure to the protein probe. Interactions that occur are enriched by panning giving this assay high sensitivity.

A method called 'peptides-on-plasmids' is another library based screening method (Schatz et al., 1996). In this case, libraries of random peptides are fused to the carboxy terminus of the Lac repressor protein (LacI). Within the bacterial cell, LacI will recognize a LacI binding site (*LacO*) present on the same plasmid containing the gene that encodes the LacI fusion protein. The bacterial cells are lysed and panning of the lysate over immobilized probe allows peptides with which the probe can interact to be enriched. Each peptide that binds the protein probe carries along with it the plasmid that encodes it. The plasmid is then eluted from the interaction complex for isolation and sequencing. This is a very sensitive and unique assay that has been shown to work well for PDZ domain containing proteins (Stricker et al., 1997; van Huizen et al., 1998).

The random peptides generated may not occur *in vivo* yet they may be used to predict a consensus recognition sequence.

The yeast two-hybrid system developed by Fields and Song (1989), exploits the modular nature of transcriptional activation (Fig 2-1). There are two functions in initiation of transcription: DNA-binding for site-specific recognition and transcriptional activation. Two separate domains in the yeast GAL4 transcriptional activation protein, that is, the DNA binding domain (DBD) and the activation domain (AD), supply these two functions. These two domains can be physically separated into two proteins and when brought in close proximity, are able to act as the native transcriptional activator. Alternative DNA binding domains from other transcription activation proteins (e.g. LexA, large T antigen) have also been used successfully in combination with the GAL4 activation domain.

In the yeast two-hybrid system, the cDNA encoding the protein of interest is fused to the cDNA of a DBD, in our case LexA, in a vector which drives the expression of the fusion protein in the yeast cells (Fig. 2-1). A library of cDNAs which have been fused to the GAL4 AD cDNA are co-expressed in the yeast cells. This allows interactions to occur between the protein of interest and an unknown protein encoded by a library cDNA. The protein-protein interaction is detected when the reconstituted transcriptional activator specifically initiates transcription of reporter genes, for example, *lacZ* and *his3*. The expression of the enzymes encoded by these reporter genes is detected by β–galactosidase activity and restoration of histidine biosynthesis, respectively.

There are several advantages of yeast two-hybrid screening for protein-protein interactions over other library-based methods. The detection of an interaction is very sensitive because protein-protein interactions result in transcription of reporter genes and one interaction can cause many copies of the reporter gene to be transcribed. The two reporter genes employed encode enzymes, which catalyze the conversion of many substrate molecules to product. This serves to further amplify the signal; together this allows detection of weak interactions. It has been estimated that the minimal binding constant required to detect an interaction in this system is 1μM (Phizicky and Fields, 1995). However, this value depends on the level of expression of the hybrid proteins

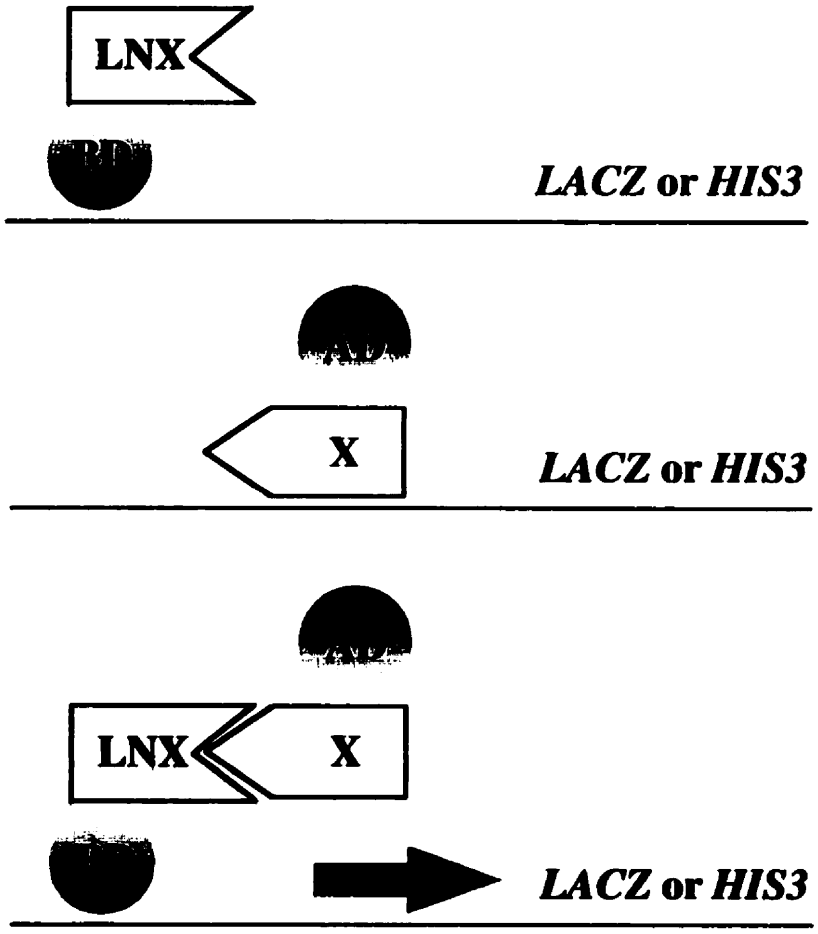

LNX - full length LNX protein
BD - LexA DNA Binding Domain (1-147)

AD - Gal4 Activation Domain (768-881)
X - cDNA hybrid

➡ - transcriptional activation

Fig. 2-1. Schematic diagram of the yeast two-hybrid system. Fusion proteins are coexpressed in yeast cells. If an interaction occurs between LNX and a library-encoded protein, transcription of reporter genes is initiated. Enzyme activity is detected by either β-galactosidase assay or growth in absence of histidine.

and the number, sequence and arrangement of DNA binding sites adjacent to the reporter genes. Although phage display screens provide high sensitivity via panning, the yeast two-hybrid system allows high sensitivity without placing size restrictions. The yeast two-hybrid screen can also detect short-lived (transient) interactions. A protein-protein interaction need not continue to occur once transcription has been initiated. Any transcribed mRNA that has been generated will be translated and active enzyme will be produced whether or not the original interaction is still occurring in the nucleus.

There are also several differences between other library-based screens and the yeast two-hybrid screen with respect to protein expression and interactions. In expression screens, phage display and peptides-on-plasmids, the interactions all occur *in vitro*, i.e., on nitrocellulose filter overlays or in a 96-well plate. A protein-protein interaction in the yeast two-hybrid screen occurs intracellularly which more closely reflects the native environment for interactions. As in bacteria, it is possible for incorrect conformation of the proteins to occur within the yeast. However, yeast is a eukaryotic organism thus somewhat more similar than bacteria to the eukaryotic organisms in which the protein of interest is naturally expressed. Within the yeast cell, more eukaryotic post-translational modifications are possible than in bacteria. Thus the yeast two-hybrid screen provides an environment which better reflects the native setting for a protein-protein interactions.

A final advantage of the yeast two-hybrid screen is that multiple clones encoding overlapping regions of one protein are often isolated which can serve to map the minimal region for interaction directly from an initial screen. As well, deletion or point mutations can easily be made in either hybrid protein for identifying specific sites of interaction between the two proteins.

Thus, the yeast two-hybrid screen was chosen as the appropriate method for identification of the LNX PDZ targets. One disadvantage of this approach was the lack of publications describing the isolation of PDZ target proteins from a yeast two-hybrid screen. However, this method allowed us to rapidly screen with all four PDZ domains of LNX within the intracellular environment and to detect both weak and transient interactions.

2.2 MATERIALS AND METHODS

2.2.1 Subcloning of LNX cDNA into pBTM116

LNX expression constructs were generated by PCR using the mouse cDNA for LNX long. The primers used were as follows. For PDZ1 (amino acids 264-376 of LNX), ACTGT CCCCG AATTC TTCCC AAGG (5') and CATCC CGAGG TCGAC AGGAG TCCG (3'). For PDZ2 (aa 367-478) CGGGA GCAGG AATTC CGTAG C (5') and GCTGA TCCAG TCGAC TTCTT G (3'). For PDZ3 (aa 495-606) GGCCC AGGAG AATTC AACAC AGC (5') and GTGGT TGGAG TCGAC GGCTG C (3'). For PDZ4 (aa 625-728) GGTCC CCATC CGAAT TCATG TGG (5') and CTGTG GTTTG TCGAC GATCC ATC (3'). For the LNX long isoform GTTTC CTGAA TTCTA CACAG C (5') and CTGTG GTTTG TCGAC GATCC ATC (3'). For LNX short isoform, TGG GGA AAT GAA TTC ATT TGC T (5') and CTGTG GTTTG TCGAC GATCC ATC (3'). Some of these same primers were used in different combinations for generating pairs of PDZ domains, e.g., for PDZ1/2 the 5' primer for PDZ1 was used with the 3' primer for PDZ2. The PCR reactions contained 40 picomoles of each primer, 20 ng of full length LNX cDNA, 1x Thermopol buffer (10mM KCl, 20 mM Tris-HCl pH8.8, 10 mM $(NH_4)_2SO_4$, 2 mM $MgSO_4$, 0.1% Triton X-100), 20 picomoles of each deoxynucleotidetriphosphate and 0.5μL Vent DNA polymerase and sterile distilled water was used to bring the total volume to 100μL. The PTC-200 Peltier Thermal Cycler from MJ Research was used with the PCR programs consisting of thirty cycles of 1 min at 95°C, 1 min of annealing at 58-60°C and an extension period (1 min/kilobase) at 72°C. This was followed by an additional extension time (1 min-5 min) at 72°C to allow reactions to go to completion.

To verify production of the correct size fragment of DNA, 10μL of the PCR reaction was separated on a 1.0 to 1.5% agarose gel. The total remaining volume of reactions with the correct size products (90μL each) were combined for precipitation by adding 2.5 volumes of 100% ethanol and 0.1 volumes of 3M sodium acetate. The samples were then put at -20°C for 20 min and centrifuged for 15 min at 12000 rpm. The pellet was washed with 70% ethanol, left to air dry, and resuspended in 16μL of 10mM Tris pH 8.0. To this was added 2μL of SuRE/Cut Buffer H (Boehringer Mannheim, Germany), 1μL EcoRI (10 units) and 1μL SalI (10 units) restriction enzymes. The samples were incubated 2 hours at 37°C to allow digestion of DNA. At the same

time, 5μg of pBTM116 was digested with EcoRI and SalI and dephosphorylated by incubation with 1μL of shrimp alkaline phosphatase (USB) for 30 min at 37°C and processed as follows. Digested vector and PCR product were run on 1.0 to 1.5% agarose gel. The appropriate sized fragment was excised, gel purified using the QiaExII kit (Qiagen) (described below) and quantified by agarose gel electrophoresis. Vector and PCR-generated inserts were ligated using 50-100ng of vector and an appropriate amount of insert to maintain 1:3 ratio of DNA fragment ends of vector:insert. Samples were incubated at 14°C overnight then left at room temperature for 3-4 hours the next day. Addition of 10μL of 10mM Tris pH8.0 to each ligation brought the final volume to 20μL. Transformation of 100μL of competent E. coli (DH5α) with 10μL of ligation mixture was performed as follows. Cells and DNA were incubated together on ice for 20 min and heat-shocked for 90 seconds at 42°C. 400μL of LB was added followed by incubation at 37°C for 30 min. 100μL of this was spread on LB plates containing 100μg/mL ampicillin. Following incubation at 37°C, bacterial colonies were picked and screened for correct ligation product by minipreps (Qiagen) (described below) followed by EcoRI/SalI digestion of 10μL of miniprep DNA and separation on 1.0-1.5% agarose gel. Plasmids containing the correct size of insert were then prepared by maxiprep (Qiagen) as described below then sequenced (Amgen, HSC or York).

To create LexA DBD and GAL4 AD fusions of the LNX RING finger, pBTM116 (created by Paul Bartel and Stan Fields) was digested with EcoRI/XhoI and pADGAL4 was digested with EcoRI/SalI and both were treated with phosphatase. The pGEX-RING construct (Dho et al., 1998) was digested with EcoRI and SalI. The appropriate vector and insert pieces were purified and quantitated and ligation mixtures were prepared as described above. The ligation mixtures were transformed into *E. coli* (DH5α), selected and sequenced as described above. Yeast cotransformations were performed as described in Section *2.2.5*.

The carboxy terminal 14 amino acids of the L61 clone (isolated from the yeast two-hybrid screen with LNX long, see Section *2.2.9*) were removed during PCR amplification. The 5' primer was ATT CGA TGA TGA AGA TAC CCC ACC and the 3' primer was CAG CTT CTC GAG TTC CTA AAT TTG, which created a premature stop codon. The PCR reaction contained the

components described above except the template used was the 20ng of L61 cDNA. Thirty cycles of 95°C for denaturation, 60°C for annealing and 72°C for extension was followed by 2 min at 72°C to allow extension to go to completion. Correct size PCR products were concentrated then PCR product and pBTM116 were EcoRI/XhoI digested. The vector was also phosphatase treated and vector and insert were purified and quantitated as above. Ligation mixtures were prepared as above then transformed, selected and sequenced as above. Yeast cotransformations were performed as described in Section *2.2.5*.

2.2.2 DNA Purification

2.2.2.1 Minipreps

An overnight culture of 2mL LB + 100μg/mL ampicillin was centrifuged to pellet the cells. The pellet was resuspended in 250μL of Buffer P1 (50mM Tris-Cl pH8.0, 10mM EDTA, 100μg/mL RNase A). An equal volume of freshly made Buffer P2 (1% SDS; 0.2M NaOH) was then added and mixed gently. Within 5 min of addition of P2, 500μL of Buffer N3 was added and again mixed gently. The samples were centrifuged 20 min at 13,000 rpm. During this time a vacuum manifold was prepared with an appropriate number of QIAprep 8 strips. The supernatant was added to each column of the strip and a vacuum source applied to allow DNA in solution to bind to the column. The columns were then washed twice with 1mL of Buffer PE with vacuum. The vacuum was left on for five min more after the last wash to dry the membrane. The strips were blotted dry and transferred to collection tubes. The DNA was eluted into the collection tubes with 150μL of 10mM Tris pH8.0.

2.2.2.2 Maxipreps

A culture of 100mL LB+100μg/mL ampicillin was grown overnight at 37°C with shaking. The cells were pelleted by centrifugation for 10 min at 5000 rpm then resuspended in 10mL of buffer P1 (50mM Tris-Cl pH8.0, 10mM EDTA, 100μg/mL RNase A). 10mL freshly made buffer P2 (1% SDS; 0.2M NaOH) was added and the sample was incubated 5 min at room temperature. Then 10mL of buffer P3 (3.0M potassium acetate pH5.5) was added and poured immediately into the barrel of the Qiafilter cartridge. The sample is then incubated 10 min at room temperature to allow separation of phases. During this time, a Qiagen-tip 500 is equilibrated with

10mL of buffer QBT (750mM NaCl, 50mM MOPS pH7.0, 15% isopropanol, 0.15% Triton X-100). The separated sample in the Qiafilter cartridge is then plunged with supplied plunger into an equilibrated Qiagen-tip500 and allowed to enter the column by gravity flow. The column is washed by gravity flow two times with 30mL of buffer QC (1.0M NaCl, 50mM MOPS pH7.0, 15% isopropanol). The DNA bound to the column is then eluted by gravity flow with 15mL buffer QF (1.25M NaCl, 50mM Tris-Cl pH8.5, 15% isopropanol). To the elution, 0.7 volumes of isopropanol was added. The sample was then centrifuged 30 min at 15,000xg. The pellet was then washed with 5mL of 70% ethanol, left to air dry and resuspended in 0.5-1.0mL of 10mM Tris pH8.0. DNA concentration was measured by OD_{280}.

2.2.2.3 Fragment purification

The excised gel slice was weighed in a microcentrifuge tube and 3 volumes of buffer QX1 was added to the gel slice. The QiaExII beads were vortexed and 30µL was added to the microcentrifuge tube. The sample was then incubated at 50°C for 10 min with vortexing every 2 min. The sample was centrifuged for 30 seconds at 12,000 rpm and the beads were resuspended in 500µL buffer QX1 to wash. The washing was repeated two more times except with 500µL of buffer PE. The pellet was air dried for 30 min at room temperature. When the pellet appeared white in colour, the beads were resuspended in 10mM Tris pH8.5. The sample was left for 5 min at room temperature to elute the DNA. The sample was centrifuged to separate the beads from the eluted DNA. DNA was quantitated by electrophoresis and compared to similar molecular weight DNA standards of known concentration.

2.2.3 Media and Plates

Luria-Bertani (LB) broth or plates:

10g bacto-tryptone (Difco), 5g bacto-yeast extract (Difco) and 10g NaCl (Fisher) were dissolved in approximately 800mL of water. The pH was brought to 7.0 and water was added to a volume of 1L and autoclaved. If used for plates, 20g of agar was added per liter before autoclaving. Alternatively, 20g of LB broth base (Sigma) was dissolved in 1L of water and autoclaved.

SD broth or plates:

6.7g of Yeast nitrogen base without amino acids/L (Difco) was dissolved in 860mL of water. For plates 20g agar/L was included. The solution was then autoclaved. Before use of broth or pouring of plates, 100mL of appropriate 10X amino acid dropout media and 40mL of 50% glucose was added.

10X amino acid dropout media:

300mg/L L-isoleucine, 1500mg/L L-valine, 200mg/L L-adenine hemisulfate salt, 200mg/L L-arginine HCl, 200mg/L L-histidine HCl monohydrate, 1000mg/L L-leucine, 200mg/L L-lysine HCl, 200mg/L L-methionine, 500mg/L L-phenylalanine, 2000mg/L L-threonine, 200mg/L L-tryptophan, 300mg/L L-tyrosine and 200mg/L L-uracil were dissolved in 1L of water and filter sterilized. All amino acids were obtained from Sigma. The appropriate component(s) were omitted for the synthetic selection medium desired.

YPD broth:

20g Difco Peptone and 10g Difco yeast extract was dissolved in water and the volume was brought up to 960mL. The solution was autoclaved; before use, 40mL of 50% glucose was added.

M9 plates:

Two separate solutions were made; the first contained 6g of Na_2HPO_4, 3g KH_2PO_4, 0.5g NaCl and 1.0gNH_4Cl in 500 mL of water and the second contained 15g agar in 500 mL of water. These two solutions were autoclaved separately then mixed. Before pouring the plates, the following ingredients were added: 1mL 1M $MgSO_4$, 100µL 1M $CaCl_2$, 4mL 50% glucose, 4mL 0.5mg/mL thiamine and 10mL of 2mg/mL uracil.

2.2.4 Expression of LNX fusion protein in transformed yeast cells

A 15mL culture of the yeast strain L40 (MATa, his3D200, trp1-901, leu2-3,112, ade2, LYS2::$(lexAop)_4$-HIS3 URA3::$(lexAop)_8$-lacZ) transformed with either pBTM116 alone, pBTM116-LNX long or pBTM116-LNX short (transformation as described below) was incubated with shaking in SD-tryptophan for 2 days at 30°C. Cells were pelleted and resuspended in 1.5mL sterile water containing 0.1M PMSF then transferred to a screwcap microcentrifuge tube. Cells were centrifuged 5 seconds at 12,000 rpm and two times the cell pellet volume of 2xSDS sample buffer with 0.1M PMSF was added. An equal volume of acid

washed glass beads (Sigma) was then added and the sample was vortexed in the cold room 3 times for 30 seconds each with incubation on ice for a minimum of 2 min between vortexes. The sample was then boiled for 3 min at 100°C and put on ice for 5 min. The sample was centrifuged for 5 min at 12,000 rpm, the supernatant was removed and 25μL of the final sample was loaded into a 10% SDS-PAGE. The separated proteins were then transferred to immobilon-P (Millipore) and blocked in 5% non-fat skim milk powder for 2 hours at room temperature. Affinity purified αJ3NPAY-L (produced as described in section *3.2.8*) was then added at a dilution of 1:250. The blot was left at 4°C overnight with gentle mixing, washed five times for 5 min each in PBS + 0.05% tween-20 (PBS-T).Then proteinA-HRP (BioRad) was added at 1:3000 in PBS-T, mixed gently for 1 hour at room temperature and washed five times for 5 min each in PBS-T. The results were then visualized by ECL (Amersham).

2.2.5 Small scale yeast cotransformations

A 50mL culture of L40 in SD lacking uracil and lysine was grown for 2 days at 30°C. 5mL of the culture was diluted into 300mL YPD, incubated at 30°C for 3-5 hours with shaking until the optical density at 600 nm reached approximately 0.5-0.6. The cells were centrifuged 5 min at 2200 rpm at room temperature and washed in 25-50mL sterile distilled water. Cells were again centrifuged for 5 min at 2200 rpm at room temperature and then resuspended in 2mL TE/LiAc (10mM Tris, 1mM EDTA, 100mM LiAc). During this time, 1μg of each of the desired DNA samples was mixed with 10μL of 10 mg/mL sonicated herring sperm DNA. A control containing no DNA but only sonicated herring sperm DNA was also made. To the DNA mix, 100μL of the cells in TE/LiAc was added followed by 0.6mL of PEG/LiAc (40% PEG4000, 10mM Tris, 1mM EDTA, 100mM LiAc); the sample was vortexed to mix. The sample was incubated at 30°C for 30 min with shaking. To this was added 70μL DMSO and the sample was mixed gently. The sample was incubated at 42°C for 15 min to heat shock, chilled briefly on ice and then centrifuged five seconds at 14,000rpm. The pellet was resuspended in 500μL of 1XTE (10mM Tris, 1mM EDTA, pH7.5). 100μL of the sample was plated on appropriate SD plates. The plates were inverted and incubated for two days at 30°C.

It was important to ensure that nonspecific interactions between bait molecules (LNX long, LNX short, each PDZ domain) and library-encoded proteins (mouse embryo heart and lung or rat brain) would not be more prevalent than true positive interactions. To this end, 1μg of each (bait and library) was cotransformed and plated on SD plates lacking leucine and tryptophan that contained varying amounts of 3-aminotriazole (AT) (Sigma) (0, 2, 5, or 10mM). The level of AT at which no colonies grew was chosen as the amount to be used in the plates on which the library scale cotransformation was to be plated.

2.2.6 Library scale cotransformations

A 50mL culture of the yeast strain L40 in SD media lacking uracil and lysine was grown for two days at 30°C with shaking. 10mL of the culture was diluted into 250 mL of YPD and incubated for 4 to 6 hours at 37°C with shaking until the OD reached 0.5-0.6. The cells were centrifuged for 5 min at 3400 rpm in 50mL conical tubes at room temperature. The pellets were resuspended in 12.5 mL LiAc mix (10mM Tris pH7.4, 1mM EDTA, 100mM LiAc). The five fractions were pooled and centrifuged for 5 min at 3400 rpm. The pellets were then resuspended in 1.5mL LiAc mix and incubated in a 15mL round bottom tube for 60 min at 30°C with shaking at 200 rpm. During this time, a DNA mix was prepared containing 60μL of 10mg/mL sonicated salmon sperm DNA, 20μL of 10XTE pH7.4, 20μL of 1M LiAc, 100μg of cDNA library and 100μg of bait DNA (LNX long, LNX short or each PDZ). A control mix was also prepared containing only 5μL of sonicated salmon sperm DNA. In round bottom tubes, 250μL of cells in LiAc mix was mixed with 40μL of DNA mix (control: 100μL of cells with 5μL sonicated salmon sperm DNA) and mixed gently. The cells and DNA were incubated at 30°C for 30 min with no shaking. Then 1.75mL of PEG mix (40% PEG4000, 10mM Tris pH7.4, 1mM EDTA, 100mM LiAc) was added to each tube (700μL added to control tube) and mixed by inverting. The sample was again incubated for 45 min at 30°C with shaking at 100 rpm. After this incubation, the samples were mixed by inversion followed by heat shock for 15 min at 42°C. The cells were then centrifuged for 1 min at 3400 rpm. The cell pellet was resuspended in 500μL SOS (5mL 2M sorbitol, 3.35mL YEP broth, 65μL 1M $CaCl_2$, 1.5mL sterile water); 200μL was added to the control. These were then incubated for 20 min at 30°C with shaking at 200 rpm. All fractions were pooled (total volume approximately 3mL) and 200μL was plated on 15cm SD plates lacking the

appropriate amino acids. The 200μL control was plated on a 10cm SD plate lacking leucine and tryptophan. Dilutions of 10^{-2}, 10^{-3} and 10^{-4} of the cotransformed cells were made and 100μL of each was plated on SD plates lacking leucine and tryptophan to monitor the transformation efficiency. The plates were incubated inverted at 30°C between 2 days and two weeks.

The library cotransformations performed with either PDZ1, PDZ2 or PDZ3 as the bait plasmid were plated on SD plates lacking leucine, tryptophan and histidine. Each library cotransformation performed with LNX long or LNX short as the bait was performed simultaneously in duplicate and plates on SD plates containing either 0 or 2mM 3-aminotriazole (a competitive inhibitor of the *HIS3* gene) and without leucine, tryptophan, histidine, uracil and lysine.

2.2.7 Selection of colonies

As colonies appeared on the library transformation plates, they were picked and restreaked to SD plates without leucine and tryptophan. This confirmed that the colony had acquired two plasmids - one cDNA library plasmid and one bait plasmid. This also allowed for testing of the β-galactosidase activity of the colony after growth at 30°C for two days to confirm interaction.

2.2.8 β-galactosidase assay

A nitrocellulose filter (Schleicher and Schuell, Keene, NH) was overlayed on the plate with yeast growth to pick up colonies. The nitrocellulose was then placed on an aluminum foil boat yeast-side up and floated on liquid nitrogen for 10-15seconds. The corners of the boat were pushed down to completely submerge the filter. After 30 seconds, the boat was removed from the liquid nitrogen and placed on a Whatman filter resting in the lid of petri dish soaked in 2.5mL Z buffer (16.1g $Na_2HPO_4 \cdot 7H_2O$, 5.5g $NaH_2PO_4 \cdot H_2O$, 0.75g KCl, 0.25g, $MgSO_4 \cdot 7H_2O$, pH7.0) containing β-mercaptoethanol (2.7μL/mL Z buffer) and Xgal (10μL of 4% Xgal (Boehringer) in dimethylformamide/mL Z buffer). The petri dish is sealed with parafilm and placed at 30°C until colour developed or for a maximum of 8 hours.

2.2.9 Isolation of library cDNA from yeast

Colonies that had grown on SD plates without histidine and had positive β-galactosidase results were selected for cDNA isolation. A 5mL culture of SD-leucine was inoculated with the selected colony. The growth media included tryptophan to encourage the growing yeast to lose the bait plasmid and retain only the prey plasmid of interest. The culture was grown for 2 days at 30°C with shaking. The cells were then pelleted and resuspended in 0.2mL of yeast lysis buffer (2% Triton-X-100, 1% SDS, 100mM NaCl, 10mM Tris pH8.0, 1.0mM EDTA). 100μL of acid washed glass beads (Sigma) and 0.2mL of phenol:chloroform:isoamylalcohol (25:24:1) were added. This mixture was vortexed for 2 min then centrifuged for 5 min at 14000rpm to separate the layers. The aqueous phase was removed to a fresh tube (approx. 200μL) and the plasmid DNA was salt precipitated. This was incubated at -20°C for 20 min then centrifuged for 20 min at 14000 rpm. The pellet was washed with 70% ethanol and left to air dry. The dried pellet was then resuspended in 20μL of 10mM tris pH8.0. To rescue the prey plasmid, 10μL of DNA was mixed with 100μL of competent *E. coli* (MH6) and incubated on ice for 20 min. The cells were heat shocked for 2-5 min at 42°C and then 400μL of LB broth was added to allow recovery of the cells shaking at 37°C for 30 min. From this, 100μL of cells were plated on LB containing 100μg/mL ampicillin and grown overnight at 37°C.

Colonies containing the leucine marker were selected and restreaked onto LB and M9 (minimal media) plates. Plates were incubated overnight at 37°C and those that were able to grow on M9 were used to inoculate 2mL of LB+ampicillin. Cultures were incubated overnight at 37°C with shaking and prepared by miniprep (Qiagen) as described above except that columns are washed once with Buffer PB before the two washes with Buffer PE. 10μL of plasmid DNA was digested with EcoRI/XhoI to check insert size. Those clones containing an insert were selected for maxiprep as in Section *2.2.2*, sequenced and retransformed with LNX long to confirm interaction and determine specificity.

Sequences were analyzed by BLAST and FASTA searches of GenBank were performed. Matching or similar sequences were verified with PILEUP and BESTFIT programs from GCG, Wisconsin Package.

2.2.10 Confirmation of relevant interacting molecules

Specific combinations of cotransformations were performed between LNX constructs and isolated clones as described in Section *2.2.5* except transformed cells were plated on SD plates without leucine and tryptophan. Interactions were then assessed using the β–galactosidase assay (See Section *2.2.8*) or restoration of histidine biosynthesis. After two days of growth on plates lacking leucine and tryptophan, 5-10 colonies were picked and dispersed in 1mL of sterile water to approximately equal turbidity. Dilutions of 1:10 and 1:100 were made and 12μL of each of the three samples from each cotransformation were spotted on plates lacking leucine, tryptophan and histidine. After spots dried at room temperature, plates were inverted and incubated at 30°C for two days.

2.3 RESULTS

2.3.1 Yeast two-Hybrid Library Screens with Individual PDZ domains

Initially, yeast two-hybrid screens of cDNA libraries were performed with bait constructs encoding individual PDZ domains (constructs as shown in Fig. 2-2). In the first attempt, the yeast strain L40 was sequentially transformed with pBTM-PDZ1 and 100μg of the mouse embryo heart and lung library (gift of Nina Jones, Table 2-1). $9.264x10^5$ transformants were screened and 62 colonies were initially selected and restreaked to SD plates lacking leucine and tryptophan. The β–galactosidase assay was performed on these plates and 25 of the 62 showed potential positive interaction. It is essential that positive interaction be seen in an isolated colony to reduce the chance that neighbouring cells containing different prey plasmids do not produce a false positive result. To confirm that these were true interactions, the 25 clones were restreaked to produce isolated colonies and retested for β–galactosidase activity. Only eight of the 25 had isolated colonies that turned blue. The sequence of these eight clones revealed that four clones were either intron sequences or out-of-frame exon sequences, two encoded ribosomal proteins and were deemed not of interest and the final two had open reading frames (ORFs) of only five and seven amino acids.

A second attempt was made using sequential cotransformation with pBTM-PDZ3 as the bait construct. $1.2x10^6$ transformants were obtained and 30 colonies were selected. However, only 3 of these 30 clones exhibited β–galactosidase activity. One cDNA encoded a transcription factor (ganglioside expression factor) while the other two cDNAs had ORFs of seven or less amino acids. A third attempt involved simultaneous cotransformation of the yeast strain L40 with pBTM-PDZ3 and the rat brain cDNA library (called concurrent cotransformation). $1.95x10^6$ transformants were screened and 56 colonies were selected. Of these, only 5 were positive for β–galactosidase activity. Two of these clones were intron sequences and two clones had ORFs of seven or 28 amino acids while the fifth clone had a large ORF (280aa) that matched an EST but not any known sequences. The carboxy terminal amino acids of this protein are predicted to be - TQA GGT LGS FGM*.

Two additional cotransformations of pBTM-PDZ4 or pBTM-PDZ1 with the rat brain library (gift

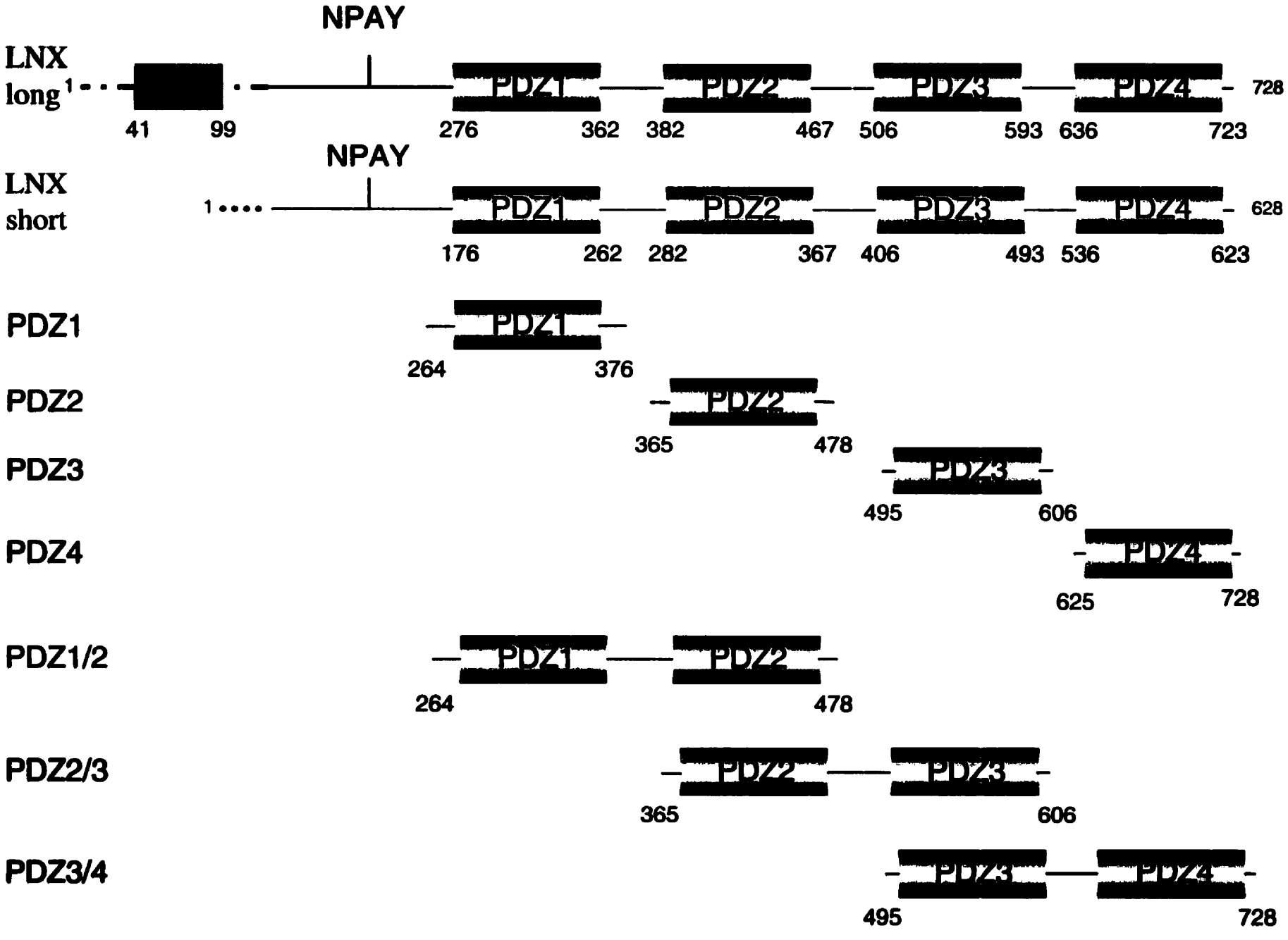

Fig. 2-2. Schematic diagram of LexA DNA binding domain-LNX fusion constructs

Table 2-1. Outcome of yeast two-hybrid library screens performed with various LNX constructs. ¶ indicates mouse embryo heart and lung cDNA library supplied by N. Jones or rat brain cDNA library supplied by B. Snow. * indicates that no colonies were picked but βgalactosidase assay was performed directly on library plates. For details see text.

BAIT	COMPLEXITY	VARIABLES	# SELECTED	# positive for βgalactosidase activity
PDZ1	$9.8X10^5$	-leu-trp-his sequential mouse¶	62	25
PDZ3	$1.2x10^6$	-leu-trp-his sequential mouse	30	3
PDZ3	$1.9x10^6$	-leu-trp-his cotransformation rat¶	56	5
PDZ4	$2.8x10^5$	-leu-trp-his+10mMAT cotransformation rat	3	0
PDZ1	$1.2x10^7$	-leu-trp-his+10mMAT cotransformation rat	none*	4
LNX long	$1.5x10^6$	-THULL and -THULL+2mMAT cotransformation mouse	77	44
LNX short	$1.9x10^6$	-THULL and -THULL+2mMAT cotranformation mouse	47	0

of Bryan Snow) were performed. The $2.8x10^5$ or $1.3x10^{10}$ cotransformed cells, respectively, were plated on SD plates lacking leucine, tryptophan and histidine but containing 10mM AT. Three colonies were selected from the pBTM-PDZ4 transformation but none of these colonies displayed β–galactosidase activity. Due to the numerous colonies that grew from the pBTM-PDZ1 cotransformation, a β–galactosidase assay was performed on all the library plates. Only 4 colonies were positive for β–galactosidase activity and these were selected for cDNA isolation. All of these clones were either from non-coding regions or were exon sequences that were out-of-frame with the GAL4 activation domain.

2.3.2 Yeast two-hybrid library screen with LNX long

Given that the above screens yielded mostly irrelevant clones, we reasoned that more relevant clones might be isolated if the entire LNX protein was used as bait. This was intended to address the possibility that the individual PDZ domains of LNX may require the presence of the other PDZ domains in order to retain proper conformation or to retain the ability to bind target molecules. Therefore, both the long and short forms of LNX fused to the LexA DNA binding domain were used to screen the mouse embryo heart and lung library. The experiments with LNX short are discussed in Section *2.3.5*.

A western blot confirmed the expression of the LexA DNA-binding domain-LNX long fusion protein (Fig. 2-3) and we therefore proceeded with the library screen. Cotransformation with 100μg of a mouse embryo heart and lung library with the LexA DBD-LNX long fusion produced $1.5x10^6$ transformants. Of the 77 colonies that were selected and restreaked from the library plates, 44 clones exhibited β–galactosidase activity. Examples of the β–galactosidase assay performed on library plates after several weeks of growth are shown in Fig 2-4. A flowchart of the process of analysis of these 77 clones is shown in Fig. 2-5.

2.3.3 Plasmid isolation and sequencing

Prey plasmid DNA was isolated from 33 of the 44 selected colonies as eleven of the plasmids could not be purified from the yeast strain and transformed into *E. coli* MH6 host cells. Several prey plasmids were cotransformed into L40 cells with LNX long to check that interaction could

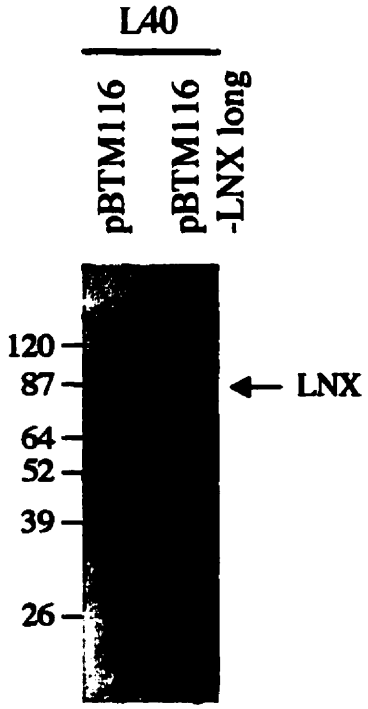

Fig. 2-3. Lysates of L40 cultures transformed with either pBTM116 or pBTM116-LNX long separated by SDS-PAGE and western blotted with α-J3-NPAY-L polyclonal antibody.

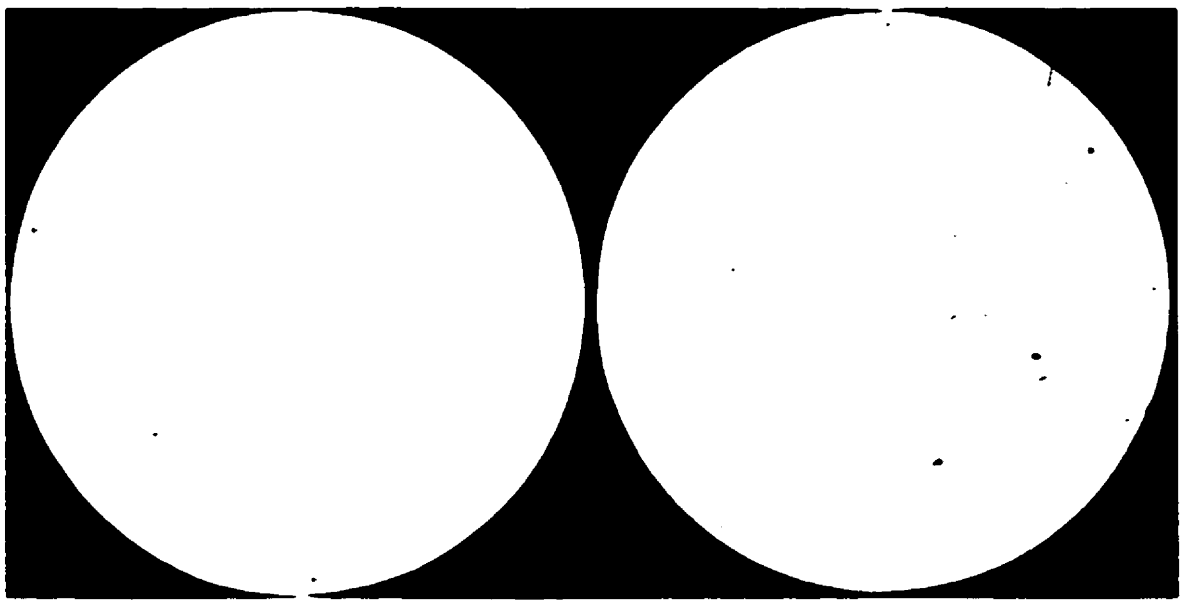

Fig. 2-4. Two examples of β–galactosidase filter assays from yeast two-hybrid library screen. β–galactosidase assays performed as described in Section 2.2.8.

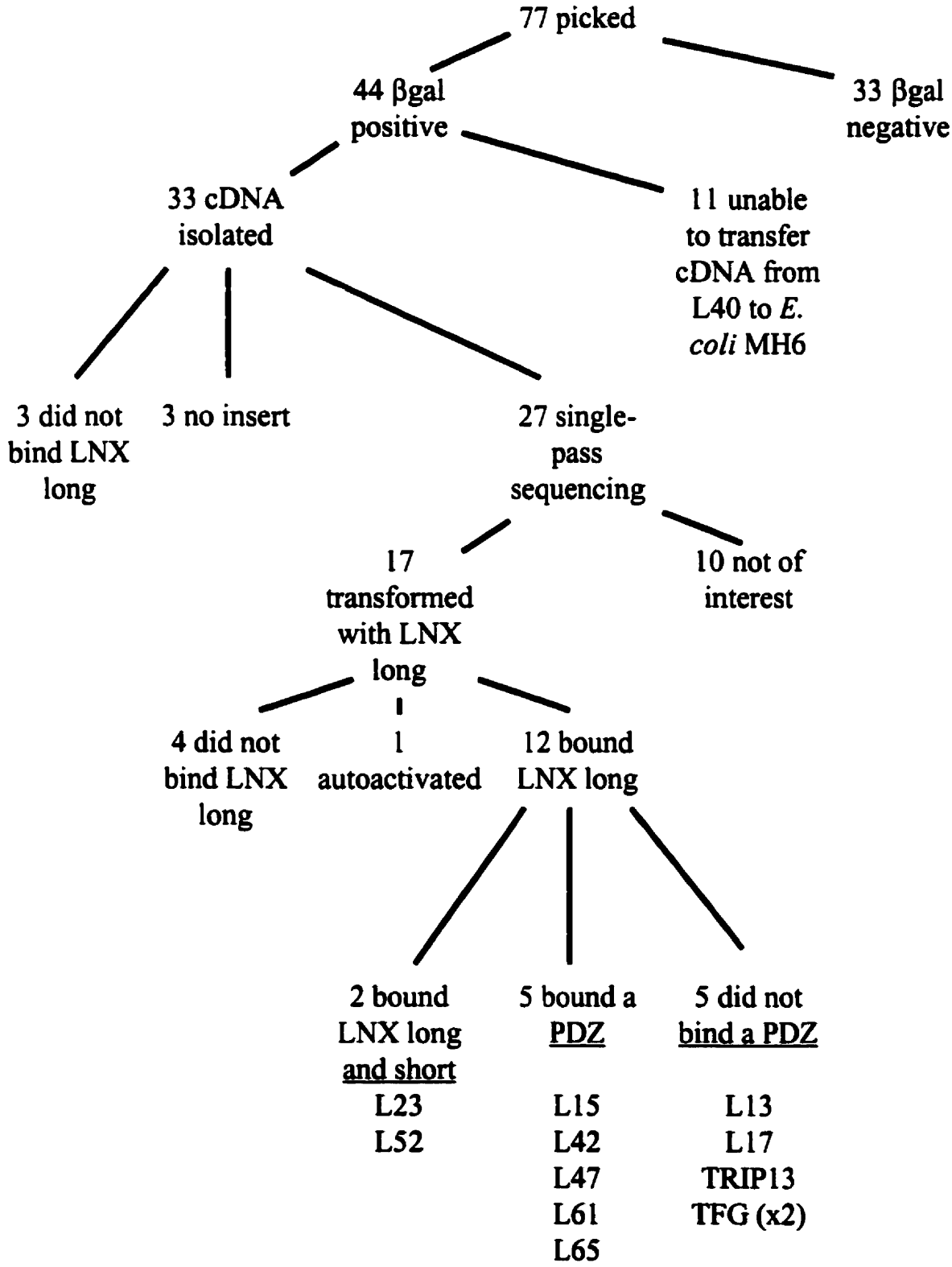

Fig. 2-5. Flowchart of selection of LNX long interacting molecules.

be observed with purified cDNAs. Three clones did not interact with LNX long and were therefore not pursued further. Upon restriction digestion, three other clones were shown to have no insert and were also not pursued. The remaining 27 clones were sent for single-pass sequencing for preliminary identification. Ten of the 27 were deemed not of interest; eight of these ten encoded ribosomal proteins, collagen, cytochrome C subunits, testin (a secreted protein) or heat-shock proteins. One plasmid encoded the αglobin cDNA but was not in the correct frame for αglobin expression. Another plasmid consisted of repetitive intron sequence. These ten clones were not relevant to our purpose of studying LNX in signal transduction pathways.

2.3.4 Confirming the interaction with LNX

The seventeen clones that remained were transformed into L40 alone to determine whether they were able to autoactivate transcription of the reporter genes. Only one clone autoactivated and was not pursued. The remaining sixteen clones were cotransformed with LNX long or LNX short to confirm interaction. Four clones did not interact with LNX long or LNX short. Three of these clones encoded TI-225/polyubiquitin (Ishiguro et al., 1996) and the other was a novel cDNA. The remaining twelve plasmids interacted with LNX long; two of these twelve interacted with both LNX long and LNX short (L23 and L52).

2.3.5 Studies with the LNX short fusion protein

The two-hybrid screen with LNX short yielded 1.9×10^6 transformants, however, none of the colonies which grew were β-galactosidase positive. A small culture of LexA DBD-LNX short transformed yeast cells was tested for expression of the fusion protein by western blotting with αLNX antisera. No specific band corresponding to the LexA DBD-LNX short fusion protein was detected (data not shown). This suggests that the fusion protein was not expressed.

Doubts about the integrity of the LNX short fusion protein are substantiated by the fact that not all of the clones that were able to interact with LNX long and an individual PDZ domain (see Section *2.3.6*) were able to interact with LNX short. However, two of the clones were able to activate transcription when cotransformed with LNX short which suggests that the protein is

expressed, contrary to the results of the western blot. It may be that very low levels are expressed, that is, below the detection level of western blotting. It is also possible that the protein does not adopt the correct conformation causing only the strongest interactions with LNX short to be detected. This is supported by the observation that some LNX long-interacting clones were able to interact with LNX short while others only showed interaction with the individual PDZ domains.

2.3.6 Testing the twelve clones with individual PDZ domains

The four LexA DBD-PDZ fusion proteins (Fig. 2-2) were cotransformed with each of the twelve clones that interacted with LNX long. Seven of these twelve were able to interact with an individual PDZ domain (Fig. 2-6; Table 2-2). However, an interaction between PDZ3 and L61 was only observed in two out of three attempts. The seven clones able to interact with an individual PDZ domain were chosen for further study in agreement with the purpose of these experiments, to identify the targets of the LNX PDZ.

Thus, the remaining five clones may interact with LNX long independent of the PDZ domains. Two of these clones are irrelevant as they encode a portion of the coding region of TFG (Trk fused gene) fused to part of its 3' untranslated region. One clone encoded TRIP13 (thyroid receptor interacting protein, GenBank accession no. L40834) which has been isolated from at least two other yeast two-hybrid screens (Lee et al., 1995; Schepens et al., 1997). The final two clones are identical and encode a novel protein that does not appear to have any known domains. They match several ESTs in GenBank (C76356, AA920753) and the carboxy terminal amino acids fit a type I PDZ consensus motif (-SFWK PEE TWV*). This suggests that these clones were nonspecifically recognized by LNX PDZ domains during the yeast two-hybrid screen.

2.3.7 Identity of the seven LNX interacting proteins

The first clone, L15, encodes the carboxy terminal portion of the previously identified protein, WWP1 (Fig. 2-7). The cDNA encodes a region beginning approximately 80 amino acids into the HECT domain (homologous to E6-AP carboxy terminus) (Huibregtse et al., 1995) and continues

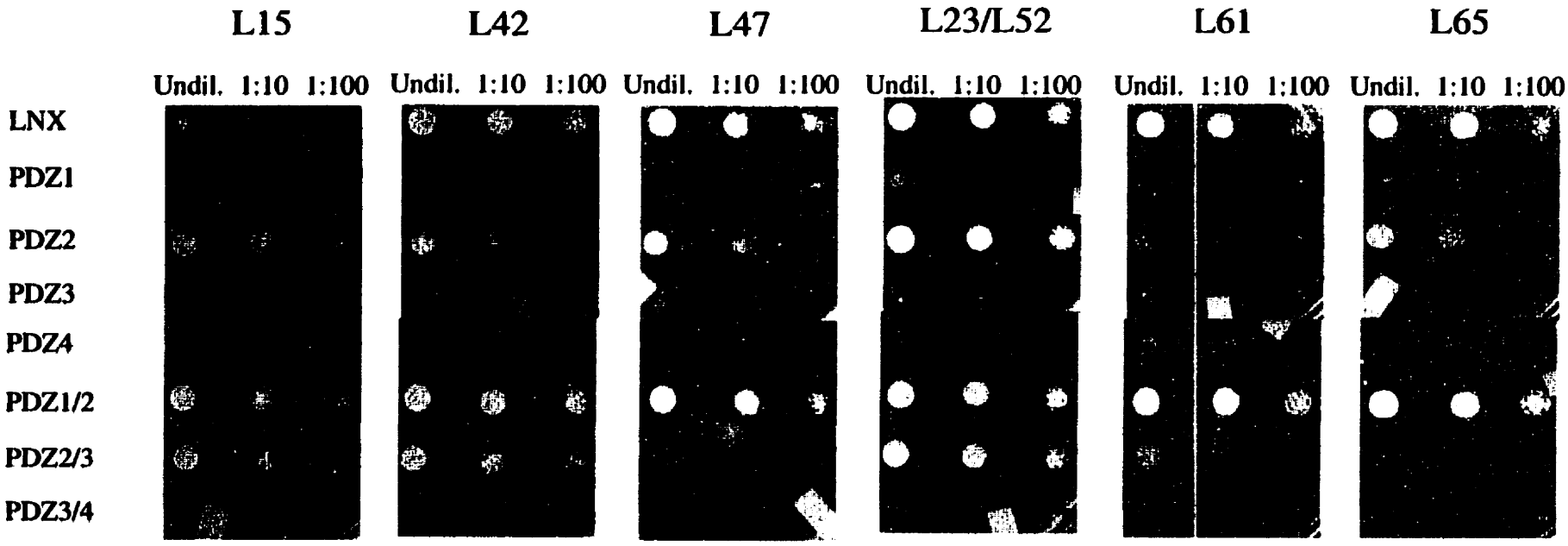

Fig. 2-6. Yeast two-hybrid assays for interaction of LNX, each PDZ or PDZ pair with seven clones. Column on left indicates bait construct; row across top indicates clone. L40 cells were cotransformed as indicated and plated on minimal media lacking leucine and tryptophan. Two days later, 5-10 colonies were picked and dispersed in 1mL of sterile water. Dilutions of 1:10 and 1:100 in sterile water were also made, then 12 μL of all three dilutions were spotted on minimal media lacking leucine, tryptophan and histidine and incubated for two days.

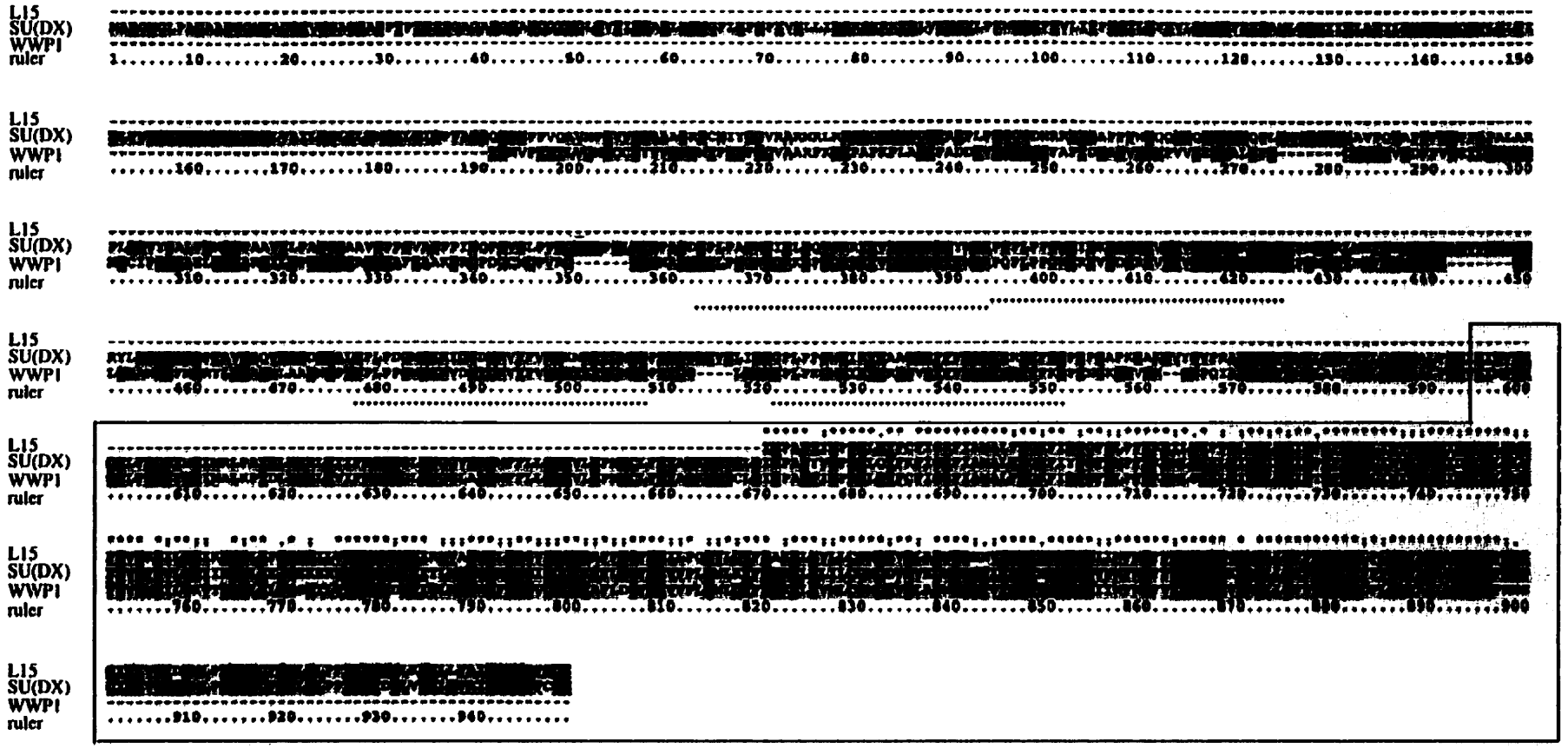

Fig. 2-7. Alignment of protein sequences of L15, WWP1 (U96113) and Suppressor of Deltex (SU(DX); AF152865). WW domains are underlined, Hect domain (homologous to E6-AP carboxy terminus) is enclosed by box.

to the carboxy terminus of WWP1. The carboxy terminal amino acids of L15 do not fit a PDZ consensus binding site (-FAIEET EGFGQE*).

Two copies of another clone, L23/L52, were isolated (Fig. 2-8). This cDNA encodes the carboxy terminal 123 amino acids of a novel protein that contains a type I PDZ recognition site at the carboxy terminal tail (-KAPPGP KGPTLV*) but no other known domains. A mouse genomic sequence deposited in GenBank (AF109905) is predicted to encode a protein (AAC84153) similar to L52. This genomic sequence maps to chromosome 17 in the mouse. There are also many expressed sequence tags (ESTs) which are identical to L52, isolated from both mouse mammary gland and thymus.

The third clone, L42, has been previously identified as a Rab interacting molecule, PRA1 (Janoueix-Lerosey et al., 1995; Martincic et al., 1997) (Fig. 2-9). There are two regions of hydrophobic residues in PRA1, which may be transmembrane domains, or the hydrophobic core of the molecule. The carboxy terminus of PRA1 has a potential PDZ recognition site (-PAD GEE QLM EPV*).

Another novel clone isolated, L47, does not contain any known domains (Fig. 2-10). In GenBank, there are 184 ESTs and one partial cDNA isolated from a pituitary tumour (PTD011, accession no. AF078864) that are identical to L47. The ESTs are expressed in many tissues including heart, kidney and skeletal muscle. The carboxy terminal amino acids (-KVG ISL LSS PHP*) do not fit a consensus for recognition by a PDZ domain; the isolated clone encodes 132 amino acids.

The clone L61 has an open reading frame of 89 amino acids that encodes a novel molecule (Fig. 2-11). There are no known domains found in the protein sequence predicted from the isolated L61 cDNA, however the carboxy terminus fits a type II PDZ domain recognition motif (-LEKLKN QNSFMV*). There are 56 mouse, rat and human ESTs that match this sequence. They have been isolated from many different tissues and therefore L61 is predicted to be widely

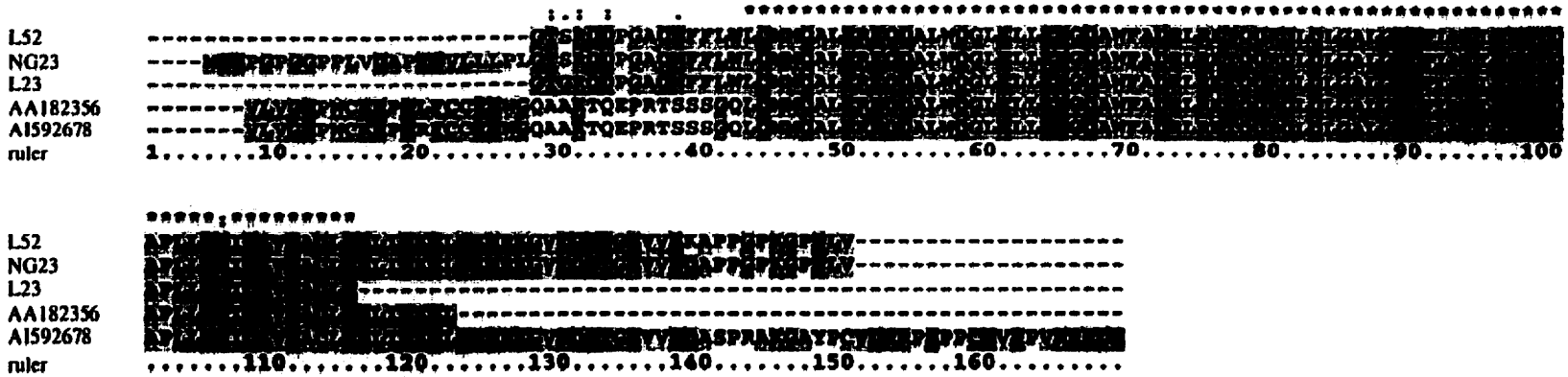

Fig. 2-8. Multiple sequence alignment of L23, L52, NG23 (AAC54153) and two ESTs (AA182356, AI592678). AI592678 is a resequence of AA182356 that shows diverging protein sequence in the carboxy terminal region.

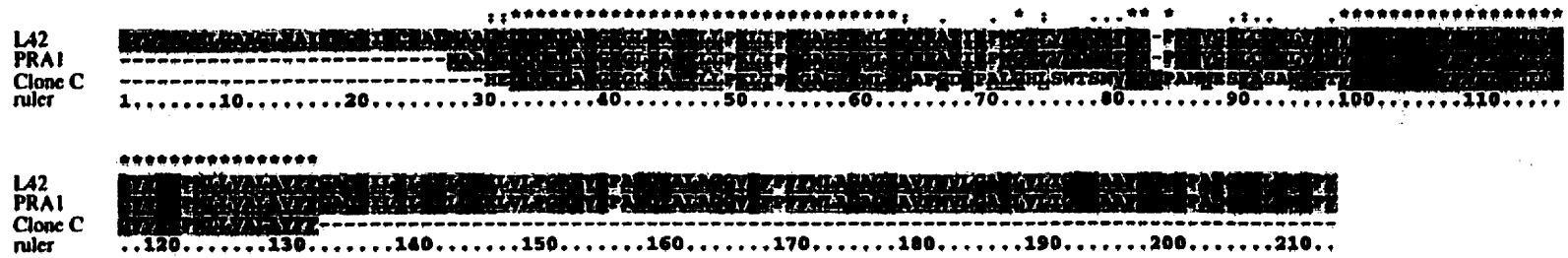

Fig. 2-9. Alignment of L42, PRA1 (AAD17296) and Clone C (L40934) (from Janoueix-Lerosy et al., 1995).

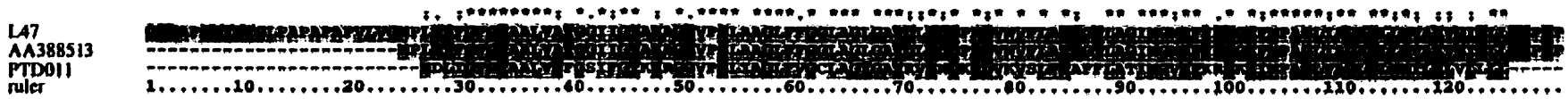

Fig. 2-10. Alignment of L47, PTD011 (AAD44496) and an EST (AA388513).

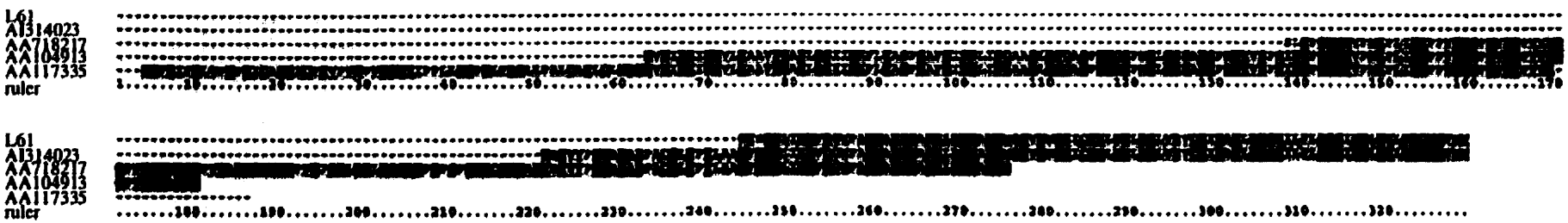

Fig. 2-11. Alignment of L61 and several ESTs to extend the predicted amino terminal protein sequence(AI314023, AA718217, AA104913, AA117335).

expressed. One of the human sequences that matches L61 has been mapped to the region 10p11.2-10p12.1 on human chromosome 10.

The final clone isolated from the yeast two-hybrid screen with LNX long, L65, is syntaxin5 (Fig. 2-12). Syntaxin5 is involved in vesicular fusion events by which proteins are transported from the endoplasmic reticulum (ER) to the golgi apparatus and within the golgi (Bennett et al., 1993; Nichols and Pelham, 1998). The carboxy-terminal 20 amino acids of syntaxin5 are embedded in the organellar membrane.

Table 2-2. Summary of the seven LNX-interacting clones selected for further study

CLONE	IDENTITY	OF NOTE	INTERACTS WITH IN Y2H:	C TERMINAL AMINO ACIDS:
L15	WWP1	Nedd4-like	PDZ2, PDZ2/3	FAI EET EGF GQE*
L23/L52	novel (NG23)		PDZ1, PDZ2, PDZ2/3	KAP PGP KGP TLV*
L42	PRA1	Rab associated protein	PDZ2, PDZ3, PDZ2/3	PAD GEE QLM EPV*
L47	Novel		PDZ2	KVG ISL LSS PHP*
L61	Novel		PDZ3	LEK LKN QNS FMV*
L65	syntaxin5	SNARE complex protein	PDZ2, PDZ2/3	IVF FII FVV FLA*
	PDZ type I recognition site:			(S/T)X(V/I/L)*
	PDZ type II recognition site:			(F/Y)X(V/I/L/A)*

2.3.8 Testing the PDZ pair fusion proteins with LNX interacting clones

Fusion proteins with the LexA DBD were constructed of each of the adjacent pairs of PDZ domains (PDZ1/2, PDZ2/3, PDZ3/4; see Fig. 2-2). Each fusion protein was tested to ensure that they were not able to autoactivate transcription of reporter genes. The PDZ1/2 pair was not capable of autoactivation but was able to activate transcription of *lacZ* when expressed together with the GAL4 activation domain alone (that is, empty pADGAL4). The seven clones that were able to interact with an individual PDZ domain were each cotransformed with the PDZ pairs. Five clones were also able to interact with a PDZ pair (Fig. 2-6). All clones nonspecifically interacted with PDZ1/2.

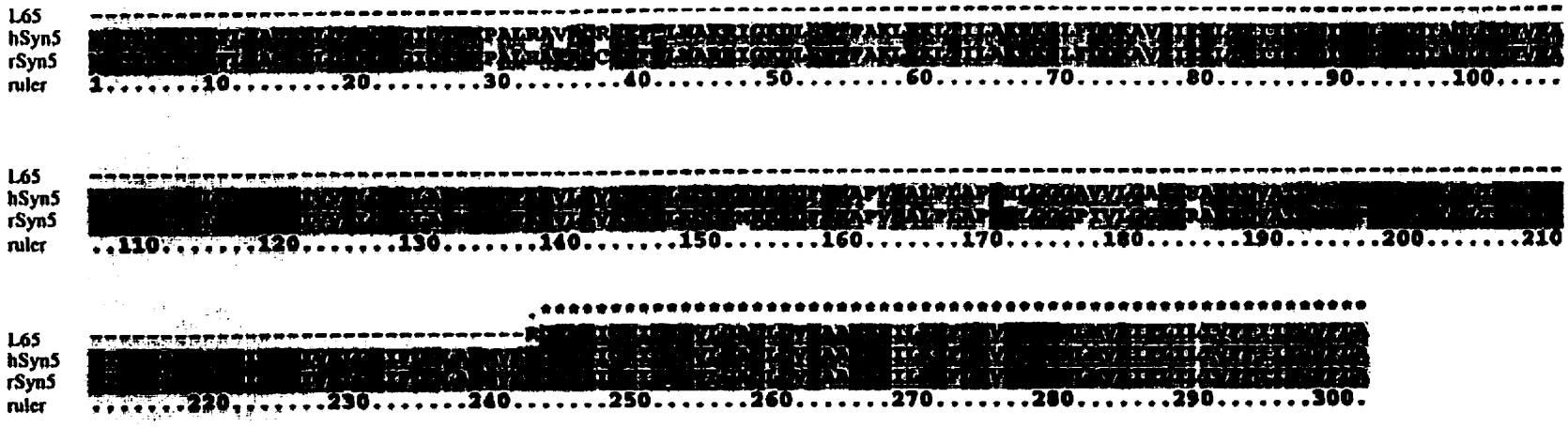

Fig. 2-12. Multiple sequence alignment of L65 with human (SwProt 2501092) and rat (SwProt 2501093) syntaxin5.

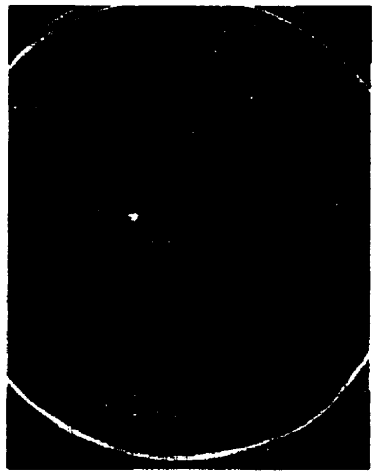

Fig. 2-13. Yeast two-hybrid assay to test for interaction between L61 (left) or L61 lacking 14 carboxy terminal amino acids (right) with LNX.

2.3.9 LNX interaction with the carboxy-terminal tail

Since PDZ domains are predicted to interact with carboxy terminal amino acids, we wished to explore whether LNX interacts with the carboxy terminal tail of the isolated clones. Although mutation of all six clones was planned, only one construct was completed due to time constraints. A construct encoding the L61 clone lacking the carboxy-terminal 14 amino acids was generated by PCR. When cotransformed with LNX long in yeast, the interaction no longer occurred as indicated by the inability to grow on media lacking histidine (Fig 2-13). This suggests that the carboxy terminus of L61 contains a recognition site for a LNX PDZ.

2.3.10 RING finger interactions

Since another RING finger containing protein had been shown to be able to homodimerize through its RING finger domains (Inouye et al., 1997), a construct encoding the RING finger domain fused to the GAL4 AD was generated. This construct was cotransformed with one of two LexA DBD fusion proteins: the RING finger domain and the full length LNX. No interaction was seen in either case (data not shown). As well, the LexA DBD-RING fusion was cotransformed with several of the clones isolated in the LNX long screen (e.g. L13, L17, L23, L52, L61, L65), none of which interacted with the isolated RING finger domain.

2.4 DISCUSSION

We have used a yeast two-hybrid screen to identify proteins that interact with the PDZ domains of the Numb-binding protein, LNX. A library of cDNA molecules from mouse embryo heart and lung tissues was screened with LNX long. Isolated clones were assessed for their ability to interact with an individual PDZ domain or a pair of PDZ domains from LNX. Seven clones were identified as specifically interacting with the LNX PDZ domains. One of these clones, L61, was shown to require its carboxy terminal 14 amino acids to maintain LNX binding which is consistent with a PDZ domain-mediated interaction. A study of the RING finger domain of LNX long revealed that LNX is not able to homodimerize through this domain.

2.4.1 The yeast two-hybrid library screen and PDZ domains

In the last two years, several PDZ domain containing molecules have been identified through yeast two-hybrid screens with intracellular portions of proteins (Bruckner et al., 1999; Hasegawa et al., 1999; Hock et al., 1998; Torres et al., 1998). Very few clones were isolated in each of these screens (i.e., one or two) yet further analyses of these proteins indicate that the interactions identified may be biologically relevant. There are also many recent examples of yeast two-hybrid screens using PDZ domain containing proteins in whole or in part as bait (Cuppen et al., 1998; Jaffrey et al., 1998; Kim et al., 1998; Masuko et al., 1999; Niethammer and Sheng, 1998; Schepens et al., 1997). In each case, a low number of specific clones (i.e., 1-12) were isolated from the screens. These examples illustrate that yeast two-hybrid screens utilizing PDZ domains or PDZ recognition sites often identify a low number of interacting molecules. This may indicate either that interactions involving PDZ domains do not readily occur in yeast or that these interactions are more selective than two-hybrid screens with other types of bait molecules. In many of these examples, biochemical techniques were used to complement the results and suggest that the interactions are biologically relevant. This would indicate that yeast two-hybrid screens involving PDZ domain containing-proteins are generally successful and identify biologically relevant interactions for future study.

2.4.2 Yeast two-hybrid screen with PDZ domain-containing protein, LNX

From the examples discussed above, a trend emerges whereby a relatively small number of clones are isolated from yeast two-hybrid screens in which the bait construct either contains a PDZ domain or a PDZ domain binding site. This is in agreement with the results obtained here. A very small number of clones were isolated from the screens performed with either individual PDZ domains (less than 8) or with the full length molecule (12).

The screen using the short form of the LNX protein did not identify any interacting clones. This may be due to little or no expression of the LNX short protein or incorrect folding of the expressed protein inside the yeast cells. Attempts to identify the LexA DBD-LNX short fusion protein by western blot analysis were unsuccessful. This could indicate that the either fusion protein is not expressed or the expressed protein is cleaved by intracellular proteases. This fusion protein contained a large linker region between the LexA DBD and the initiating methionine of the LNX short protein (23 amino acids). This may have led to, or at least contributed to, misfolding or cleavage problems. The fact that two of the seven clones isolated from the LNX long screen were able to interact with LNX short suggests that the fusion protein is expressed. However, it is likely that some misfolding of LNX short occurs making interactions more difficult or much weaker and thus below the level of detection in this assay.

2.4.3 Selection of PDZ domain interacting clones

The yeast two-hybrid screen with the full length LNX long protein was the most successful of the screens attempted. Seven clones were obtained which were able to interact with an individual PDZ domain in the yeast two-hybrid system. Further analysis of these clones may contribute to our understanding of the function of LNX within the cell as well as the role of LNX with respect to Numb.

L15 encodes part of the carboxy terminal HECT domain of a mouse homologue of the human protein WWP1. HECT domains have been shown *in vitro* to act as E3 ubiquitin ligases. Several publications have described the isolation of WWP1 from other library based screens. The first group utilized peptides containing predicted WW domain binding sites to screen an expression

library for novel WW domain containing proteins (Pirozzi et al., 1997). One of the partial cDNAs isolated, termed WWP1, contains four WW domains followed by a partial HECT domain. WWP1 was also isolated from a yeast two-hybrid screen employed to isolate proteins that interact with atrophin-1 in the vicinity of its polyglutamine repeat (Wood et al., 1998). Northern blot analysis revealed that WWP1 is widely expressed with particularly high expression in heart and skeletal muscle. This is an interesting overlap with the restricted expression pattern of LNX; both forms of LNX are expressed in heart while only the long form of LNX is found in skeletal muscle.

WWP1 is a member of a family of proteins similar to Nedd4 (Cornell et al., 1999; Pirozzi et al., 1997). The role of Nedd4 in mammalian cells is to interact with the subunits of the epithelial sodium channel (Staub et al., 1996; Staub and Rotin, 1997). Thus, WWP1 may also have a role in binding to a transmembrane or membrane-associated complex; this is very similar to the predicted role of LNX. Interestingly, nNOS, a PDZ domain-containing protein, is known to associate via α1-syntrophin with the dystrophin complex (Brenman et al., 1996; Brenman et al., 1995). Dystrophin is a WW domain-containing protein found in a multiprotein, membrane associated signaling complex important for muscle cell function (Pirozzi et al., 1997). In the same way, WWP1 and LNX may work in concert to nucleate multiprotein signaling complexes at the membrane.

Recently, a new member of the Nedd4 family was identified in Drosophila when the gene encoding the *Suppressor of Deltex (Su(dx))* mutation was cloned (Cornell et al., 1999). *Su(dx)* is known to be a negative regulator of the Notch pathway, as is dNb. It is very interesting to note that in Drosophila there is a connection between Notch and a Nedd4-like molecule while in mammals there is a connection through LNX between Nb and another Nedd4-like molecule.

The carboxy terminal amino acids of WWP1 do not match a PDZ recognition site thus LNX is most likely to recognize WWP1 at an internal site. The site of interaction between LNX and WWP1 could be mapped by creating several GAL4 AD fusion proteins of different regions of WWP1 and testing their ability to interact with LNX or an individual PDZ domain.

The second known protein identified in the LNX yeast two-hybrid screen was PRA1, which is a Rab associated protein. Rabs are small GTPases of the Rac/Rho family found in submembranous regions as well as associated with intracellular vesicles. Rabs are associated with either GDP (inactive form) or GTP (active form). Rab also cycles between the prenylated and unprenylated state, which alters its ability to associate with the membrane. PRA1 was identified in two different yeast two-hybrid screens for Rab-interacting molecules (Janoueix-Lerosey et al., 1995; Martincic et al., 1997). PRA1 was found to interact with both Rab5 and Rab6 in the yeast two-hybrid system but it appeared to preferentially interact with the GDP bound form of Rab6 (Janoueix-Lerosey et al., 1995). PRA1 mRNA and protein are both widely expressed in rat tissues (Martincic et al., 1997). PRA1 is capable of interaction with Rab3A and VAMP2, although forms of Rab3A that could not be lipid modified were not able to interact with PRA1. VAMP2 is known to be a downstream target of Rabs and a component of SNARE complexes involved in synaptic vesicle fusion to target membranes. These experiments suggest that PRA1 can bind to several Rab proteins and is involved in general Rab GTPase function. PRA1 has a potential PDZ recognition site at its carboxy terminus (-PAD GEE QLM EPV*). If an interaction occurs between LNX and PRA1 *in vivo*, this may indicate a role for LNX in intracellular vesicles and/or fusion of these vesicles to target membranes.

Syntaxin5 is involved in membrane fusion events during ER to golgi transport and intra-golgi transport (Nichols and Pelham, 1998). The 20 carboxy terminal amino acids of syntaxin5 are known to be embedded in organellar membrane therefore we would predict that an interaction between LNX and the carboxy terminus of syntaxin5 is not possible *in vivo*. It is possible that the hydrophobic tail of syntaxin5 was not embedded in the membrane when expressed in yeast and therefore was available for binding by the LNX PDZ domains resulting in a fortuitous interaction. Several PDZ domains have been shown in the past to preferentially recognize sequences containing hydrophobic amino acids, called a type II PDZ recognition site. Thus, a non-specific interaction between a LNX PDZ and the hydrophobic tail of syntaxin5 may have occurred. However, an interaction between LNX and syntaxin5 is still possible through an internal site on syntaxin5. If an interaction does occur between LNX and syntaxin5, this would

correspond well with an interaction between LNX and PRA1 and a role in intracellular vesicles, possibly in the trans-golgi network.

It is difficult to predict the role of L23/L52, L47 and L61 since they are novel and do not resemble other known proteins. Some relevant information about L61 may be obtained from a human EST matching the L61 cDNA that has been mapped to 10p11.2-10p12.1. Many cancers are linked to this region such as primary sarcomas (Tarkkanen et al., 1999), lymphoma (Bea et al., 1999), bladder cancer (Simon et al., 1998), glioblastoma multiforme (Mao et al., 1999), astrocytoma (Nishizaki et al., 1998) and neuroblastoma (Altura et al., 1997). The carboxy terminal amino acids of L61 fit a consensus type II PDZ recognition site. In support of this, we showed that deletion of the 14 carboxy terminal amino acids from L61 results in the loss of interaction between LNX and L61 in the yeast two-hybrid system. This would suggest the interaction between LNX and L61 is mediated by PDZ domain recognition of the carboxy terminal amino acids of L61. It will be important to isolate the full length sequence of each of these three clones and determine their expression patterns in order to establish how they are involved in LNX function.

2.4.4 Preliminary RING finger studies

The RING finger of the yeast protein Ste5 is able to homodimerize through its RING finger domain (Inouye et al., 1997). Therefore we tested the ability of a GAL4 AD fusion of the LNX long RING finger domain to interact with either LexA DBD-RING or LexA DBD-LNX long. No interaction was seen with either fusion protein, suggesting that the RING finger domain of LNX long does not homodimerize. As mentioned above, there were two clones that interacted with LNX long but did not interact with an individual PDZ domain. These were cotransformed with the LexA DBD-RING finger domain but no interaction was seen.

Chapter III Characterization of the interactions between LNX PDZ domains and their interaction partners

3.1 INTRODUCTION

We have identified six proteins from a yeast two-hybrid screen that interact with the PDZ domains of LNX. We then utilized *in vitro* methods in order to validate these interactions. Surface plasmon resonance is used to detect protein-protein interactions and measure binding affinities *in vitro*. A protein or peptide of interest is immobilized and a second protein flows past the immobilized protein in a fluid phase. If an interaction occurs between the two proteins, a change in optical properties is detected by the apparatus and reported in real-time. Using this technique, we undertook a study to 1) confirm the interactions observed in the yeast two-hybrid system and 2) test for novel interactions between LNX PDZ domains and potential targets. These potential targets are previously identified proteins that were selected on the basis of function and carboxy terminal sequences that contain potential PDZ binding sites.

A second approach to confirm the interactions observed in the yeast two-hybrid system involves recombinant fusion proteins. These fusion proteins were tested for their ability to bind exogenously expressed LNX in cell lysates. This method was utilized because appropriate antibodies and/or techniques were not available for identifying the endogenously expressed proteins. Recombinant proteins are often produced as a fusion of the protein of interest with a large molecular tag, for example, glutathione-S-transferase (GST) or maltose binding protein (MBP). These fusion proteins can be expressed at high levels in bacteria and are easy to purify via their affinity for glutathione and maltose, respectively. In this chapter, we have created GST fusions of the proteins identified by the yeast two-hybrid screen to verify their interaction with LNX.

Once a protein-protein interaction is verified *in vitro*, the next step is to demonstrate that the interaction occurs *in vivo* and determine its biological relevance. This requires appropriate methods and antibodies to detect the endogenous protein. Thus, it was important in studying LNX and its interaction partners to establish a method by which endogenous LNX protein can be

detected and isolated. Endogenous proteins may sometimes be difficult to detect because they may be expressed at a very low level or be located within a region of the cell, such as the submembranous region, from which it is difficult to extract proteins. Previously we have shown restricted expression of LNX mRNA and have been unable to detect endogenous LNX in cell lines commonly used in our laboratory. This suggests that either the protein is not expressed in cell lines or we are not able to extract it. As a first step to being able to study the LNX protein and its binding partners *in vivo*, we sought to identify endogenous LNX using tissue lysates prepared by a modified technique.

3.2 MATERIALS AND METHODS

3.2.1 Subcloning directly or by PCR

GST fusion proteins of each of the LNX PDZ domains were generated by PCR with the primers and methods as described in Section *2.2.1*. The only exception is that the recipient vector was pGEX4T1 in place of pBTM116. For subcloning PDZ pairs from pBTM116 to pGEX4T1, 5μg of pBTM116-PDZ pairs were digested with EcoRI/SalI, pGEX4T1 was prepared as described in Section *2.2.1*.

The isolated cDNA from six clones (L15, L42, L47, L52, L61, L65) were excised from pADGAL4 by EcoRI/XhoI or EcoRI/SalI digestion and ligated into pGEX4T1 EcoRI/SalI digested as described under Section *2.2.1*. GST fusion proteins were produced as described under Section *3.2.2*.

3.2.2 Preparation of fusion proteins expressed in E. coli (BL21) cells

Constructs encoding GST fusion proteins of LNX PDZ domains and adjacent pairs of PDZ domains were transformed into *E.coli* (BL21) as described for *E.coli* (DH5α) except that transformed cells were plated on LB plates containing 100μg/mL ampicillin and 50μg/mL kanamycin (LB+amp+kan). One colony from these plates was chosen to inoculate a 50mL culture of LB+amp+kan and incubated overnight at 37°C with shaking. A portion of the culture (5 to 10mL) was diluted the next morning into 250mL LB+amp+kan and incubated for 2 hours at 37°C with shaking. The culture was then induced to express the GST fusion proteins with 1mM isopropylthiogalactoside (IPTG, Boehringer Mannheim) and incubated for a further 3-6 hours at 30°C or 37°C. It was found that the most efficient expression of each fusion protein occurred at the following incubation times and temperatures: PDZ1 was induced for 3 hours at 30°C, PDZ2 and PDZ3 were induced for 3 hours at 37°C and PDZ1/2, PDZ2/3 and PDZ3/4 were induced for 5 hours at 30°C. The induced cells were then pelleted by centrifugation for 10 min at 4000-5000 rpm. The pellets were resuspended in 10-25mL of PBS (8g NaCl, 0.2g KCl, 1.44g Na_2HPO_4, 0.24g KH_2PO_4, pH7.4) containing Complete® protease inhibitor tablets (PBS+) (Boehringer Mannheim) and sonicated 2-4 times for 20 seconds with one-second-on/one-second-off bursts. The sonicated cells were incubated on ice for 5 min after addition of Triton-X-100 (Sigma) to a

final concentration of 1%. The mixture was centrifuged 30 min at 12000 rpm. The supernatant was mixed with 100-250μL glutathione sepharose beads (Pharmacia) that had been washed once with PBS containing 1% Triton-X-100 and Complete® protease inhibitor tablets (PBS++). The GST fusion proteins were bound to the beads by incubation for 15 min at 4°C with gentle mixing. The glutathione sepharose beads were washed three times with PBS++ then washed two times with PBS+. The beads were then resuspended to 50% with PBS+ containing 1mM dithiothreitol and a 10μL sample was removed and checked on 10% SDS-PAGE stained with Coomassie Brilliant Blue (2.5g Coomassie Brilliant Blue dissolved in 200mL glacial acetic acid, 900mL methanol and 900mL H_2O).

3.2.3 Elution of Fusion Proteins from Glutathione Sepharose Beads for BiaCore studies

After quantification, GST fusion proteins were eluted from the sepharose beads by incubation with elution buffer containing 5-10mM glutathione, 50mM tris pH8.0 for 20 min at 4°C. The beads were pelleted and the supernatant was removed; this was the primary elution. To each elution, 1mM dithiothreitol was added to prevent oxidation. These steps were repeated for a secondary elution and the remaining beads were resuspended to 50% with PBS+ containing 1mM dithiothreitol. A 10μL sample of each elution and the fusion protein that remained on the beads was taken to be checked on 10% SDS-PAGE stained with Coomassie Brilliant Blue.

3.2.4 The BiaCore apparatus

N-terminally biotinylated peptides were made by various sources (Amgen and HSC Laboratory Services). The peptides were dissolved to 1mg/mL concentration in 10mM Tris pH 8.0 and immobilized on streptavidin coated chips on the BiaCore apparatus. The purified GST fusion proteins were injected at 1mM into the BiaCore flow chamber for exposure to immobilized peptides. If binding occurred between a peptide and the fusion protein, a change in optical properties was displayed as Resonance Units (RU) by the BiaCore program.

The detection chamber of the BiaCore apparatus is composed of three layers: a layer of glass, a 50 nm layer of gold and a liquid layer in which the peptide of interest is immobilized (Fig. 3-1) (O'Shannessy et al., 1994). Plane-polarized, monochromatic light travels through the glass layer

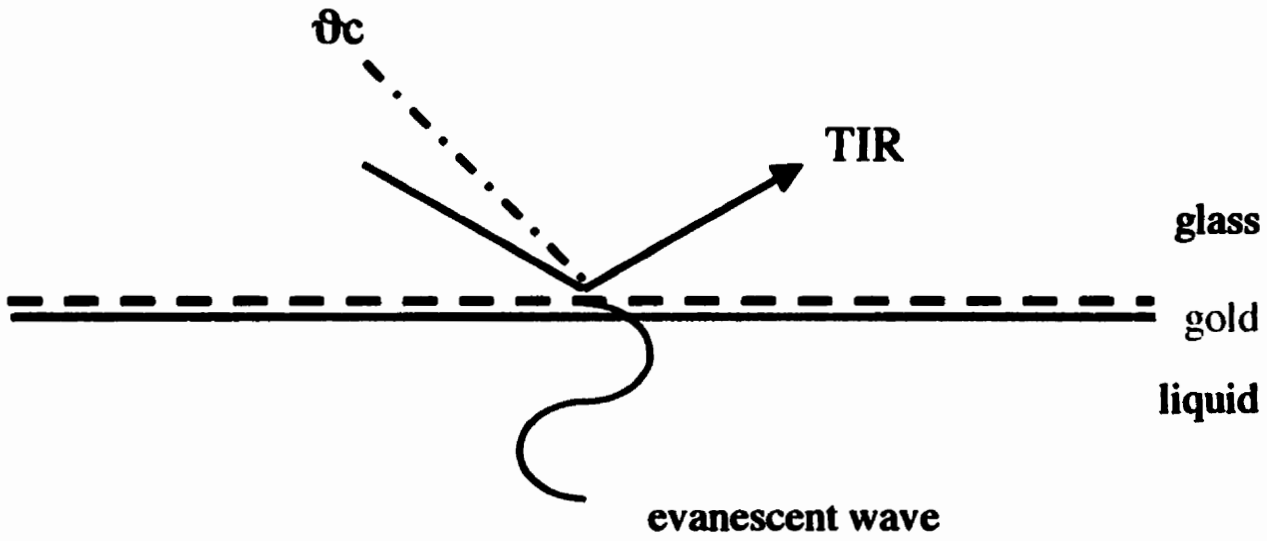

Fig. 3-1. The theory of plasmon resonance. A beam of light that is plane-polarized and monochromatic is shone through a glass layer and, below a critical angle (ϑc) of incidence, undergoes total internal reflection (TIR). At a specific angle, the evanescent wave emitted by the reflected light induces resonance in the plasmons of the 50 nm thick layer of gold. The angle at which plasmon resonance occurs depends on the refractive index of the adjacent solution.

and undergoes total internal reflection (TIR) when incident below a critical angle (ϑ_c). As TIR occurs, a component of the momentum of the plane-polarized light, called the evanescent wave, penetrates into the liquid layer up to a distance of one wavelength. At a specific angle of incidence, this evanescent wave is able to induce plasmons (free oscillating electrons) in the gold layer to resonate which causes a decrease in intensity of the reflected light. The angle at which resonance of the plasmons occurs depends on the refractive index of the adjacent liquid layer; the refractive index of the liquid layer depends on its composition. Therefore, when a protein interacts with the peptide, the composition of the liquid layer is modified which alters its refractive index. The change in refractive index alters the resonance angle, which is then detected by the BiaCore apparatus. A 0.1° change in the resonance angle results in an output of 100 response units.

3.2.5 Transient expression of FLAG-LNX in 293T cells

An expression construct of the pFLAGCMV2 (Sigma) vector containing the LNX long cDNA was a gift of Sascha Dho. 293T cells were grown at 37°C in DMEM+10% FBS containing 100μg/mL penicillin, 100IU streptomycin and 2mM glutamine. These cells were transfected at 50-60% confluency with 5-10μg of pFLAGCMV2-LNX long using OPTI-MEM and lipofectamine (GibcoBRL). Briefly, 5-10μg DNA and 8μg lipofectamine reagent were separately mixed with 800μL of OPTI-MEM then mixed together and incubated at room temperature for 15-40 min. Cells were washed once with sterile PBS. Then, 1.6mL of the DNA-lipofectamine mixture was brought to 8.0mL with OPTI-MEM and this was added to the washed cells. After incubation for 5 hours at 37°C, the DNA solution was removed and 10mL of growth media was added. After incubation at 37°C for 24-36 hours, cells were lysed in 1mL PLC lysis buffer (50mM HEPES pH7.5, 150mM NaCl, 10% glycerol, 1.5mM $MgCl_2$, 1% Triton-X-100, 1mM EGTA, 10mM $NaPP_i$, 100mM NaF, Complete® protease inhibitor tablet) and centrifuged 20 min at 14000 rpm. The supernatant was removed and stored at -80°C until use.

3.2.6 Western blotting

Samples (20μL unless otherwise stated) were separated by 8, 10 or 12% SDS-polyacrylamide gel electrophoresis (PAGE). Separated proteins were transferred to immobilon-P (Millipore) either

by a semi-dry or a submerged transfer apparatus (BioRad). Immobilon-P was blocked in 5% nonfat, skim milk powder dissolved in PBS (blotto) for 1-3 hours at room temperature. An appropriate antibody was added at specified concentration and incubated with mixing at 4°C overnight. Immobilon-P was washed five times for 5 min each in PBS containing 0.05% Tween-20 (Sigma) (PBS-T), then incubated with either protein A-HRP (BioRad) at 1:3000 concentration in PBS-T for one hour at room temperature or with goat anti-rabbit-HRP (BioRad) at 1:30000 concentration in 5% blotto for 45 min at room temperature. Immobilon was then washed five times for 5 min each in PBS-T. Either ECL (Amersham) or Chemiluminescence Reagent Plus (NEN) was used to develop blot according to manufacturer's instructions.

3.2.7 Production and affinity purification of antibodies

Three peptide antibodies were generated against different regions of LNX. αLNX-N rabbit polyclonal antibody was raised against a peptide antigen of amino acids 2-13 of LNX long (H2N-NQPDLADDPDPSPEPLC-COOH). αMid-J3 was raised against a peptide sequence from within PDZ2 of LNX (H2N-CVSRQVRQSSPDIFQE-COOH) and αJ3-QED was raised against a sequence found between PDZ3 and PDZ4 of LNX (H2N-CVLKALEVKEQETQED-COOH). Keyhole limpet hemocyanin-conjugated peptides were generated and used to immunize rabbits. The antiserum was tested for reactivity against *in vitro* transcribed and translated LNX long cDNA (pFLAG-LNX) produced in a T7 TNT-coupled reticulocyte lysate reaction (Promega). Five μl of the reaction was boiled in an equal volume of SDS-sample buffer, separated by SDS-PAGE and immunoblotted as described above.

αLNX-N, αmid-J3 and αJ3-QED rabbit polyclonal antibodies were individually affinity purified using the SulfoLink Kit from Pierce (Rockford, IL). Briefly, 5mg of each of the above peptides were dissolved in 1mL of Sample Preparation Buffer and coupled to a SulfoLink Coupling Gel column according to manufacturer's instructions. Crude serum was incubated with the appropriate column for 1 hour at room temperature with gentle mixing; the column was then washed with 16mL of PBS. The purified antibodies were eluted from the column with the addition of 8mL of Immunopure IgG Elution Buffer and collection of 1mL fractions in microcentrifuge tubes containing 50μL of 1M Tris pH9.5. The presence of protein in each

fraction was measured by absorbance at 280nm; the fractions containing protein were pooled and dialyzed overnight at 4°C against PBS. Protein concentration was measured by both absorbance at 280nm and SDS-PAGE and Coomassie staining of the gel.

αJ3NPAY-L rabbit polyclonal antibody was raised against a GST fusion protein of the NPAY region of LNX long. The GST-LNX NPAY fusion protein was purified by glutathione affinity chromatography and used to immunize rabbits. The antiserum was tested for reactivity against the GST-fusion immunogen and FLAG-LNX that had been transcribed and translated from pFLAG-LNX cDNA as described above.

αJ3NPAY-L rabbit polyclonal antibody was affinity purified by the following method. A nitrocellulose filter was incubated with bacterial lysate expressing GST for 1 hour and then blocked with BSA/ovalbumin in TBS (8g NaCl, 0.2g KCl, 3g Tris base, pH7.4 in 1L) for 30-60 min. After a quick rinse with TBS, the nitrocellulose was incubated with crude serum to remove antibodies recognizing GST or other bacterial proteins. During this time a second nitrocellulose filter was incubated with purified GST-J3NPAY-L construct for 1-2 hours, washed briefly with TBS and blocked for one hour with BSA/ovalbumin. Again after a brief wash, this second nitrocellulose was incubated with the precleared serum for 1-2 hours at room temperature or overnight at 4°C. The nitrocellulose was then washed 3-4 times with TBS containing 0.05% Triton X-100 (TBS-T) and two times with TBS. Adding 1mL of 0.2M glycine pH2.6 for approximately 2 min eluted the purified antibody. The solution was removed and added to a microcentrifuge tube containing 128 μL of 1M Tris pH9. The elution was repeated a second time with 0.5 mL of glycine. The two elutions were combined and dialyzed overnight at 4°C against PBS. The concentration was obtained by measurement of A_{280} as well as SDS-PAGE followed by staining of the gel with Coomassie Brilliant Blue.

3.2.8 GST fusion protein binding experiments

In a microcentrifuge tube 50-100 μL of transfected cell lysate was mixed with 3 μg of immobilized purified GST fusion proteins in a total of 1 mL of PLC lysis buffer for 90 min at 4°C to allow interaction to occur. Sepharose beads were pelleted and washed five times with 1

mL PLC lysis buffer. The beads were resuspended in 70μL of 2x SDS sample buffer (100mMTris pH6.8, 200mM dithiothreitol, 4% sodium dodecyl sulfate, 0.2% bromophenol blue, 20% glycerol, 5% β-mercaptoethanol) and boiled 5-7 min at 100°C. The samples were separated by 10% SDS-PAGE to perform western blotting as described above. αLNX-N was used as the primary antibody at a dilution of 1:250, protein A-HRP (BioRad) was the secondary reagent and the blot was developed as described above with ECL (Amersham).

3.2.9 Mouse brain homogenates

Adult mouse brains and mouse embryos were lysed in one of three buffers. The buffer PLC contained 50mM HEPES pH7.5, 150mM NaCl, 10% glycerol, 1.5mM $MgCl_2$, 1% Triton-X-100, 1mM EGTA, 10mM $NaPP_i$ (sodium pyrophosphate) and 100mM NaF (sodium fluoride). RIPA (radio-immuno precipitation assay) buffer contained 1% Nonidet P-40, 1% sodium deoxycholate, 0.1% SDS, 150mM NaCl, 10mM sodium phosphate pH7.2, 2mM EDTA, 50mM NaF. CHAPS buffer contained 50mM HEPES pH7.5, 150mM NaCl, 10% glycerol, 1.5mM $MgCl_2$, 10mM CHAPS, 1mM EGTA, 10mM $NaPP_i$ and 100mM NaF. A final method was used as follows. Two mouse brains were mechanically separated in 5mL of sonication buffer (10mM HEPES pH7.4, 100mg/L PMSF). 5mL of a second buffer (10mM HEPES pH7.4, 0.2M NaCl, 100mg/L PMSF, 2mM EDTA, 2% Triton-X-100) was added and the mixture was incubated at 4°C with end-over-end rotation for 4 hours. The sample was then ultracentrifuged at 100 000xg for 30 min in TLA100.2 (Beckman). The supernatant was removed at stored at -80°C until use. The protein concentration was determined by MicroBCA Protein Assay Reagent kit (Pierce, Rockford, IL).

An appropriate volume of brain homogenate containing 2.0mg of protein (286μL) was incubated with 10μL of αJ3NPAY-L and 50μL of 20% proteinA-sepharose or 5μg of GST alone, GST-L52 fusion or GST-NumbPTB fusion in a total of 1mL PLC lysis buffer. These mixtures were incubated for 90 min at 4°C with gentle mixing. The beads were pelleted and washed three times with 1mL PLC lysis buffer then resuspended in 70μL 2xSDS sample buffer. The samples were separated by 10% SDS-PAGE and transferred, αJ3NPAY-L (1:200) was then added, and the blot was incubated overnight at 4°C. The secondary antibody was goat-anti-rabbit-HRP and the blot was developed using Chemiluminescence Reagent Plus (NEN).

3.2.10 Preparation of HIS-HA-PRA1 in E. coli (M15 (pREP4)) cells

A construct encoding a hexahistidine (his) and hemagglutinin (HA) tagged PRA1 (L42) cDNA was generously provided by Dr. Johnny Ngsee at the Loeb Research Institute, Ottawa. This construct was transformed into competent *E. coli* (M15 (pREP4)) cells as described in Section *3.2.2*. A culture of 2mL LB+amp+kan was grown overnight at 37°C. The next day, 500μL of the culture was diluted into 5mL LB+amp+kan, and cultures were grown 2 hours at 37°C with shaking. The culture was then induced to produce fusion protein for 5 hours at 37°C with 1mM IPTG. The cells were pelleted and resuspended in sonication buffer (50mM phosphate buffer pH8.0, 300mM NaCl, 1% Triton-X-100). After sonication, as described in Section *3.2.2*, the sample was centrifuged for 10 min at 14000rpm. The supernatant was removed to a fresh tube with 30μL of Ni-NTA agarose beads (Qiagen) that had been washed once in sonication buffer. This mixture was incubated for 30 min at room temperature with gentle mixing then briefly centrifuged to pellet beads. The beads were washed three times in 0.5mL wash buffer (50mM phosphate buffer pH6.0, 300mM NaCl, 10% glycerol, 1% Triton-X-100). The fusion protein was then eluted with 0.3M imidazole in wash buffer. A small sample (3-5μL) was quantitated on 10% SDS-PAGE and the gel was stained with Coomassie Brilliant Blue.

3.2.11 Co-immunoprecipitation of HIS-HA-PRA1 and FLAG-LNX

To test for interaction between PRA1 and LNX, eluted HA-PRA1 fusion protein was mixed with 50-100μL of 293T-LNX lysate in the presence of αHA(12CA5) or αLNX-N (1:100) and 50μL of 20% protein A-sepharose in a total of 1mL PLC lysis buffer. The mixtures were incubated for 90 min at 4°C with gentle mixing followed by three washes of 1mL of PLC lysis buffer. The beads were resuspended in 70μL of 2xSDS sample buffer. Samples were separated by 10% SDS-PAGE and transferred. αHA(12CA5) or αLNX-N (1:250) was added and incubated overnight at 4°C. The secondary reagent was protein A-HRP, and the blot was developed using ECL (Amersham).

An alternate method was used to examine the PRA1-LNX interaction that was not observed in the initial co-immunoprecipitation studies. Induced M15(pREP4) cultures were pelleted and

resuspended in sonication buffer, sonicated and centrifuged as described above. The supernatant, however, was then incubated with αHA(12CA5) and 50μL of 20% protein A-sepharose to immunoprecipitate the HA-PRA1 fusion. The beads were washed three times with sonication buffer, 50-100μL of 293T-LNX was added, and the volume brought to 1mL with PLC lysis buffer. The mixture was then incubated for 90 min at 4°C with gentle mixing and washed three times with PLC lysis buffer. The beads were resuspended in 70μL of 2xSDS sample buffer, separated by 10% SDS-PAGE and transferred. The primary antibodies were αHA(12CA5) or αLNX-N (1:250), the secondary reagent was protein A-HRP and the blot was developed by ECL (Amersham).

3.3 RESULTS

3.3.1 BiaCore Studies

Biotinylated peptides consisting of the carboxy-terminal twelve amino acids of known proteins containing potential PDZ domain-binding motifs (Table 3-1) were synthesized and assayed for LNX binding using the BiaCore system (described in detail in Section *3.2.4*). These peptides had either been identified in a search of GenBank for proteins with a Ser/Thr-Xaa-Val* motif or as proteins potentially relevant to the function of Numb and LNX in mammalian cells (JM, unpublished data). For example, the carboxy terminal tails of Inscuteable, Jagged, Notch and several of the Frizzled isoforms were included since the Drosophila homologues of these proteins are connected to dNb and/or Notch. The biotinylated peptides were immobilized on streptavidin-coated sensorchips. Purified GST fusion proteins were injected at a constant rate (5 μl/min) and flowed past each peptide individually. Resonance units were simultaneously plotted v. time to show any interactions that occurred.

In the initial stages, only PDZ1, PDZ3 and PDZ4 purified fusion proteins were analyzed because we did not recognize PDZ2 as a PDZ domain at the time. Only PDZ1 bound to some of the peptides whereas PDZ3 and PDZ4 did not. The peptides recognized by PDZ1 were: mFz8, dFz1, dFz2, Sina, dINSC, dToll, hAPC, hFas, rNMDAR2β, mPKCα and rNaC.

3.3.2 BiaCore analysis of peptides based on yeast two-hybrid clones

The observation that PDZ3 and PDZ4 did not interact with any of the peptides tested suggests that the domains were not folded correctly. One reason for this may be that an insufficient number of amino acids were included on either side of the domains to allow for proper conformation. Therefore, new constructs with larger boundaries were designed and generated for PDZ3 and PDZ4 for both the yeast two-hybrid interactions (fusion to LexA DBD) and for *in vitro* binding experiments (fusion to GST). At this time, it was also recognized that another PDZ domain existed between PDZ1 and PDZ3. Fusion proteins of the PDZ2 domain with LexA DBD and GST were also created.

The new GST-PDZ4 fusion protein with larger boundaries accumulated within the bacterial cells

Table 3-1. Sequence of biotinylated peptides used in BiaCore studies using single letter amino acid codes; * indicates carboxy terminus.

Name of Peptide	Source	Sequence
L45	TI-225/polyubiquitin	SKK SPP CAC SWV*
L61	novel	LEK LKN QNS FMV*
L42	PRA1	AD GEE LQM EPV*
L19	TRIP13/HPVE16PBP	QFE ERK KLA AYI*
L52	novel	KAP PGP KGP TLV*
mFz8	mouse Frizzled8	VSY PKQ MPL SQV*
mFz7	mouse Frizzled7	RLS HSS KGE TAV*
mFz4	mouse Frizzled4	WVK PGK GNE TVV*
hFz5	human Frizzled5	ATY HKQ VSL SHV*
dFz1	Drosophila Frizzled1	GKE PRT RAQ AYV*
dFz2	Drosophila Frizzled2	HHV LKQ PAA SHV*
Sina`	Drosophila seven-in-absentia	GNL GIN VTI SLV*
dINSC	Drosophila Inscuteable	LKF NLT RQE SFV*
dToll	Drosophila Toll	FII NTN AKQ SDV*
mNotch1	mouse Notch1	PSQ ITH IPE AFK*
mNotch2	mouse Notch2	SEP PHS NMQ VYA*
mJGD1	mouse Jagged1	SAQ SLN RME YIV*
hAPC	human adenopolyposis carcinoma	KRH SGS YLV TSV*
hFas	human Fas	NSN FRN EIQ SLV*
rNMDAR2β	rat glutamate receptor, NMDAR2 β subunit	VYE KLS SIE SDV*
mPKCα	mouse protein kinase Cα	PQF VHP ILQ SAV*
rNaC	rat sodium channel, cardiac subtype, α subunit	YSG AIV VRE SIV*
rNGFR	rat neurotrophic growth factor receptor	SLC SES TAT SPV*
rVCAM	rat vascular cell adhesion molecule	SYS LVE AQK SKV*
mLERK5	mouse Eph receptor ligand, ephrinB1	PPQ SPA NIY YKV*
mSyn	mouse syndecan	YQK PTK QEE FYA*
NbC	Numb C terminus	SSD LQK TFE IEL*

in inclusion bodies making it difficult to purify sufficient amounts of protein for experiments. Because attempting to purify the protein by denaturation and renaturation would generate a protein of unknown conformation, we chose not to study PDZ4 further in this experiment. However, we were able to purify sufficient amounts of the new PDZ2 and PDZ3 fusion proteins, thus they were included in subsequent experiments.

Peptides were synthesized representing the clones isolated from the yeast two-hybrid screen that contained potential PDZ consensus motifs. The peptides were based on the novel clones L42, L52 and L61 and the clone L45 which encodes TI-225/polyubiquitin. A peptide based on the carboxy terminus of L65 (syntaxin5) was attempted but was too insoluble to purify. These new peptides as well as some of the original peptides generated were tested with PDZ1 and the new PDZ2 and PDZ3 fusion proteins. Once again, PDZ3 did not interact with any of the selected peptides. However, PDZ1 interacted with both L45 and L52 and PDZ2 interacted with L45, L52, L61, mSyn and hAPC (Figs. 3-2 and 3-3).

The fusion proteins encoding pairs of PDZ domains, that is, PDZ1/2, PDZ2/3 and PDZ3/4 were also tested with L42, L52, L61 and a peptide based on the carboxy terminus of Numb (NbC). PDZ1/2 recognized L52 and L61 (Fig. 3-4a). The interaction with L52 appeared to be quite strong.

The response in RU between L52 and PDZ1/2 was measured at several concentrations of PDZ1/2 in order to estimate a constant of dissociation (K_d) for the interaction (Fig. 3-4b). Analysis of the association and dissociation rates predicts a K_d of 0.76 μM between PDZ1/2 and L52.

3.3.3 In vitro mixing experiments with the yeast two-hybrid isolated clones

To verify if the six clones selected in the yeast two-hybrid screen bind to LNX *in vitro*, the open reading frame of each of the clones was inserted into the vector pGEX4T1 for fusion to

Fig. 3-2. Interaction of L42, L52, L61 and NbC peptides with PDZ1 in BiaCore. Bulk change in response units upon injection of fusion protein due to change in running buffer.

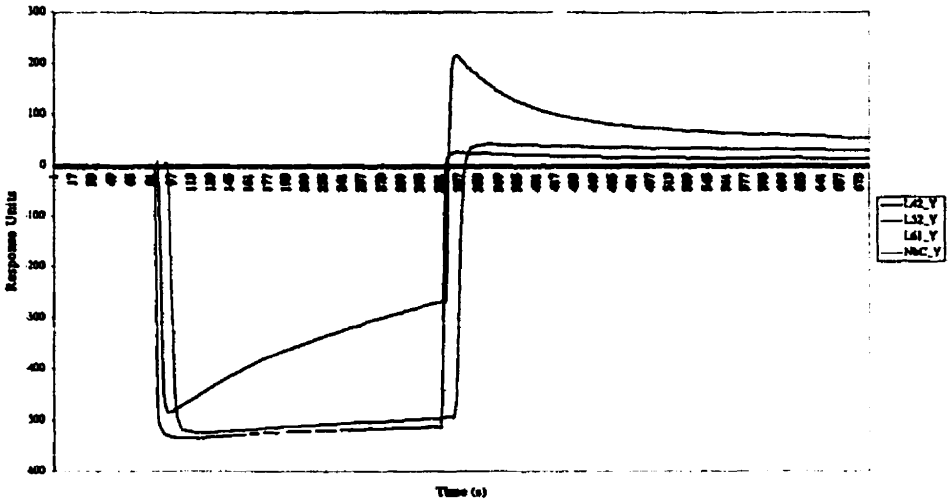

Fig. 3-3 Interaction of L42, L52, L61 and NbC peptides with PDZ2 in BiaCore.

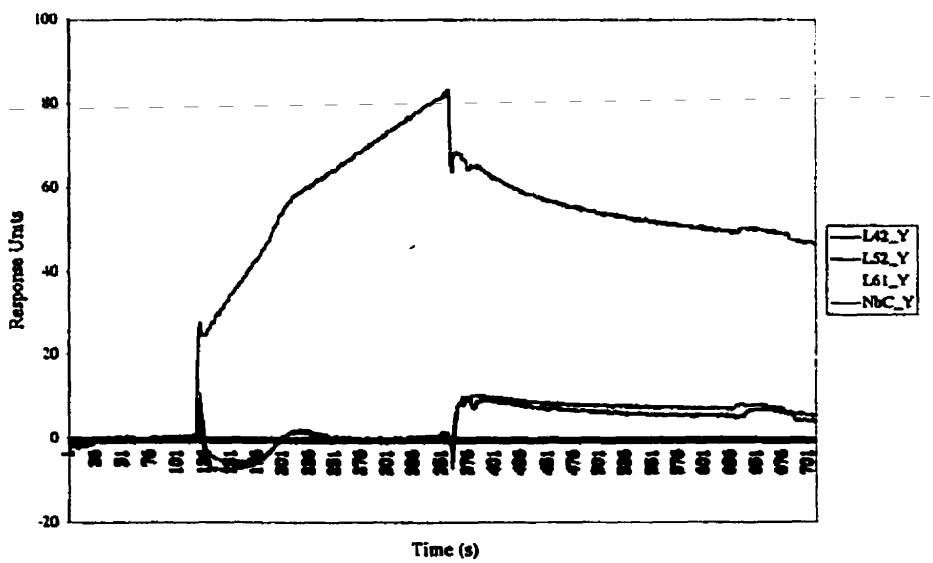

Fig. 3-4a. Interaction of L42, L52, L61 and NbC peptides with PDZ1/2 in Biacore

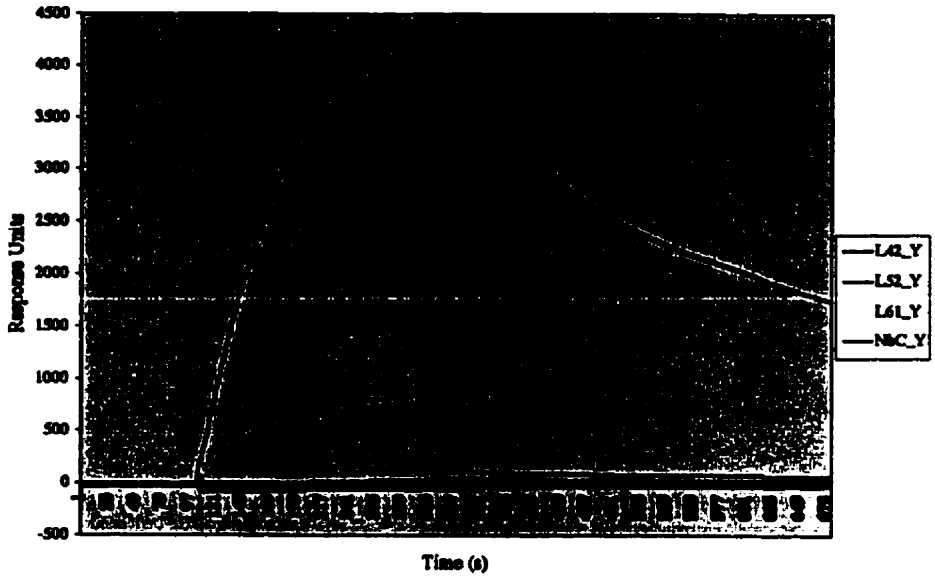

Fig. 3-4b. Increasing concentrations of PDZ1/2 (from bottom (grey) to top (light blue): 0.15 μM, 0.3 μM, 0.6 μM, 1.2 μM, 2.4 μM and 9.6 μM) with L52 peptide in BiaCore apparatus for estimation of K_d.

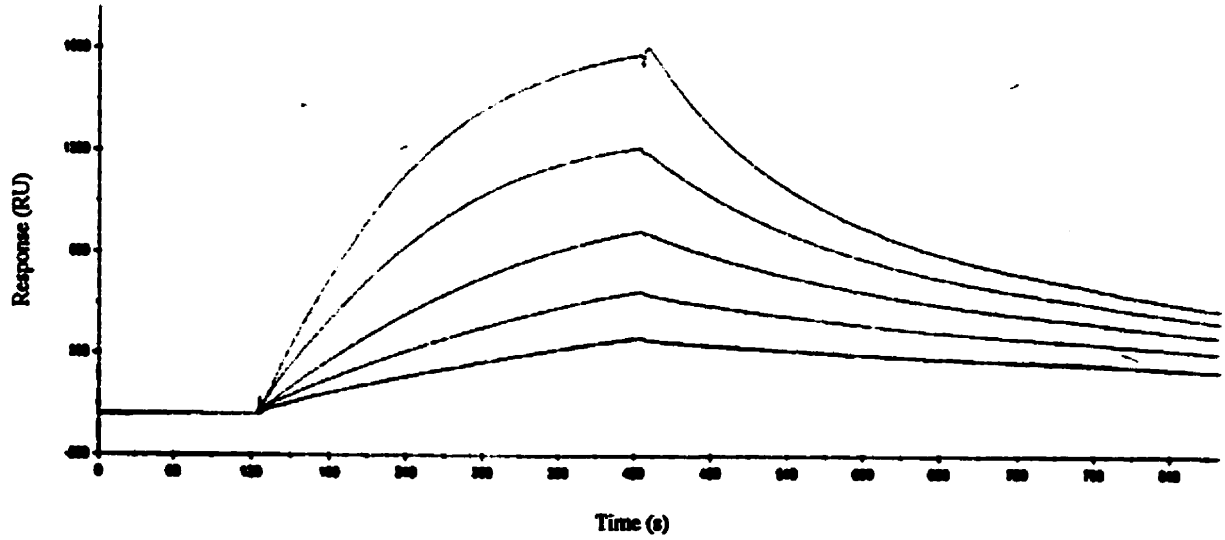

glutathione-S-tranferase (GST). Five of the six clones were successfully purified as GST fusion proteins. The sixth, GST-L61, was insoluble and collected in inclusion bodies within the bacterial cells making immobilization of protein on glutathione-sepharose beads with the proper conformation difficult.

These five fusion proteins bound to glutathione-sepharose beads were mixed *in vitro* with lysate from 293T cells that had been transfected with the pFLAG-LNX expression construct. The bound complexes were washed, separated by SDS-PAGE, transferred to immobilon and precipitated LNX was detected using αLNX-N (Fig. 3-5). Only L52 bound to LNX long in this assay.

We have not tested the binding of these fusion proteins to LNX short in a similar assay since we were not able to detect the expression of the LNX short protein transfected into 293T cells. The reason for this is unknown since the sequence of the construct has been confirmed and proteins were made when the cDNA was tested by *in vitro* transcription and translation. This suggests that either 293T cells do not use this translation start site or the protein which is generated is extremely unstable.

3.3.4 In vitro mixing experiments with PRA1

A six-histidine (his) and hemagglutinin (HA) tagged version of PRA1 (L42), a generous gift from Dr. Johnny Ngsee, Loeb Research Institute, Ottawa, was also utilized to test for *in vitro* interaction between PRA1 and LNX. Despite a variety of methods attempted for mixing the two fusion proteins *in vitro*, no interaction was seen (data not shown). The first method consisted of adding his-HA-PRA1 fusion protein purified from *E. coli* (M15 (pREP4)) cells to 293T-LNX transfected lysates. Mixtures were immunoprecipitated with either αHA(12CA5) or αLNX-N and western blotted for both PRA1 and LNX. It was observed that both PRA1 and LNX were present but were not able to associate. A second method that confirmed these results involved incubating αHA(12CA5) immunoprecipitations from *E. coli* (M15 (pREP4)) lysates with 293T-LNX lysates.

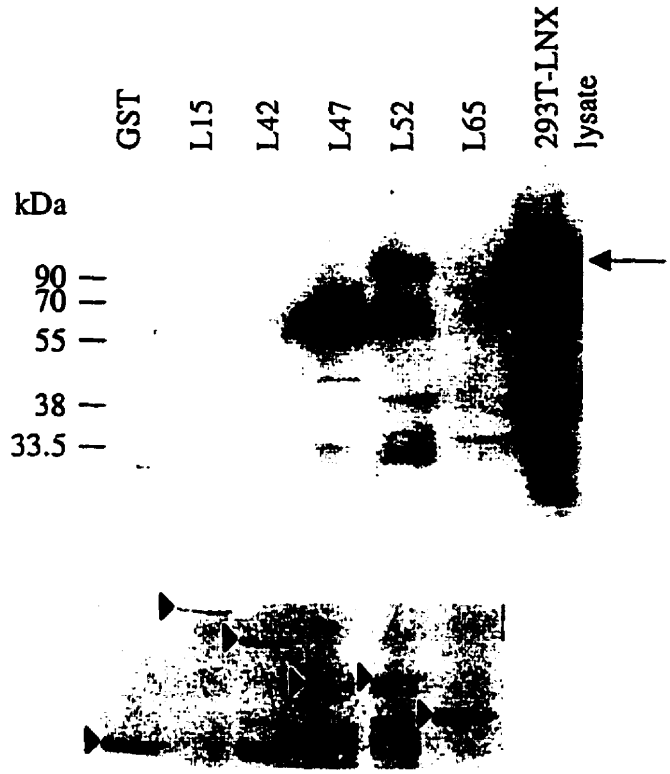

Fig. 3-5. Upper panel: *In vitro* mixing of GST fusion proteins with LNX-transfected 293T lysate, western blot with αLNX-N. Arrow indicates LNX long. Lower panel: Commassie stain of same blot, arrowheads indicate position of GST fusion proteins

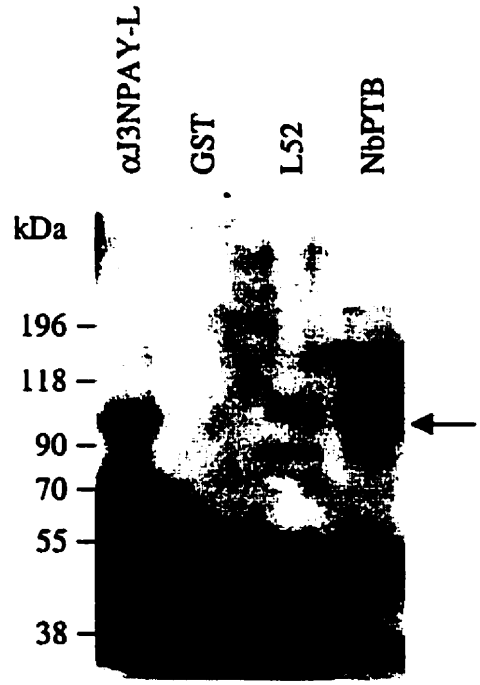

Fig. 3-6. Immunoprecipitation and GST pulldown of endogenous LNX short from mouse brain homogenates. Arrow indicates LNX short.

3.3.5 In vivo expression studies

The tissue distribution of LNX mRNA has been previously examined (Dho et al., 1998). It was found that the two isoforms of LNX are differentially expressed in adult mouse tissues. While both isoforms are expressed in heart, only LNX long is expressed in lung, skeletal muscle and kidney and LNX short is expressed in brain. Using this information, several cell lines commonly used in our laboratory (NIH 3T3, P19, C2C12, MDCKII) were tested for LNX expression by immunoprecipitation, western blotting, northern blotting and reverse-transcriptase (RT)-PCR. Very low amounts of expression were observed by RT-PCR in NIH3T3 and C2C12 cells at specific stages of culture. Several antibodies have been generated against various regions of LNX long and short and have been shown to recognize FLAG-LNX in transfected cell lysates. However, we have had difficulty visualizing endogenous LNX from cell lines with these same antibodies. A few immunofluorescence experiments in NIH3T3 and MDCKII cells were attempted but were not reproducible.

Several attempts were made to isolate the LNX short endogenous protein from embryo or brain homogenates using three different lysis conditions. PLC, RIPA and CHAPS buffer were all employed in making tissue homogenates however neither immunoprecipitation nor western blotting of LNX short protein was observed. An alternative method that proved to be successful was adapted from Wang et al. (1997) who used this procedure to isolate a neuronal PDZ protein, Rim, which is thought to be closely associated with the membrane. Rat brains were placed in hypotonic buffer for homogenization followed by addition of an equal volume of more complex buffer. The mixture was incubated at 4°C for 4 hours with end-over-end rotation and then centrifuged in an ultracentrifuge. Using this method, we generated mouse brain homogenates with a protein concentration of 7mg/mL.

Several antibodies predicted to recognize the LNX short protein were then used for immunoprecipitation from lysate containing 1.0mg of protein followed by western blotting. A band of the appropriate size was observed in the immunoprecipitation using the αJ3-NPAY-L antiserum (Fig. 3-6). We then tested whether the panel of antibodies generated against LNX were able to recognize this same band from a volume of homogenate which contained 2.0mg of

protein. Only αJ3-NPAY-L recognized the band corresponding to LNX short, which may suggest that the band observed is an artifact generated by one antibody. We therefore confirmed that this was the LNX short protein by using GST fusions of either the Numb PTB domain or L52 to identify an αLNX immunoreactive band of the appropriate size.

3.4 DISCUSSION

3.4.1 PDZ1 and PDZ2 may recognize a classical PDZ motif

Comparison of the amino acid sequences of the peptides recognized by PDZ1 allowed some preliminary prediction of PDZ1 binding specificity. PDZ1 appears to preferentially recognize E/Q-S-X-V*, a type I PDZ recognition motif. Although not all of the peptides bound by PDZ1 fit this consensus, all of the available peptides which contained this motif were recognized by PDZ1 however, the basis of the selectivity of interaction was not always clear. For example, PDZ1 recognized the following peptides: mFz8 with a carboxy terminus of -LSQV*, dFz2 (-ASHV*), Sina (-ISLV*), rNMDAR2β (-ESDV*) and rNaC (-ESIV*) and yet did not recognize hFz5 (-LSHV*). This suggests that amino acids upstream of the last four may be involved in target recognition by a PDZ domain. However, in the experiments performed here, no consensus was seen with any amino acids from the -4 to the -12 position. Some of the peptides that were recognized by PDZ1 may be indicative of physiologically relevant interactions. Both the frizzled family of proteins and the inscuteable protein are known to be important in Numb and Notch function (Gho and Schweisguth, 1998; Kraut and Campos-Ortega, 1996; Kraut et al., 1996). However, a mammalian inscuteable counterpart has not yet been isolated making it difficult to predict whether an inscuteable- like molecule plays a role in signaling by mammalian Numb.

A consensus recognition motif based on the four peptides recognized by PDZ2 may be T/F-X-V/A*. If this was true, it would be expected that both mFz7 (ETAV*) and mFz4 (ETVV*) would also be recognized by PDZ2. Since this did not occur, I believe that the recognition of peptide targets by PDZ2 involves more than just the last three amino acids of the peptide. However, no consensus amino acids at any other position were readily apparent when the four peptides that were recognized by PDZ2 were examined. Further experimentation is required to determine the specificity of PDZ2.

Isolated PDZ1 and PDZ2 domains both recognized L52, and the fusion protein encoding both PDZ domains, PDZ1/2, recognized L52 and L61. The interaction between L52 and PDZ1/2 appeared to be the strongest of all the interactions tested. It is possible that the PDZ1/2 construct was able to cooperatively bind to L52. Preliminary interaction kinetics were measured and

predicted a K_d of 0.76 μM, however, this may be an overestimation. Several factors can contribute to overestimation of the K_d for a specific association using this BiaCore method. It is known that GST is able to dimerize in solution (Ji et al., 1992) and that this dimerization can have an avidity effect on BiaCore measurements when the immobilized ligand is above a threshold concentration of 0.1ng/mm^2 (Ladbury et al., 1995). Also, the observed response in the BiaCore is directly proportional to the size of the molecule in solution (Ladbury et al., 1995). Although the K_d measured here is similar to BiaCore measurements from other PDZ domains (Hirao et al., 1998; Irie et al., 1997), this interaction should be tested again using two different surface concentrations of peptide that are both below 0.1ng/mm^2.

Although the clone L45 was not recognized by an individual PDZ domain in the yeast two-hybrid assay, a peptide based on the L45 carboxy terminus was recognized by PDZ1 and PDZ2 in the BiaCore. This clone has a type I PDZ recognition motif at the carboxy terminus. It is possible that the PDZ domains do not recognize those amino acids in the context of the fusion protein and may be an example of the loss of selectivity for biologically relevant interactions when isolated PDZ domains are used in the BiaCore. Likewise, PDZ1 of murine LNX recognized several peptides based on Drosophila proteins that may be addressed by two explanations. Either LNX can interact with as-of-yet unidentified mammalian counterparts to these proteins or there is a loss of selectivity in these interactions. The issue of biological relevance of an interaction can be addressed by comparison of results from a number of techniques (i.e., yeast two-hybrid assays, *in vitro* mixing and BiaCore experiments).

3.4.2 PDZ3 and PDZ4 may have unique target sequences

No interaction between PDZ3 or PDZ4 and any of the peptides was observed. It is possible that the interaction motifs recognized by PDZ3 and PDZ4 were not represented in the group of peptides generated based on the carboxy terminal sequence of known proteins. As well, no interaction was observed between L42, L52, L61 or NbC and PDZ3, PDZ2/3 or PDZ3/4. Both classes of PDZ recognition motifs (Songyang et al., 1997) were represented the group of peptides tested however, there may not have been sufficient variation in these sequences to identify interacting molecules.

3.4.3 Testing the interaction between LNX PDZ domains and the Numb C terminus

We also tested the carboxy terminus of Numb in these studies because of previous results indicating that there may be a second interaction site between LNX and Numb independent of the described PTB-NPAY interaction (Dho et al., 1998). Residual interaction was observed between a fusion protein of LNX encoding the PDZ1 but lacking the NPAY recognition site. However we did not observe an interaction between any of the PDZs or PDZ pairs and the NbC peptide in the BiaCore.

3.4.4 In vitro interactions with LNX

We have demonstrated an interaction between LNX and L52 in the yeast two-hybrid setting, in BiaCore and *in vitro* which may be indicative of an *in vivo* interaction between these two proteins. L52 encodes a novel protein with little homology to any known proteins. This makes it very difficult to predict the role of an interaction between L52 and LNX. There are several expressed sequence tags (ESTs, AA182356, AA612528, AI603957, AI666282) isolated from mammary gland and thymus that are identical to L52 indicating that the mRNA is expressed *in vivo*. In addition, the genomic sequence NG23 (AF109905) is predicted to encode a protein identical to L52 (AAC84153). This sequence predicts a protein of 146 amino acids. If this is correct, then our cDNA sequence is missing only the amino terminal 23 amino acids. An important next step is to examine the size of the mRNA by northern blot analysis to confirm that the genomic sequence predicts the entire protein.

It is important not to exclude other clones from consideration as encoding true *in vivo* interacting proteins. It may be that some other requirement for interaction is met inside the yeast cell, which is not available in BiaCore and *in vitro* mixing of GST fusion proteins. In addition, it is possible that these proteins interact with LNX short but not LNX long in spite of the results in the yeast two-hybrid assays or that the interaction may only be detected in the intracellular environment. It will be interesting to see if the GST fusion proteins encoded by any of the other clones are able to interact with LNX short using the brain homogenates that are described below.

3.4.5 Endogenous LNX short

In the search for endogenous LNX protein, we tested several different lysis conditions on different tissues to address potential differences in the ability to solubilize and isolate the protein. Mouse brains and embryos were homogenized in three standard buffers but LNX short was not observed by immunoprecipitation or western blotting. In all three cases, many non-specific bands were seen in the lysate and no bands of appropriate size were seen in immunoprecipitations (data not shown). The method previously used to isolate the PDZ protein Rim was then identified and employed to successfully extract LNX short from brain homogenate (Wang et al., 1997).

We found that only one of the αLNX antibodies recognized the LNX short protein from brain. It may be that αJ3-NPAY preferentially recognizes more of the RING finger and thus does not recognize LNX short very strongly. As well, the recognition site for αmidJ3 is within the PDZ2 domain and αJ3-QED recognizes LNX between the PDZ3 and PDZ4 region. In both of these cases, the epitope may be inaccessible when LNX is in its native conformation, which would explain why these two antibodies were unable to immunoprecipitate LNX short. However, this does not explain why an immunoprecipitation with αJ3-NPAY-L followed by western blot with αmidJ3 or αJ3-QED did not work. It is possible that the affinity of the peptide antibodies for LNX is too low. Regardless, GST fusion proteins of the Numb PTB and L52 were used to show that the band isolated by αJ3-NPAY-L can also be isolated through interacting molecules. This establishes the identity of this protein as LNX short.

3.4.6 Interaction with PRA1

The clone identified as L42 is reported to interact with Rab proteins in the yeast two-hybrid system (Janoueix-Lerosey et al., 1995; Martincic et al., 1997). Rab proteins are members of the Rac/Rho family of small G protein binding molecules. They are associated with intracellular vesicles and juxta-membrane regions and are involved in membrane fusion events. One group identified PRA1 (L42) from a yeast two-hybrid screen with Rab5 (Janoueix-Lerosey et al., 1995) while another group was interested in identifying molecules which interact with Rab3A (Martincic et al., 1997). The lack of interaction seen between LNX and his-HA-PRA1 *in vitro* corresponds with the results seen from mixing LNX with GST-tagged L42 and from the BiaCore.

However, lipid modification is required for interaction to occur between PRA1 and Rab3A fusion proteins so it is possible that post-translational modification is also required for a PRA1-LNX interaction. In any *in vitro* mixing experiment, the fusion proteins (either fused to GST or his-HA in this case) are generated in bacterial cells where post-translational modifications, like those seen in mammalian or yeast cells, cannot occur.

PRA1 is expressed in all rat tissues examined (Martincic et al., 1997)) including those tissues in which LNX is expressed in mouse (i.e., heart, brain, lung, skeletal muscle and kidney). Thus, a physiological interaction is possible between these two molecules. However, rat tissue lysates of Triton-X-100 soluble proteins were shown to contain PRA1, which is in contrast to the results presented here whereby endogenous LNX is not observed in Triton-X-100-solubilized lysates. Thus, in the tissues examined, PRA1 was not associated with the membrane whereas LNX must be isolated in a unique way in which membrane associated proteins can be separated from the membrane fraction after cell lysis. It is possible, however, that, similar to Rab molecules (Martinez and Goud, 1998), PRA1 translocates to the submembranous region at different points in its signaling pathway to permit interaction with LNX. Further experiments should be performed to confirm whether PRA1 is an *in vivo* interaction partner for LNX. For example, the brain and lung lysates from which endogenous LNX has been isolated may be tested for LNX-PRA1 coimmunoprecipitation.

Chapter IV Conclusions and Future Directions

4.1 CONCLUSION

A yeast two-hybrid screen was performed in order to identify target proteins of the LNX PDZ domains. Six candidate molecules were identified and preliminary analyses of the interactions were performed. Each of the isolated clones was assessed for its ability to interact with individual PDZ domains in the yeast two-hybrid system. One of the clones, L61, was shown to require its 14 carboxy terminal residues for LNX binding in a yeast two-hybrid assay. Interactions between LNX and five of the clones were examined *in vitro*; the clone L23/L52 was bound by LNX. Peptides based on the carboxy terminus of three of the clones were utilized in BiaCore studies with some of the PDZ domains. Many other peptides based on known proteins were also tested with each of the LNX PDZ domains. The *in vivo* relevance of these results could next be examined using the technique described herein for isolation of endogenous LNX short protein.

4.2 COMPARING THE LNX PDZ DOMAINS TO SOLVED PDZ STRUCTURES

Some preliminary predictions can be made by comparing the sequences of the LNX PDZ domains to those PDZ domains whose structures have been solved. The structures of the third PDZ domains of PSD-95 and hDlg, which are both type I PDZ domains, have been described and critical residues for structure and function were identified (Doyle et al., 1996; Morais Cabral et al., 1996). Notably, these two structure studies described similar domain structure and conserved residues. As well, the crystal structure of the type II PDZ domain of hCASK has been determined (Daniels et al., 1998). Most recently, a PDZ-PDZ heterodimer was crystallized and described (Hillier et al., 1999). Described below is a comparison of each PDZ domain of LNX to these crystal structures.

The residues important for the creation of a hydrophobic pocket for the carboxy-terminus of a target peptide are highly conserved in their hydrophobic nature between type I and type II PDZ domains (Daniels et al., 1998; Doyle et al., 1996). The four residues lining the hydrophobic pocket of PSD-95 PDZ3 are Leu-323, Phe-325, Ile-327 and Leu-379. These correspond to Met-501, Ile-503, Leu-505 and Leu-556 in hCASK. In each of the LNX PDZ domains, hydrophobic

residues are found in the corresponding positions. Both the PDZ1 and PDZ2 domains substitute Ile for the residue corresponding to Phe-325 and Leu for the Ile-327 position while the leucine residues corresponding to Leu-323 and Leu-379 are conserved. The LNX PDZ3 domain is slightly different; Leu519, Met521, Val523 and Leu579 line the hydrophobic pocket. The residues involved in forming the hydrophobic pocket in LNX PDZ4 are identical to those in PSD-95 PDZ3 suggesting that PDZ4 might bind a carboxy-terminal valine residue. It has been proposed that the minor variation seen between PDZ domain hydrophobic pockets may be responsible for the variable 0 position residues observed in target molecules (Doyle et al., 1996). That is, the size of the hydrophobic pocket created will prefer a larger or smaller residue at the 0 position.

The differences observed between the type I and type II PDZ domains lie in the residues found to determine the sequence specificity for the -2 position amino acid of the target peptide. Gly-329 and His-372 of PSD-95 PDZ3 were identified as important for specific recognition of Thr-2 in the target peptide. For the type II PDZ domain of hCASK, the residues interacting with the -2 position are Met507 and Val549. These residues correlate well to a hydrophobic -2 position residue in the target peptide. Both PDZ1 and PDZ4 of LNX have Gly and His residues at the corresponding sites for -2 position recognition. This would suggest recognition of a Ser or Thr in the target peptide. LNX PDZ2 has Arg403 and Pro446 at the corresponding positions for -2 residue recognition. It is difficult to predict what residues would be recognized at this position by comparing it to PDZ domains with known targets because these residues are rarely seen at these positions. From the yeast two-hybrid and BiaCore studies described here, PDZ2 appears to recognize Thr and Phe at the -2 position. It may be that these particular residues in PDZ2 (Arg403 and Pro446) facilitate unique specificity for Thr or Phe at the –2 position of the peptide. LNX PDZ3 has Gly525 and Arg572 at the -2 position-binding sites. This may suggest that PDZ3 recognizes Ser or Thr at the -2 position since several other type I PDZ domains are known to have Arg rather than His at this position.

The structure predictions can then be compared to the consensus interaction sequences observed in the experiments described in this work. By sequence-structure comparison, PDZ1 is predicted

to recognize Ser/Thr-Xxx-Val-COOH. From the BiaCore analysis, a preliminary consensus of Glx-Ser-Xxx-Val was generated which corresponds well to the prediction. PDZ2 would be predicted to recognize a carboxy-terminal valine but the -2 position residue would be difficult to predict due to the unique residues that create the -2 position binding pocket. A preference for peptides containing the sequence Thr/Phe-Xxx-Val/Ala-COOH was observed in BiaCore studies. PDZ3 is predicted to recognize Ser/Thr-Xxx-Phe/Tyr/Ile. None of the peptides used in this study were recognized by PDZ3 so the prediction could not be tested. Consistent with this prediction, this motif was not present in any of the peptides used here. PDZ4 is likely to recognize Ser/Thr-Xxx-Val, however, there were problems with the conformation and solubility of the PDZ4 constructs so we were unable to determine its binding specificity.

Another sequence-structure relation that can be studied involving the LNX PDZ domains is whether they can form or recognize βfingers as seen in nNOS and α1-syntrophin, respectively (Hillier et al., 1999). Since only one example of such an interaction has been described structurally, it is difficult to reliably predict whether this type of interaction occurs with other PDZ domains. However, performing a direct comparison between the LNX PDZ domains and nNOS or α1-syntrophin may provide some preliminary indications. Despite the few residues found between PDZ1 and PDZ2 of LNX, there is still potential for formation of a βfinger in this region. An Asp is conserved in βD of PDZ1 for stabilization of the βfinger structure by salt bridge formation with Arg380, located in a potential βH region in the linker between PDZ1 and PDZ2. As well, the linker region contains a potential pseudo-peptide motif (Ser-Asn-Ala-His-Val) followed by potential βturn residues (Pro-Asp or Gly-Pro).

The region between PDZ2 and PDZ3 is much larger and is expected to be able to accommodate a βfinger much more easily. Residues are present in this region that could potentially participate in the βturn and salt bridge, however, there does not appear to be a pseudo-peptide motif. It is unlikely that PDZ2 and the adjacent residues are able to form a βfinger according to the current structural understanding. The linker between PDZ3 and PDZ4 has a potential pseudo-peptide motif followed by potential βturn residues but they are not contiguous as would be expected for βfinger formation. In addition, there is no Arg residue to participate in a salt bridge with the Asp

in βD, but this could conceivably be provided by another type of residue. Nonetheless, it appears unlikely that PDZ3 and the adjacent residues are able to form a βfinger based on the results from Hillier et al. (1999). Lastly, there are only five residues at the carboxy-terminus of LNX following PDZ4, which is not enough for a potential βfinger. In all of these cases it is important to remember that there is only one example of a βfinger structure determined, thus the important residues for generating this type of a structure are not yet well-defined. The predictions described here are solely based on these results and are entirely speculative.

The other sequence-structure relationship described by Hillier et al. (1999) is the ability of α1-syntrophin to recognize a βfinger. The residues deemed critical for this type of interaction were Ser95, Asn102, Ser109, His142 and Asp143. Residues corresponding to these positions are not conserved in LNX PDZ1, PDZ3 and PDZ4. Some of the corresponding residues in PDZ2 have conservative changes: Asp406 of LNX PDZ2 corresponds to Asn102 and Glu447 in PDZ2 is at the position corresponding to Asp143 of α1-syntrophin. However, the other residues specified are not conserved between α1-syntrophin and LNX PDZ2. Although it may still be possible for PDZ2 to bind a βfinger, analysis of more βfinger-interacting PDZ domains must be performed in order to better predict whether this is in fact the case.

4.3 LNX AND EPHRINS

Concurrent with this yeast two-hybrid study, LNX was isolated in a yeast two-hybrid screen utilizing the cytoplasmic tail of the transmembrane ligand, ephrinB1 (C. Cowan, M. Henkemeyer, personal communication). In initial experiments, we have not been able to co-immunoprecipitate LNX and ephrinB1 or ephrinB2 from cell lysates. However, interaction between cotransfected LNX and Ephrin B1 has been observed (C. Cowan, M. Henkemeyer, unpublished results). The next step will be to determine whether LNX and ephrinB molecules are localized to similar intracellular structures and whether the endogenously expressed proteins co-immunoprecipitate. These studies are an ongoing collaboration with the lab of Mark Henckemeyer at the University of Texas, Southwestern Medical Center, Dallas.

4.4 FUTURE EXPERIMENTS

4.4.1 LNX PDZ-mediated interactions

From the yeast two-hybrid screen, LNX was found to associate with two different molecules that are (or are possibly) involved in vesicular trafficking through the ER and golgi, syntaxin5 and PRA1. Syntaxin5 is required for vesicle fusion events as are certain Rab isoforms with which PRA1 has been shown to associate. It is possible that LNX plays a role in localizing cytoplasmic or transmembrane proteins to the ER or golgi apparatus. Immunohistochemistry of endogenous LNX is one method that could be used to examine whether LNX exhibits a perinuclear staining pattern.

To further examine the interaction of LNX with all of the clones isolated, it will be helpful to generate deletion mutants like L61. The carboxy terminal regions of the other five clones should also be deleted and tested for interaction with LNX. As well, all six deletion mutants could be tested for interaction with each of the PDZ domains and pairs of PDZ domains.

There are examples of PDZ domain mutations that have eliminated the ability of the PDZ domain to bind its target. Several of these mutations have been at a conserved site within the PDZ domain that disrupts the tertiary structure of the PDZ domain. INAD Met442Lys, a mutation in the third PDZ domain, abolishes the ability of INAD to bind to and localize the transmembrane protein TRP (Shieh and Zhu, 1996; Tsunoda et al., 1997). A similar mutation has been made in PDZ2 of PSD-95 (Leu241Lys) and the nNOS PDZ (Val93Lys) domain (Christopherson et al., 1999). In all four PDZ domains of LNX, there is a leucine at the corresponding sites (Leu357, Leu462, Leu588 and Leu718 in LNX long). Mutations at these sites could be generated and tested for loss of specific interactions or changes in protein stability and localization of LNX or other putative target molecules.

4.4.2 In vivo LNX

It will be interesting to examine whether LNX is phosphorylated on serine or threonine *in vivo*. This may regulate the localization of LNX and its binding partners within the cell or the function of LNX in Numb signaling pathways. A putative serine/threonine kinase, Nak, has been found to

associate with dNb (Chien et al., 1998). Studies are ongoing in our laboratory to isolate and characterize a mammalian homologue of Nak.

Gene-targeted deletion of Nb in mice is currently underway in our laboratory. It will be interesting to examine LNX in the various tissues of these mice with respect to protein expression and stability and subcellular localization.

4.4.3 The RING finger domain

The function of the RING finger in signal transduction molecules is not well understood. Some RING fingers homodimerize (Inouye et al., 1997), and there is recent evidence that other RING fingers are involved in the ubiquitin pathway (Hu and Fearon, 1999; Lorick et al., 1999; Tyers and Willems, 1999). As the RING finger of LNX long is not able to homodimerize in the yeast two-hybrid assay, it may be capable of acting as an E3 ubiquitin ligase. Experiments are currently underway in our laboratory to investigate this possibility. Interestingly, polyubiquitin was isolated three times from the yeast two-hybrid screen with LNX long but did not interact specifically with LNX upon back-transformation. It may be that another plasmid was present in the yeast colonies picked from the library screen that facilitated interaction with LNX. In the same vein, another molecule predicted to have E3 ubiquitin ligase activity, WWP1, was observed to interact with LNX. Although it is not clear why this type of interaction occurs, it does lend support to the hypothesis that LNX is involved in the ubiquitination pathway. These studies will be extended by directly testing the ubiquitinating activity of LNX. Some of the proteins isolated from the yeast two-hybrid screen may in fact be substrates of the LNX E3 ubiquitin ligase activity.

4.5 MODELS OF LNX FUNCTION

From these results, we can propose several models of the intracellular role of LNX; these models are not mutually exclusive. There are two isoforms of LNX with unique expression patterns and LNX could have different roles in different cell types.

Two of the proteins that we identified as LNX interacting molecules, syntaxin5 and PRA1, are (or are potentially) involved in intracellular vesicle trafficking. Syntaxin5 and its yeast homologue Sed5p are important for the fusion of transport vesicles through the cisternae of the ER and golgi (Nichols and Pelham, 1998). PRA1 interacts with several rab family members, including Rab6 (Janoueix-Lerosey et al., 1995). Rab6 and its yeast homologue Ypt6 are important in several steps of vesicular protein trafficking: ER to golgi, intra-golgi and possibly retrograde traffic (Martinez and Goud, 1998). Rab6 is found on the transport vesicles as they travel through the ER and golgi while syntaxin5 is found on the ER and golgi target membranes. Although neither is solely responsible, both rabs and syntaxins are critical for the specificity of vesicles fusing to target membranes (Waters and Pfeffer, 1999). Molecules such as LNX, which may interact with both rabs (via PRA1) and syntaxins, could provide a bridge from an intracellular vesicle to its specific target. Due to its multiple interaction motifs, LNX may even recruit other signaling molecules, such as Nb, and/or enzymes important for recognition, vesicle fusion or downstream signaling.

The finding that RING finger domains are able to act as E3 ubiquitin ligases introduces new possibilities for LNX. In certain asymmetric cell divisions during Drosophila and mouse development, distinct daughter cells inherit different amounts of the cell-fate determinant Nb (Guo et al., 1996; Zhong et al., 1997). In the daughter cell which inherits it, Nb somehow downregulates Notch signaling pathways. It is possible that Nb also recruits LNX and its associated proteins to that daughter cell and causes the degradation of Notch by the ubiquitin-proteosome pathway. If WWP1 interacts with LNX in vivo, the HECT domain of WWP1, another domain with E3 ubiquitin ligase activity, may also be involved in degradation of Notch or its downstream signaling targets. In fact, a gene known to be capable of downregulation of Notch signaling, *suppressor of deltex* (*Su(dx)*, has recently been cloned and found to be a Nedd4 family member (Cornell et al., 1999). Thus the way in which Nb inhibits Notch signaling may be through targeted degradation of Notch and its downstream targets.

Both of these models require further validation and refinement but they provide a basis on which to investigate the molecular function of Numb and LNX.

Chapter V References

Altura, R. A., Maris, J. M., Li, H., Boyett, J. M., Brodeur, G. M., and Look, A. T. (1997). Novel regions of chromosomal loss in familial neuroblastoma by comparative genomic hybridization. Genes Chromosomes Cancer *19*, 176-84.

Andre, B., and Springael, J. Y. (1994). WWP, a new amino acid motif present in single or multiple copies in various proteins including dystrophin and the SH3-binding Yes- associated protein YAP65. Biochem Biophys Res Commun *205*, 1201-5.

Aoki, E., Takeuchi, I. K., Shoji, R., and Semba, R. (1993). Localization of nitric oxide-related substances in the peripheral nervous tissues. Brain Res *620*, 142-5.

Bea, S., Ribas, M., Hernandez, J. M., Bosch, F., Pinyol, M., Hernandez, L., Garcia, J. L., Flores, T., Gonzalez, M., Lopez-Guillermo, A., Piris, M. A., Cardesa, A., Montserrat, E., Miro, R., and Campo, E. (1999). Increased number of chromosomal imbalances and high-level DNA amplifications in mantle cell lymphoma are associated with blastoid variants. Blood *93*, 4365-74.

Bennett, M. K., Garcia-Arraras, J. E., Elferink, L. A., Peterson, K., Fleming, A. M., Hazuka, C. D., and Scheller, R. H. (1993). The syntaxin family of vesicular transport receptors. Cell *74*, 863-73.

Blaikie, P., Immanuel, D., Wu, J., Li, N., Yajnik, V., and Margolis, B. (1994). A region in Shc distinct from the SH2 domain can bind tyrosine- phosphorylated growth factor receptors. J Biol Chem *269*, 32031-4.

Bloomquist, B. T., Shortridge, R. D., Schneuwly, S., Perdew, M., Montell, C., Steller, H., Rubin, G., and Pak, W. L. (1988). Isolation of a putative phospholipase C gene of Drosophila, norpA, and its role in phototransduction. Cell *54*, 723-33.

Borg, J. P., Ooi, J., Levy, E., and Margolis, B. (1996). The phosphotyrosine interaction domains of X11 and FE65 bind to distinct sites on the YENPTY motif of amyloid precursor protein. Mol Cell Biol *16*, 6229-41.

Bork, P., and Margolis, B. (1995). A phosphotyrosine interaction domain [letter]. Cell *80*, 693-4.

Bork, P., Schultz, J., and Ponting, C. P. (1997). Cytoplasmic signalling domains: the next generation. Trends Biochem Sci *22*, 296-8.

Bork, P., and Sudol, M. (1994). The WW domain: a signalling site in dystrophin? Trends Biochem Sci *19*, 531-3.

Brenman, J. E., Chao, D. S., Gee, S. H., McGee, A. W., Craven, S. E., Santillano, D. R., Wu, Z., Huang, F., Xia, H., Peters, M. F., Froehner, S. C., and Bredt, D. S. (1996). Interaction of nitric oxide synthase with the postsynaptic density protein PSD-95 and alpha1-syntrophin mediated by PDZ domains. Cell *84*, 757-67.

Brenman, J. E., Chao, D. S., Xia, H., Aldape, K., and Bredt, D. S. (1995). Nitric oxide synthase complexed with dystrophin and absent from skeletal muscle sarcolemma in Duchenne muscular dystrophy. Cell *82*, 743-52.

Brenman, J. E., Christopherson, K. S., Craven, S. E., McGee, A. W., and Bredt, D. S. (1996). Cloning and characterization of postsynaptic density 93, a nitric oxide synthase interacting protein. J Neurosci *16*, 7407-15.

Bruckner, K., Pablo Labrador, J., Scheiffele, P., Herb, A., Seeburg, P. H., and Klein, R. (1999). EphrinB ligands recruit GRIP family PDZ adaptor proteins into raft membrane microdomains. Neuron *22*, 511-24.

Bryant, P. J., Watson, K. L., Justice, R. W., and Woods, D. F. (1993). Tumor suppressor genes encoding proteins required for cell interactions and signal transduction in Drosophila. Dev Suppl, 239-49.

Chevesich, J., Kreuz, A. J., and Montell, C. (1997). Requirement for the PDZ domain protein, INAD, for localization of the TRP store-operated channel to a signaling complex. Neuron *18*, 95-105.

Chien, C. T., Wang, S., Rothenberg, M., Jan, L. Y., and Jan, Y. N. (1998). Numb-associated kinase interacts with the phosphotyrosine binding domain of Numb and antagonizes the function of Numb in vivo. Mol Cell Biol *18*, 598-607.

Cho, K. O., Hunt, C. A., and Kennedy, M. B. (1992). The rat brain postsynaptic density fraction contains a homolog of the Drosophila discs-large tumor suppressor protein. Neuron *9*, 929-42.

Christopherson, K. S., Hillier, B. J., Lim, W. A., and Bredt, D. S. (1999). PSD-95 assembles a ternary complex with the N-methyl-D-aspartic acid receptor and a bivalent neuronal NO synthase PDZ domain [In Process Citation]. J Biol Chem *274*, 27467-73.

Cornell, M., Evans, D. A., Mann, R., Fostier, M., Flasza, M., Monthatong, M., Artavanis-Tsakonas, S., and Baron, M. (1999). The Drosophila melanogaster Suppressor of deltex gene, a regulator of the Notch receptor signaling pathway, is an E3 class ubiquitin ligase. Genetics *152*, 567-76.

Cuppen, E., Gerrits, H., Pepers, B., Wieringa, B., and Hendriks, W. (1998). PDZ motifs in PTP-BL and RIL bind to internal protein segments in the LIM domain protein RIL. Mol Biol Cell *9*, 671-83.

Daniels, D. L., Cohen, A. R., Anderson, J. M., and Brunger, A. T. (1998). Crystal structure of the hCASK PDZ domain reveals the structural basis of class II PDZ domain target recognition. Nat Struct Biol *5*, 317-25.

Dho, S. E., French, M. B., Woods, S. A., and McGlade, C. J. (1999). Characterization of Four Mammalian Numb Protein Isoforms. Identification of cytoplasmic and membrane-associated variants of the phosphotyrosine binding domain. J Biol Chem *274*, 33097-33104.

Dho, S. E., Jacob, S., Wolting, C. D., French, M. B., Rohrschneider, L. R., and McGlade, C. J. (1998). The mammalian numb phosphotyrosine-binding domain. Characterization of binding specificity and identification of a novel PDZ domain-containing numb binding protein, LNX. J Biol Chem *273*, 9179-87.

Doyle, D. A., Lee, A., Lewis, J., Kim, E., Sheng, M., and MacKinnon, R. (1996). Crystal structures of a complexed and peptide-free membrane protein- binding domain: molecular basis of peptide recognition by PDZ. Cell *85*, 1067-76.

Etemad-Moghadam, B., Guo, S., and Kemphues, K. J. (1995). Asymmetrically distributed PAR-3 protein contributes to cell polarity and spindle alignment in early C. elegans embryos. Cell *83*, 743-52.

Fanning, A. S., and Anderson, J. M. (1999). PDZ domains: fundamental building blocks in the organization of protein complexes at the plasma membrane. J Clin Invest *103*, 767-72.

Fanning, A. S., and Anderson, J. M. (1999). Protein modules as organizers of membrane structure [In Process Citation]. Curr Opin Cell Biol *11*, 432-9.

Feng, S., Chen, J. K., Yu, H., Simon, J. A., and Schreiber, S. L. (1994). Two binding orientations for peptides to the Src SH3 domain: development of a general model for SH3-ligand interactions. Science *266*, 1241-7.

Gee, S. H., Sekely, S. A., Lombardo, C., Kurakin, A., Froehner, S. C., and Kay, B. K. (1998). Cyclic peptides as non-carboxyl-terminal ligands of syntrophin PDZ domains. J Biol Chem *273*, 21980-7.

Gho, M., and Schweisguth, F. (1998). Frizzled signalling controls orientation of asymmetric sense organ precursor cell divisions in Drosophila. Nature *393*, 178-81.

Guo, M., Jan, L. Y., and Jan, Y. N. (1996). Control of daughter cell fates during asymmetric division: interaction of Numb and Notch. Neuron *17*, 27-41.

Guo, S., and Kemphues, K. J. (1996). Molecular genetics of asymmetric cleavage in the early Caenorhabditis elegans embryo. Curr Opin Genet Dev *6*, 408-15.

Harrison, S. C. (1996). Peptide-surface association: the case of PDZ and PTB domains. Cell *86*, 341-3.

Hasegawa, M., Cuenda, A., Spillantini, M. G., Thomas, G. M., Buee-Scherrer, V., Cohen, P., and Goedert, M. (1999). Stress-activated protein kinase-3 interacts with the PDZ domain of alpha1-syntrophin. A mechanism for specific substrate recognition. J Biol Chem *274*, 12626-31.

Hata, Y., Butz, S., and Sudhof, T. C. (1996). CASK: a novel dlg/PSD95 homolog with an N-terminal calmodulin-dependent protein kinase domain identified by interaction with neurexins. J Neurosci *16*, 2488-94.

Hillier, B. J., Christopherson, K. S., Prehoda, K. E., Bredt, D. S., and Lim, W. A. (1999). Unexpected modes of PDZ domain scaffolding revealed by structure of nNOS-syntrophin complex. Science *284*, 812-5.

Hirao, K., Hata, Y., Ide, N., Takeuchi, M., Irie, M., Yao, I., Deguchi, M., Toyoda, A., Sudhof, T. C., and Takai, Y. (1998). A novel multiple PDZ domain-containing molecule interacting with N-methyl-D-aspartate receptors and neuronal cell adhesion proteins. J Biol Chem *273*, 21105-10.

Hock, B., Bohme, B., Karn, T., Yamamoto, T., Kaibuchi, K., Holtrich, U., Holland, S., Pawson, T., Rubsamen-Waigmann, H., and Strebhardt, K. (1998). PDZ-domain-mediated interaction of the Eph-related receptor tyrosine kinase EphB3 and the ras-binding protein AF6 depends on the kinase activity of the receptor. Proc Natl Acad Sci U S A *95*, 9779-84.

Hofmann, K., and Bucher, P. (1995). The rsp5-domain is shared by proteins of diverse functions. FEBS Lett *358*, 153-7.

Horvitz, H. R., and Herskowitz, I. (1992). Mechanisms of asymmetric cell division: two Bs or not two Bs, that is the question. Cell *68*, 237-55.

Hoskins, R., Hajnal, A. F., Harp, S. A., and Kim, S. K. (1996). The C. elegans vulval induction gene lin-2 encodes a member of the MAGUK family of cell junction proteins. Development *122*, 97-111.

Howell, B. W., Lanier, L. M., Frank, R., Gertler, F. B., and Cooper, J. A. (1999). The disabled 1 phosphotyrosine-binding domain binds to the internalization signals of transmembrane glycoproteins and to phospholipids. Mol Cell Biol *19*, 5179-88.

Hu, G., and Fearon, E. R. (1999). Siah-1 N-terminal RING domain is required for proteolysis function, and C-terminal sequences regulate oligomerization and binding to target proteins. Mol Cell Biol *19*, 724-32.

Huber, A., Sander, P., Gobert, A., Bahner, M., Hermann, R., and Paulsen, R. (1996). The transient receptor potential protein (Trp), a putative store- operated Ca2+ channel essential for

phosphoinositide-mediated photoreception, forms a signaling complex with NorpA, InaC and InaD. Embo J *15*, 7036-45.

Huber, A., Sander, P., and Paulsen, R. (1996). Phosphorylation of the InaD gene product, a photoreceptor membrane protein required for recovery of visual excitation. J Biol Chem *271*, 11710-7.

Huibregtse, J. M., Scheffner, M., Beaudenon, S., and Howley, P. M. (1995). A family of proteins structurally and functionally related to the E6-AP ubiquitin-protein ligase [published erratum appears in Proc Natl Acad Sci U S A 1995 May 23;92(11):5249]. Proc Natl Acad Sci U S A *92*, 2563-7.

Inouye, C., Dhillon, N., and Thorner, J. (1997). Ste5 RING-H2 domain: role in Ste4-promoted oligomerization for yeast pheromone signaling. Science *278*, 103-6.

Irie, M., Hata, Y., Takeuchi, M., Ichtchenko, K., Toyoda, A., Hirao, K., Takai, Y., Rosahl, T. W., and Sudhof, T. C. (1997). Binding of neuroligins to PSD-95. Science *277*, 1511-5.

Ishiguro, T., Nakajima, M., Naito, M., Muto, T., and Tsuruo, T. (1996). Identification of genes differentially expressed in B16 murine melanoma sublines with different metastatic potentials. Cancer Res *56*, 875-9.

Izumi, Y., Hirose, T., Tamai, Y., Hirai, S., Nagashima, Y., Fujimoto, T., Tabuse, Y., Kemphues, K. J., and Ohno, S. (1998). An atypical PKC directly associates and colocalizes at the epithelial tight junction with ASIP, a mammalian homologue of Caenorhabditis elegans polarity protein PAR-3. J Cell Biol *143*, 95-106.

Jaffrey, S. R., Snowman, A. M., Eliasson, M. J., Cohen, N. A., and Snyder, S. H. (1998). CAPON: a protein associated with neuronal nitric oxide synthase that regulates its interactions with PSD95. Neuron *20*, 115-24.

Janoueix-Lerosey, I., Jollivet, F., Camonis, J., Marche, P. N., and Goud, B. (1995). Two-hybrid system screen with the small GTP-binding protein Rab6. Identification of a novel mouse GDP dissociation inhibitor isoform and two other potential partners of Rab6. J Biol Chem *270*, 14801-8.

Ji, X., Zhang, P., Armstrong, R. N., and Gilliland, G. L. (1992). The three-dimensional structure of a glutathione S-transferase from the mu gene class. Structural analysis of the binary complex of isoenzyme 3- 3 and glutathione at 2.2-A resolution. Biochemistry *31*, 10169-84.

Kaech, S. M., Whitfield, C. W., and Kim, S. K. (1998). The LIN-2/LIN-7/LIN-10 complex mediates basolateral membrane localization of the C. elegans EGF receptor LET-23 in vulval epithelial cells. Cell *94*, 761-71.

Kameya, S., Miyagoe, Y., Nonaka, I., Ikemoto, T., Endo, M., Hanaoka, K., Nabeshima, Y., and Takeda, S. (1999). alpha1-syntrophin gene disruption results in the absence of neuronal- type nitric-oxide synthase at the sarcolemma but does not induce muscle degeneration. J Biol Chem *274*, 2193-200.

Kavanaugh, W. M., and Williams, L. T. (1994). An alternative to SH2 domains for binding tyrosine-phosphorylated proteins. Science *266*, 1862-5.

Kemphues, K. J., Priess, J. R., Morton, D. G., and Cheng, N. S. (1988). Identification of genes required for cytoplasmic localization in early C. elegans embryos. Cell *52*, 311-20.

Kennedy, M. B. (1995). Origin of PDZ (DHR, GLGF) domains [letter; comment]. Trends Biochem Sci *20*, 350.

Kim, E., DeMarco, S. J., Marfatia, S. M., Chishti, A. H., Sheng, M., and Strehler, E. E. (1998). Plasma membrane Ca2+ ATPase isoform 4b binds to membrane-associated guanylate kinase (MAGUK) proteins via their PDZ (PSD-95/Dlg/ZO-1) domains. J Biol Chem *273*, 1591-5.

Kim, E., Niethammer, M., Rothschild, A., Jan, Y. N., and Sheng, M. (1995). Clustering of Shaker-type K+ channels by interaction with a family of membrane-associated guanylate kinases. Nature *378*, 85-8.

Knoblich, J. A., Jan, L. Y., and Jan, Y. N. (1995). Asymmetric segregation of Numb and Prospero during cell division. Nature *377*, 624-7.

Koch, C. A., Moran, M., Sadowski, I., and Pawson, T. (1989). The common src homology region 2 domain of cytoplasmic signaling proteins is a positive effector of v-fps tyrosine kinase function. Mol Cell Biol *9*, 4131-40.

Kornau, H. C., Schenker, L. T., Kennedy, M. B., and Seeburg, P. H. (1995). Domain interaction between NMDA receptor subunits and the postsynaptic density protein PSD-95. Science *269*, 1737-40.

Kraut, R., and Campos-Ortega, J. A. (1996). inscuteable, a neural precursor gene of Drosophila, encodes a candidate for a cytoskeleton adaptor protein. Dev Biol *174*, 65-81.

Kraut, R., Chia, W., Jan, L. Y., Jan, Y. N., and Knoblich, J. A. (1996). Role of inscuteable in orienting asymmetric cell divisions in Drosophila. Nature *383*, 50-5.

Kuchinke, U., Grawe, F., and Knust, E. (1998). Control of spindle orientation in Drosophila by the Par-3-related PDZ- domain protein Bazooka. Curr Biol *8*, 1357-65.

Ladbury, J. E., Lemmon, M. A., Zhou, M., Green, J., Botfield, M. C., and Schlessinger, J. (1995). Measurement of the binding of tyrosyl phosphopeptides to SH2 domains: a reappraisal. Proc Natl Acad Sci U S A *92*, 3199-203.

Lee, J. W., Choi, H. S., Gyuris, J., Brent, R., and Moore, D. D. (1995). Two classes of proteins dependent on either the presence or absence of thyroid hormone for interaction with the thyroid hormone receptor. Mol Endocrinol *9*, 243-54.

Li, X. J., Xu, R. H., Guggino, W. B., and Snyder, S. H. (1995). Alternatively spliced forms of the alpha subunit of the epithelial sodium channel: distinct sites for amiloride binding and channel pore. Mol Pharmacol *47*, 1133-40.

Lim, W. A., Richards, F. M., and Fox, R. O. (1994). Structural determinants of peptide-binding orientation and of sequence specificity in SH3 domains [see comments] [published erratum appears in Nature 1995 Mar 2;374(6517):94]. Nature *372*, 375-9.

Lioubin, M. N., Algate, P. A., Tsai, S., Carlberg, K., Aebersold, A., and Rohrschneider, L. R. (1996). p150Ship, a signal transduction molecule with inositol polyphosphate-5- phosphatase activity. Genes Dev *10*, 1084-95.

Lorick, K. L., Jensen, J. P., Fang, S., Ong, A. M., Hatakeyama, S., and Weissman, A. M. (1999). RING fingers mediate ubiquitin-conjugating enzyme (E2)-dependent ubiquitination. Proc Natl Acad Sci U S A *96*, 11364-9.

Mao, X., Jones, T. A., Tomlinson, I., Rowan, A. J., Fedorova, L. I., Zelenin, A. V., Mao, J. I., Gutowski, N. J., Noble, M., and Sheer, D. (1999). Genetic aberrations in glioblastoma multiforme: translocation of chromosome 10 in an O-2A-like cell line. Br J Cancer *79*, 724-31.

Martincic, I., Peralta, M. E., and Ngsee, J. K. (1997). Isolation and characterization of a dual prenylated Rab and VAMP2 receptor. J Biol Chem *272*, 26991-8.

Martinez, O., and Goud, B. (1998). Rab proteins. Biochim Biophys Acta *1404*, 101-12.

Masuko, N., Makino, K., Kuwahara, H., Fukunaga, K., Sudo, T., Araki, N., Yamamoto, H., Yamada, Y., Miyamoto, E., and Saya, H. (1999). Interaction of NE-dlg/SAP102, a neuronal and endocrine tissue-specific membrane-associated guanylate kinase protein, with calmodulin and PSD- 95/SAP90. A possible regulatory role in molecular clustering at synaptic sites. J Biol Chem *274*, 5782-90.

Mayer, B. J., Hamaguchi, M., and Hanafusa, H. (1988). A novel viral oncogene with structural similarity to phospholipase C. Nature *332*, 272-5.

Mayer, B. J., and Hanafusa, H. (1990). Mutagenic analysis of the v-crk oncogene: requirement for SH2 and SH3 domains and correlation between increased cellular phosphotyrosine and transformation. J Virol *64*, 3581-9.

Montell, C. (1998). TRP trapped in fly signaling web. Curr Opin Neurobiol *8*, 389-97.

Montell, C., and Rubin, G. M. (1989). Molecular characterization of the Drosophila trp locus: a putative integral membrane protein required for phototransduction. Neuron *2*, 1313-23.

Morais Cabral, J. H., Petosa, C., Sutcliffe, M. J., Raza, S., Byron, O., Poy, F., Marfatia, S. M., Chishti, A. H., and Liddington, R. C. (1996). Crystal structure of a PDZ domain. Nature *382*, 649-52.

Muller, H. A., and Wieschaus, E. (1996). armadillo, bazooka, and stardust are critical for early stages in formation of the zonula adherens and maintenance of the polarized blastoderm epithelium in Drosophila. J Cell Biol *134*, 149-63.

Nichols, B. J., and Pelham, H. R. (1998). SNAREs and membrane fusion in the Golgi apparatus. Biochim Biophys Acta *1404*, 9-31.

Niethammer, M., and Sheng, M. (1998). Identification of ion channel-associated proteins using the yeast two- hybrid system. Methods Enzymol *293*, 104-22.

Nishizaki, T., Ozaki, S., Harada, K., Ito, H., Arai, H., Beppu, T., and Sasaki, K. (1998). Investigation of genetic alterations associated with the grade of astrocytic tumor by comparative genomic hybridization. Genes Chromosomes Cancer *21*, 340-6.

O'Shannessy, D. J., Brigham-Burke, M., Soneson, K. K., Hensley, P., and Brooks, I. (1994). Determination of rate and equilibrium binding constants for macromolecular interactions by surface plasmon resonance. Methods Enzymol *240*, 323-49.

Pak, W. L., and Pinto, L. H. (1976). Genetic approach to the study of the nervous system. Annu Rev Biophys Bioeng *5*, 397-448.

Pascal, S. M., Singer, A. U., Gish, G., Yamazaki, T., Shoelson, S. E., Pawson, T., Kay, L. E., and Forman-Kay, J. D. (1994). Nuclear magnetic resonance structure of an SH2 domain of phospholipase C-gamma 1 complexed with a high affinity binding peptide. Cell *77*, 461-72.

Pawson, T. (1995). Protein modules and signalling networks. Nature *373*, 573-80.

Pawson, T., and Scott, J. D. (1997). Signaling through scaffold, anchoring, and adaptor proteins. Science *278*, 2075-80.

Pelicci, G., Lanfrancone, L., Grignani, F., McGlade, J., Cavallo, F., Forni, G., Nicoletti, I., Pawson, T., and Pelicci, P. G. (1992). A novel transforming protein (SHC) with an SH2 domain is implicated in mitogenic signal transduction. Cell *70*, 93-104.

Phizicky, E. M., and Fields, S. (1995). Protein-protein interactions: methods for detection and analysis. Microbiol Rev *59*, 94-123.

Pirozzi, G., McConnell, S. J., Uveges, A. J., Carter, J. M., Sparks, A. B., Kay, B. K., and Fowlkes, D. M. (1997). Identification of novel human WW domain-containing proteins by cloning of ligand targets. J Biol Chem *272*, 14611-6.

Ponting, C. P., Phillips, C., Davies, K. E., and Blake, D. J. (1997). PDZ domains: targeting signalling molecules to sub-membranous sites. Bioessays *19*, 469-79.

Ranganathan, R., and Ross, E. M. (1997). PDZ domain proteins: scaffolds for signaling complexes. Curr Biol *7*, R770-3.

Rhyu, M. S., Jan, L. Y., and Jan, Y. N. (1994). Asymmetric distribution of numb protein during division of the sensory organ precursor cell confers distinct fates to daughter cells [see comments]. Cell *76*, 477-91.

Rhyu, M. S., and Knoblich, J. A. (1995). Spindle orientation and asymmetric cell fate. Cell *82*, 523-6.

Sadowski, I., Stone, J. C., and Pawson, T. (1986). A noncatalytic domain conserved among cytoplasmic protein-tyrosine kinases modifies the kinase function and transforming activity of Fujinami sarcoma virus P130gag-fps. Mol Cell Biol *6*, 4396-408.

Saras, J., and Heldin, C. H. (1996). PDZ domains bind carboxy-terminal sequences of target proteins. Trends Biochem Sci *21*, 455-8.

Schatz, P. J., Cull, M. G., Martin, E. L., and Gates, C. M. (1996). Screening of peptide libraries linked to lac repressor. Methods Enzymol *267*, 171-91.

Schepens, J., Cuppen, E., Wieringa, B., and Hendriks, W. (1997). The neuronal nitric oxide synthase PDZ motif binds to -G(D,E)XV* carboxyterminal sequences. FEBS Lett *409*, 53-6.

Shieh, B. H., and Niemeyer, B. (1995). A novel protein encoded by the InaD gene regulates recovery of visual transduction in Drosophila. Neuron *14*, 201-10.

Shieh, B. H., and Zhu, M. Y. (1996). Regulation of the TRP Ca2+ channel by INAD in Drosophila photoreceptors. Neuron *16*, 991-8.

Simon, R., Burger, H., Brinkschmidt, C., Bocker, W., Hertle, L., and Terpe, H. J. (1998). Chromosomal aberrations associated with invasion in papillary superficial bladder cancer. J Pathol *185*, 345-51.

Smith, D. P., Ranganathan, R., Hardy, R. W., Marx, J., Tsuchida, T., and Zuker, C. S. (1991). Photoreceptor deactivation and retinal degeneration mediated by a photoreceptor-specific protein kinase C. Science *254*, 1478-84.

Songyang, Z., Fanning, A. S., Fu, C., Xu, J., Marfatia, S. M., Chishti, A. H., Crompton, A., Chan, A. C., Anderson, J. M., and Cantley, L. C. (1997). Recognition of unique carboxyl-terminal motifs by distinct PDZ domains. Science *275*, 73-7.

Songyang, Z., Shoelson, S. E., Chaudhuri, M., Gish, G., Pawson, T., Haser, W. G., King, F., Roberts, T., Ratnofsky, S., Lechleider, R. J., and et al. (1993). SH2 domains recognize specific phosphopeptide sequences. Cell *72*, 767-78.

Spana, E. P., and Doe, C. Q. (1996). Numb antagonizes Notch signaling to specify sibling neuron cell fates. Neuron *17*, 21-6.

Spana, E. P., Kopczynski, C., Goodman, C. S., and Doe, C. Q. (1995). Asymmetric localization of numb autonomously determines sibling neuron identity in the Drosophila CNS. Development *121*, 3489-94.

Staub, O., Dho, S., Henry, P., Correa, J., Ishikawa, T., McGlade, J., and Rotin, D. (1996). WW domains of Nedd4 bind to the proline-rich PY motifs in the epithelial Na+ channel deleted in Liddle's syndrome. Embo J *15*, 2371-80.

Staub, O., and Rotin, D. (1997). Regulation of ion transport by protein-protein interaction domains. Curr Opin Nephrol Hypertens *6*, 447-54.

Staub, O., and Rotin, D. (1996). WW domains. Structure *4*, 495-9.

Stricker, N. L., Christopherson, K. S., Yi, B. A., Schatz, P. J., Raab, R. W., Dawes, G., Bassett, D. E., Jr., Bredt, D. S., and Li, M. (1997). PDZ domain of neuronal nitric oxide synthase recognizes novel C- terminal peptide sequences. Nat Biotechnol *15*, 336-42.

Tabuse, Y., Izumi, Y., Piano, F., Kemphues, K. J., Miwa, J., and Ohno, S. (1998). Atypical protein kinase C cooperates with PAR-3 to establish embryonic polarity in Caenorhabditis elegans. Development *125*, 3607-14.

Tarkkanen, M., Huuhtanen, R., Virolainen, M., Wiklund, T., Asko-Seljavaara, S., Tukiainen, E., Lepantalo, M., Elomaa, I., and Knuutila, S. (1999). Comparison of genetic changes in primary sarcomas and their pulmonary metastases. Genes Chromosomes Cancer *25*, 323-31.

Tochio, H., Zhang, Q., Mandal, P., Li, M., and Zhang, M. (1999). Solution structure of the extended neuronal nitric oxide synthase PDZ domain complexed with an associated peptide [see comments]. Nat Struct Biol *6*, 417-21.

Torres, R., Firestein, B. L., Dong, H., Staudinger, J., Olson, E. N., Huganir, R. L., Bredt, D. S., Gale, N. W., and Yancopoulos, G. D. (1998). PDZ proteins bind, cluster, and synaptically colocalize with Eph receptors and their ephrin ligands [see comments]. Neuron *21*, 1453-63.

Tsunoda, S., Sierralta, J., Sun, Y., Bodner, R., Suzuki, E., Becker, A., Socolich, M., and Zuker, C. S. (1997). A multivalent PDZ-domain protein assembles signalling complexes in a G- protein-coupled cascade. Nature *388*, 243-9.

Tyers, M., and Willems, A. R. (1999). One ring to rule a superfamily of E3 ubiquitin ligases [comment]. Science *284*, 601, 603-4.

Uemura, T., Shepherd, S., Ackerman, L., Jan, L. Y., and Jan, Y. N. (1989). numb, a gene required in determination of cell fate during sensory organ formation in Drosophila embryos. Cell *58*, 349-60.

van der Geer, P., Wiley, S., Lai, V. K., Olivier, J. P., Gish, G. D., Stephens, R., Kaplan, D., Shoelson, S., and Pawson, T. (1995). A conserved amino-terminal Shc domain binds to phosphotyrosine motifs in activated receptors and phosphopeptides. Curr Biol *5*, 404-12.

van Huizen, R., Miller, K., Chen, D. M., Li, Y., Lai, Z. C., Raab, R. W., Stark, W. S., Shortridge, R. D., and Li, M. (1998). Two distantly positioned PDZ domains mediate multivalent INAD-phospholipase C interactions essential for G protein-coupled signaling. Embo J *17*, 2285-97.

Verdi, J. M., Bashirullah, A., Goldhawk, D. E., Kubu, C. J., Jamali, M., Meakin, S. O., and Lipshitz, H. D. (1999). Distinct human NUMB isoforms regulate differentiation vs. proliferation in the neuronal lineage. Proc Natl Acad Sci U S A *96*, 10472-6.

Verdi, J. M., Schmandt, R., Bashirullah, A., Jacob, S., Salvino, R., Craig, C. G., Program, A. E., Lipshitz, H. D., and McGlade, C. J. (1996). Mammalian NUMB is an evolutionarily conserved signaling adapter protein that specifies cell fate. Curr Biol *6*, 1134-45.

Vervoort, M., Merritt, D. J., Ghysen, A., and Dambly-Chaudiere, C. (1997). Genetic basis of the formation and identity of type I and type II neurons in Drosophila embryos. Development *124*, 2819-28.

Wakamatsu, Y., Maynard, T. M., Jones, S. U., and Weston, J. A. (1999). NUMB localizes in the basal cortex of mitotic avian neuroepithelial cells and modulates neuronal differentiation by binding to NOTCH-1. Neuron *23*, 71-81.

Waksman, G., Shoelson, S. E., Pant, N., Cowburn, D., and Kuriyan, J. (1993). Binding of a high affinity phosphotyrosyl peptide to the Src SH2 domain: crystal structures of the complexed and peptide-free forms. Cell *72*, 779-90.

Wang, Y., Okamoto, M., Schmitz, F., Hofmann, K., and Sudhof, T. C. (1997). Rim is a putative Rab3 effector in regulating synaptic-vesicle fusion. Nature *388*, 593-8.

Waters, M. G., and Pfeffer, S. R. (1999). Membrane tethering in intracellular transport [In Process Citation]. Curr Opin Cell Biol *11*, 453-9.

Watts, J. L., Etemad-Moghadam, B., Guo, S., Boyd, L., Draper, B. W., Mello, C. C., Priess, J. R., and Kemphues, K. J. (1996). par-6, a gene involved in the establishment of asymmetry in early C. elegans embryos, mediates the asymmetric localization of PAR-3. Development *122*, 3133-40.

Wieschaus, E., Nusslein-Volhard, C., and Kluding, H. (1984). Kruppel, a gene whose activity is required early in the zygotic genome for normal embryonic segmentation. Dev Biol *104*, 172-86.

Wittekind, M., Mapelli, C., Farmer, B. T., 2nd, Suen, K. L., Goldfarb, V., Tsao, J., Lavoie, T., Barbacid, M., Meyers, C. A., and Mueller, L. (1994). Orientation of peptide fragments from Sos

proteins bound to the N- terminal SH3 domain of Grb2 determined by NMR spectroscopy. Biochemistry *33*, 13531-9.

Wood, J. D., Yuan, J., Margolis, R. L., Colomer, V., Duan, K., Kushi, J., Kaminsky, Z., Kleiderlein, J. J., Sharp, A. H., and Ross, C. A. (1998). Atrophin-1, the DRPLA gene product, interacts with two families of WW domain-containing proteins. Mol Cell Neurosci *11*, 149-60.

Xu, X. Z., Choudhury, A., Li, X., and Montell, C. (1998). Coordination of an array of signaling proteins through homo- and heteromeric interactions between PDZ domains and target proteins. J Cell Biol *142*, 545-55.

Zhong, W., Feder, J. N., Jiang, M. M., Jan, L. Y., and Jan, Y. N. (1996). Asymmetric localization of a mammalian numb homolog during mouse cortical neurogenesis. Neuron *17*, 43-53.

Zhong, W., Jiang, M. M., Weinmaster, G., Jan, L. Y., and Jan, Y. N. (1997). Differential expression of mammalian Numb, Numblike and Notch1 suggests distinct roles during mouse cortical neurogenesis. Development *124*, 1887-97.

Zhou, M. M., Huang, B., Olejniczak, E. T., Meadows, R. P., Shuker, S. B., Miyazaki, M., Trub, T., Shoelson, S. E., and Fesik, S. W. (1996). Structural basis for IL-4 receptor phosphopeptide recognition by the IRS-1 PTB domain. Nat Struct Biol *3*, 388-93.

Zhou, M. M., Ravichandran, K. S., Olejniczak, E. F., Petros, A. M., Meadows, R. P., Sattler, M., Harlan, J. E., Wade, W. S., Burakoff, S. J., and Fesik, S. W. (1995). Structure and ligand recognition of the phosphotyrosine binding domain of Shc. Nature *378*, 584-92.